The effect of weather and climate on siphonic rainwater drainage system operation

Thesis submitted for the degree of

Doctor of Philosophy

by

Richard K. Beattie

School of the Built Environment,
Heriot-Watt University,
March 2013

Submitted in accordance with the requirements of Heriot-Watt University
for the degree of Doctor of Philosophy.

Abstract

This thesis establishes important siphonic rainwater outlet loss coefficients which may be incorporated into a mathematical model capable of accurately simulating such networks.

The siphonic rainwater drainage system principally operates under sub-atmospheric pressures based upon the potential energy of the disposable head, resulting in depressurization and full-bore flow. These abilities generate many beneficial characteristics, but when in operation the system will be influenced by physical and external conditions, in particular, those introduced when flow pathways are compromised by detritus accumulation at outlets.

Appropriate siphonic outlet loss coefficients have been established from changes in pressure in the discharge pipe and gutter depths as a product of partial blockages at the outlet due to either detritus or percentage coverage barriers. These coefficients were derived from analysis of laboratory data informed by photographic and weather station data established from two major site investigations. Utilising these new loss coefficients allows accurate consequences of particular rainfall events to be predicted using a version of ROOFNET- a Method of Characteristics based simulation model. From this, a rainfall intensity simulated with outlet blockage has produced results similar to those recorded from site.

Acknowledgements

The author would like to express his sincere thanks to the following:

- Professor Lynne B Jack;
- EPSRC (EP/F038143/1) for funding part of this research;
- National Records of Scotland;
- Glasgow Rangers Football Club;
- All staff of the Drainage Research Group, School of the Built Environment at Heriot-Watt University;
- David Walker for his creativity and manufacturing skills;
- Lastly, I would like to thank my family and my close friends.

"*the only thing that interferes with my learning is my education*"

Albert Einstein

ACADEMIC REGISTRY
Research Thesis Submission

Name*:*	Richard K Beattie		
School/PGI:	School of the Built Environment		
Version: *(i.e. First, Resubmission, Final)*	Final	Degree Sought (Award **and** Subject area)	Doctor of Philosophy (Construction)

Declaration

In accordance with the appropriate regulations I hereby submit my thesis and I declare that:

1) the thesis embodies the results of my own work and has been composed by myself
2) where appropriate, I have made acknowledgement of the work of others and have made reference to work carried out in collaboration with other persons
3) the thesis is the correct version of the thesis for submission and is the same version as any electronic versions submitted*.
4) my thesis for the award referred to, deposited in the Heriot-Watt University Library, should be made available for loan or photocopying and be available via the Institutional Repository, subject to such conditions as the Librarian may require
5) I understand that as a student of the University I am required to abide by the Regulations of the University and to conform to its discipline.

* *Please note that it is the responsibility of the candidate to ensure that the correct version of the thesis is submitted.*

Signature of Candidate*:*		Date:	

Submission

Submitted By *(name in capitals):*	
Signature of Individual Submitting:	
Date Submitted:	

For Completion in the Student Service Centre (SSC)

Received in the SSC by *(name in capitals):*			
Method of Submission *(Handed in to SSC; posted through internal/external mail):*			
*E-thesis Submitted (**mandatory for final theses)***			
Signature:		Date:	

Contents

Chapter 4

Siphonic rainwater drainage site investigations

Notation

The topics that follow require definitions by the parameters of the Greek Alphabet. There is no conflict in the text resulting from repeated symbols with a number of definitions. SI units are used as standard within.

		Units
A	cross-sectional area	(m^2)
d_p	internal pipe diameter	(m)
g	gravity	(m/s^2)
H_T	total head loss from pipes and fittings	(m)
h_o	pressure head loss at outlet	(m)
h_E	pressure head loss at exit	(m)
h_{vp}	head water pressure	(m)
i_F	frictional head loss gradient	(m/m)
K	non-dimensional head loss coefficient	-
k_p	pipe roughness	(mm)
L_y	design lifetime of the building	(years)
P_r	probability of exceeding the statistical rate of rainfall during the lifetime of the building	-
p	point pressure of the fluid	(m)
Q	flow rate	(l/s)
T	return period	(years)
T_F	filling time	(seconds)
V	velocity	(m/s)
V_E	velocity flow at discharge point	(m/s)
V_p	collector pipe volume	(m/s)
ΔE_{12}	energy loss between points 1 point 2	(J/kg)
ΔH_{12}	head loss between points 1 and 2	(m)
ΔH_f	losses due to fittings	(m)
ΔH_p	hydraulic resistance of pipe walls	(m)
ΔZ	difference in vertical height	(m)
ρ	density	(kg/m^3)
z	vertical elevation	(m)
σ	cavitation index	-

Subscripts

a	air
w	water
u	upstream
D	downstream
E	point of discharge
T	total
K	kinetic

Other terms

K1, K4	constant in Method of Characteristic equations based on known parameters
C^+, C^-	characteristic equations sloping downstream and upstream respectively

Abbreviations

ASPE	American Society of Plumbing Engineers
BBA	British Board of Agrément
BRE	British Research Establishment, UK
BS	British Standard, UK
CIBW62	International Council for Research and Innovation in Building and Construction Working Commission W62 *'Water Supply and Drainage for Buildings'*
EN	European Standard
EPSRC	Engineering and Physical Sciences Research Council
MoC	Method of Characteristics
NRS	National Records building

List of Publications

A number of papers have been presented and published during the development of this research. These papers are listed in chronological order as follows:

Kelly D.A, Jack L.B, & **Beattie R.K,** *'An investigation into the impact of climate change on the performance of property drainage systems'*. Proceedings from the CIBW62 36th International Symposium on Water Supply and Drainage for Buildings, Sydney, Australia, 8th to 10th November 2010.

Beattie R.K, *'Examining the effects of partially blocked siphonic outlets on system performance'*. Proceedings from the 1st World Plumbing Symposium, Edinburgh, Scotland, 7th to 11th September 2011.

Beattie R.K, & Jack L.B, *'An investigation into how siphonic roof drainage systems perform in a future climate'*. Proceedings from the CIBW62 37th International Symposium on Water Supply and Drainage for Buildings, Aveiro, Portugal, 25th to 28th September 2011.

Beattie R.K, & Schee W.G,Van,der, *'Vervuiling bij de afvoertrechter'*. TVVL Magazine, Dutch, Juli/Augustus: Nr 7/8, 2012.

Beattie R.K, & Jack L.B, *'Investigation of outlet detritus accumulation at two monitored siphonic roof drainage sites'* Proceedings from the CIBW62 38th International Symposium on Water Supply and Drainage for Buildings, Edinburgh, Scotland, 27th to 30th August 2012.

Jack L.B, & **Beattie R.K,** *'Detritus accumulation at, and impact on performance of, siphonic rainwater outlets'*. Building Services Engineering Research and Technology 2012 – Submitted.

Chapter 1
Introduction to roof drainage systems

1.1 Introduction

It would be reasonable to assume the *'out of sight out of mind'* adage often applies to roof drainage systems, which may often lack the necessary design and maintenance attention they deserve. However, presenting but a small portion of the total construction cost, their importance should not be underestimated, given the cost of building content damages and disruption if the drainage system fails to protect from water ingress.

The principle objective for all roof drainage systems is the transfer of rainwater from the roof to the below-ground network or – increasingly - to SUDS. Typically two types of rainwater systems exist; conventional gravity systems and siphonic full-bore flow systems, each with three central components: gutters, outlets and downpipes. Although there is scope, in conventional systems, for a variation in the design intensity, there is little, if any, *'spare'* capacity in siphonic systems.

If climate predictions are true, it leads to the question: *'should rainwater systems be designed in order to accommodate for changes in precipitation and how are installed systems currently performing?'*. This presents two problems. Firstly, higher intensity rainfall or greater volumetric runoff may lead to system under-capacity, flooding, noise and vibration. Secondly, higher temperatures and longer dry spells may result in an increase in detritus build-up at siphonic outlets, which will directly impact system operation where the decreased water volumes may lack the necessary wash effect on detritus accumulation.

In summary, several variables may impact upon detritus build-up in a roof gutter; the varying nature and duration of rainfall events, the time between events; and even increased air temperature may influence air borne matter. Individually these may result in possible changes in detritus accumulation at outlets, and hence systems may fail at a lower rate of runoff.

1.2 Roof drainage design

As mentioned, two types of rainwater drainage systems exist, the conventional system and the siphonic system. These systems with their components may be seen in Figure 1.1 (a & b) respectively.

Significant differences between the conventional system and the siphonic system are twofold. Firstly, in a conventional system, gutter outlets are appropriately sized open holes in the gutter sole, whereas in a siphonic system the gutter outlets are of a type that restricts air entrainment. Secondly, conventional system downpipes are designed to run at approximately one fifth to one third full, whereas siphonic systems are designed to run at 100% full-flow from the outlet to the point of discharge.

For a conventional system, flow conveyance capacity is dependent on the depth of gutter water as the driving head, and the diameter of the outlet pipe. As the rainwater flows over the weir edge of the gutter outlet and into the downpipe, air is entrained. Depending on the gutter water depth, the flow may be categorised as either weir or orifice type. The falling water around the inner walls of the downpipe causes a central air core, whereby the downpipes are in a part-filled state. This system necessitates many individual downpipes each relatively large in diameter, where generally each outlet has its own discharge downpipe to enable the gutters to drain quickly. High level horizontal pipework must also be laid, at gradient, to allow for flow. Additionally, extensive underground pipework is a prerequisite of the conventional drainage system.

A siphonic system maximizes on elevation differences between gutter levels and the point of discharge, equating to the systems head loss, to achieve significantly higher flow capacities, offering fewer downpipes of smaller diameter. Achieving siphonic action at the design rainfall intensity also requires the inhibition of air intake to facilitate full-bore flow. A specially designed outlet baffle, as Figure 1.2 illustrates, inhibits air ingress when the gutter water depth is sufficiently high. This outlet allows the downpipe to fill quickly. This operational stage is referred to as *'priming'*, and defines the transitional phase from part-full two phase flow to full-bore, single phase flow. There are five water flow phases; these are discussed in Chapter 2.

System benefits have been seen by industry where many large international projects have been installed in structures such as sports stadia, airport terminals, factories and large commercial outlets. However siphonic system failures do occur, and can be catastrophic to the building and its contents, caused by the collapse of vapour cavities and pipe implosion. These occur from incorrect design and the format of the small diameter pipes used and the free surface area at the baffle plate, which leaves siphonic systems susceptible to blockages.

1.3 Climate change effects on siphonic roof drainage systems

Presently roof drainage systems are designed to manage rainfall intensities based on a defined '*return period*' representing one specific storm intensity. As mentioned, conventional systems are generally oversized with excess capacity, while a siphonic system is designed with little to no excess capacity. This is because the design intensity of the rainfall is equated to the known flow conveyance capacity of the siphonic system once all head losses have been calculated, and as such the design capacity is fixed. What is unknown is the frequency with which the design capacity will be exceeded. Design exceedance may result from extreme precipitation, the influence of climate change on detritus accumulation, or whether the secondary system or overflow can accommodate the excess rainfall.

The Meteorological Office (MET office) and the United Kingdom climate change projections (UKCP09) highlight that the United Kingdom is likely to endure wetter winters, drier summers and a higher probability of extreme weather conditions in the future. This presents two problems. Firstly, higher intensity rainfall may lead to system under-capacity and flooding, secondly, higher temperatures and longer dry spells may result in detritus build-up at siphonic outlets, each directly impacting system performance.

Further, the varying nature of rainfall events, the time between events, the predicted change in rainfall intensities, and a possible change in the accumulation of detritus at outlets will all affect system performance. A key component of this research has been to monitor how these factors affect priming and operational performance of the siphonic system from chosen sites.

1.4 Research aim and objectives

The overall aim is to increase knowledge of how local weather parameters can alter the performance of siphonic rainwater drainage systems. The study comprises two parts. The first studies the type and rate of detritus build-up at outlets over time, examining event-related network responses. The second examines the relationship between outlet blockage and system under-capacity.

This research had three objectives:

Objective 1, Investigate on-site detritus build-up at siphonic outlets.

This objective can be divided into three sub-objectives:

1. To monitor and capture detritus accumulation information at selected system sites and predefined siphonic outlets;
2. To establish the rate of build-up, or other accumulation characteristics, for this detritus - within the context of observed rainfall and temperature data recorded using installed weather stations;
3. To establish how the siphonic systems are currently performing.

From records of maintenance schedules for each site, particular gutter outlets were selected for monitoring. Weather-protected web cameras were used to provide continuous images. These images were then interrogated and, for times of interest, analysed and detritus characterised. This allowed an analysis of how weather, location and time of year affect the build-up. Sub-objective two was then addressed by comparing the images and characterisation of detritus build-up with weather station recordings. This allowed mapping detritus build-up with weather conditions. The weather station consisted of a single rain gauge, temperature and relative humidity sensor and a sonic anemometer. Sub-objective three was addressed by the installation of pipework pressure transducers and gutter depth sensors. The pressure transducers allowed for a detailed analysis into system priming, while the depth sensors allowed for the frequency of system failure to be established.

Objective 2, Investigate, through laboratory work, how detritus accumulations affect head loss of siphonic outlets.

Laboratory investigations established how materials typically found at siphonic outlets affect system performance. Two kinds of siphonic outlet were tested with the empirical findings used to enhance the simulation of partial blockage conditions in a numerical model. A detailed examination of blockages could only be undertaken in a laboratory environment where blockage materials and flow extremes can be controlled and accurately monitored. However, to inform this aspect of the research, images captured from site provided an indication of the types of detritus accumulated and the degree to which build-up occurs. Various quantities of leaves, twigs, feathers etc were positioned at the outlets and the response, in terms of gutter depths and system pressures recorded. As a result, a set of loss coefficients has been derived.

Objective 3, Assess, using the numerical simulation model, the performance of a siphonic system, based on data from objectives 1&2.

This objective can be divided into two sub-objectives:

1. Compare simulated system pressures against site-measured system pressures;
2. Investigate and analyse any anomalies, with the aim of identifying potential limitations of findings.

Two geographically-different case study sites were monitored, as mentioned above. Each site yielded data that allowed a comparison between theoretical and measured system pressures and flow-rates. One such system has been fully investigated.

This thesis establishes that weather variables play an important role in the operation of a siphonic rainwater drainage system, where the collection of detritus, influenced by weather, at the siphonic outlet will inhibit the inflow of water to the system causing possible system failure through gutter overtopping.

1.5 Layout of thesis

Chapter 1 has given reasons for this area of research and highlighted the issues that climate change may have on siphonic rainwater systems. Chapter 2 then provides an introduction to the basic concept of siphonic rainwater drainage systems, discussing the history, research undertaken and potential causes of system failure. The hydraulic principles are identified, indicating relationships between roof gutters and the siphonic system.

Industrial and research based simulation techniques used for designing and assessing siphonic rainwater systems are discussed in Chapter 3. This highlights how many industrial models are based on the assumption of instantaneous full-bore flow throughout the system, and how research models have the ability to simulate unsteady flow.

In order to obtain information on the volume and impact of detritus accumulation at siphonic outlets, a monitoring arrangement was installed at two geographically different sites in Scotland. Chapter 4 discusses the monitoring programme and the recording equipment installed that was necessary to understand the way local weather parameters affect detritus accumulation and the effect build-up has on the performance of the system. Further, images also indicated the materials that typically accumulate, and as such, this finding influenced the subsequent laboratory experiments.

Chapter 5 describes the laboratory experiments undertaken to derive outlet loss coefficients for two different baffle types subject to varying outlet blockages. The experimental arrangement and results established are discussed. Derivation of outlet loss coefficients are described in Chapter 6. Formulae for head loss coefficients are expressed with the experimental values of flow velocity and pressure loss. The resulting loss coefficients are then compared with the current form of partial blockage used in a simulation model.

Chapter 7 reports the findings of one siphonic system at the National Records of Scotland building in Edinburgh, where one recorded rainfall event is matched to the system predictions of a numerical simulation model. Finally, a summary of the research undertaken and recommendations given for further work are described in Chapter 8.

Chapter 2
Siphonic roof drainage system - historical perspective and development

2.1 Introduction

This Chapter discusses the literature applicable to siphonic rainwater systems, beginning with industry growth and siphonic rainwater developments. Particular attention is given to areas relevant to this research – namely outlet blockages. The discussion highlights the consequences of outlet blockages on the operational performance of the siphonic system.

2.2 Beginning of the siphonic roof drainage industry

Siphonic roof drainage is a relatively new concept; the theory was first patented in Finland by Consulting Engineer Mr. Olavi Ebeling in 1969 and initially advertised by Swedish based company Aeromotor. The first major scale siphonic system installation was for a turbine factory in Sweden in 1972 (May *et al*, 1996), which saw Mr Ebeling work alongside a Norwegian consulting engineer Dr Per Sommerhein. This collaboration led to the development of a siphonic system, the *'UV system'*, *'unpivirtaus'* meaning full-bore flow (UV Systems, 2011).

From this, the first research conducted on siphonic rainwater systems was undertaken in 1971 by the Finnish State Institute for Technical Research (Bramhall, 2005). In this study they evaluated the siphonic outlet performance compared to traditional outlets. They concluded that outlet dimensions determine maximum capacity.

A Swiss company, Geberit A G, started in 1978, manufactured the UV outlet under a license agreement. Following this, in 1981, the UV system came to the UK with a licensing agreement with a Danish company, Sapolite UK Limited. Also, in 1981 Sapolite installed the first major UK siphonic system in an IKEA, Warrington. Geberit then started to produce its own *'Pluvia'* siphonic system a few years later in 1985 (May *et al*, 1996).

Initially, interest in the UK was limited and slow to develop, until 1986, when a siphonic rainwater system was chosen by Foster Associates and Ove Arup Engineers for London's Stansted Airport (May *et al*, 1996). The success of the building highlighted the advantages the system offers in pipe routing and savings in underground drainage. In 1988, Geberit's *'Pluvia'* system began to be sold and installed by sub-contractors such as JIS, later known as Fullflow Systems Limited. In 1992, Fullflow parted from Geberit whereby Fullflow Systems Limited started to market their own outlets, *'Primaflow'* (Fullflow, 2011). Later in 1992, Sapolite UK Limited were taken over by Sapoflow Limited but continued to market the original UV system design; previously a Sapoflow sub-contractor (May *et al*, 1996). At this time in the UK, the foremost competitors within the siphonic market; Geberit, Sapoflow and Fullflow Systems Limited, had several different variations of outlets available and an estimated 10,000 installations between 1982 and 1996 (May *et al*, 1996).

However, during the 1990s, the UK siphonic market was damaged by some manufacturers practice of installing systems to a general 75mm/hr rainfall intensity (Wearing, 2005). System failures occurred, but unfortunately for the reputation of the siphonic system, the design technique was blamed and not the low design rainfall levels (Wearing, 2005).

Eventually, a number of rainwater outlet companies, ranging across numerous countries, emerged. Countries included: Switzerland (Geberit, 1995), America (Hydromax (Ross group), 1947) Australia (Syfon systems, 1992) and more recently in the United Kingdom (RWP Ltd, 2003). Recent industry literature and company mergers beyond the 1990s to present are currently difficult to obtain.

It follows from this siphonic rainwater industry overview that the potential benefits of siphonic systems were being noticed, and thus starting to advance in the market. However, until 1995 minimal siphonic research had been undertaken, indicating that the system fundamentals were at that time, not fully understood. Clearly research was necessary regarding design, fundamental principles and pipework material. May and Escaraemia (1996) started to investigate the basic principles. Heriot-Watt University, research generally led by Arthur, Swaffield, Wright and Campbell forged ahead and filled many gaps in knowledge.

2.3 Establishment of siphonic rainwater interest in research

In 1995, the Construction Sponsorship Directorate of the UK Department of the Environment (DoE) employed HR Wallingford to undertake a comprehensive study of siphonic systems to inform then current guidelines which had omitted siphonic rainwater systems from its contents (May, 1995). May and Escarameia, at HR Wallingford, investigated and published their findings in SR463 '*Performance of siphonic drainage systems for roof gutters'* in 1996. The investigation involved testing four separate siphonic systems (from three specialist suppliers) and comparing measured flow capacities and pressures to the design predictions given by the specifiers. It is interesting to note that design values supplied by the specialists were accurate when compared with measured values. In two systems, design capacities exceeded measured values by up to 4%. However, as highlighted by the report, the designs were based on available head with no reserve capacity. Tests were also carried out to assess system performances with and without air baffles. They found that depending upon the system and thus the manufacturer, results varied where two systems reduced their flow capacity by 2%, while the other two systems had a 1–2% increase in capacity. The most interesting find, was that in all cases, pipes filled at lower flow rates when the baffle was not in place. Additionally, tests with and without leaf-guards in position were investigated. The results indicated leaf-guards increased water depths in the gutter, but had no effect on pipework capacities. One system did achieve a slightly higher capacity without the guard.

May (1995) also spoke of the theory for conventional systems and compared this to that for siphonic systems. He discussed the main advantages of a siphonic system. The importance of different aspects needed in the evaluation of siphonic performance, i.e. margins of safety, outlet design, negative pressures and the priming of the siphonic system were all discussed.

The first research into siphonic systems at Heriot-Watt University was presented by Arthur *et al* (1998). This study investigated the priming process for siphonic systems with the aim of developing a numerical model capable of simulating contributory phases. Arthur *et al*. described a typical siphonic system as having three components - a siphonic outlet, horizontal pipework and vertical pipework. From the investigation, developments were made to *'SIPHONET'*, a Heriot-Watt University numerical model,

based on the Method of Characteristics, which at this time could simulate the development of the hydraulic jump in the upstream horizontal pipe, development of full-bore flow and system priming.

Sommerhein (1999) discussed the '*Design parameters for roof drainage systems'*. He identified the fundamental differences between gravity and siphonic systems. Also discussed were water depths in gutters, disposable heads, and priming sequences, finishing by suggesting siphonic failures in the UK were based upon poor design and possibly also poor installation. He supported the use of siphonic systems, when designed correctly, for their high levels of building protection and concluded by suggesting siphonic design procedures should be openly explained and presented by authorities, so that standards can be set and performance met.

Gutter water levels and siphonic outlets were discussed further by Bramhall and Saul (1999). They discovered that the outlet position in the gutter greatly effects gutter water levels. They highlighted that careful consideration is required with positioning of the outlets to minimize risk of gutter overtopping.

Tests undertaken by Slater *et al*. (1999) investigated the application of non-dimensional loss coefficients, using 6l/s and 12l/s outlets and the CFD model, '*FLUENT'*. Also, in 1999, Arthur and Swaffield presented work describing the phasing flow-patterns occurring in siphonic systems during priming. Three main principle routes of air entry into a system were noted, i.e. air which existed within the system before the rainfall event began, air which is held within the inflowing rainwater and air which is entrained directly into the system via the outlet. Each condition was fully explained. They also explained and measured the air entrainment through an outlet, and highlighted that under the design conditions for a siphonic system the internal flow conditions are unsteady. The priming and maintenance of siphonic systems was also highlighted and discussed. The numerical model '*SIPHONET'* was discussed in more detail than previously, where the authors presented the priming procedure and the required input data for system simulation. All investigations undertaken at this stage had utilized a single outlet and the authors therefore suggested additional research to assess the operation of a multiple-outlet system. Following Arthur and Swaffield in 1999, Wright *et al*. (2002) reported ongoing investigations and initial results into the operation of a multiple-outlet system tested at Heriot-Watt University. This research enhanced the

existing single-outlet numerical model. The findings concluded that even with more complex hydraulic considerations, multiple-outlet systems operate in much the same manner as single-outlet systems.

May (2003) simplified and discussed the background to the BSEN 12056-3, giving explanations of hydraulic calculations and the principles used for the siphonic system. May gave a more comprehensive view and design advice regarding priming, flow velocities, allowable pressures, balancing and safety factors than that which could be obtained from any previous design guide. This privately-funded research guide described the basic operating principles of siphonic systems. In 2003, Swaffield and Campbell presented information on the performance of multiple-outlet siphonic systems (Swaffield and Campbell, 2003). The simulation model *'SIPHONET2'* was introduced and the background to the model, with the techniques and equations used, explained.

Siphonic monitoring results, recorded by Arthur *et al* (2005) at the National Records building, Edinburgh, identified all but one rainfall intensity rate below the maximum system design capacity, this being 75mm/hr; the one event that eclipsed this was 105mm/hr. Continuous siphonic action occurred for approximately 500 seconds. This single event was estimated to have a 1 in 67 year return period, verifying that the system is capable of running siphonically but not frequently. Arthur *et al* (2005) also identified flow conditions as adequate for self-cleansing purposes, however proposed that regular gutter cleaning was necessary as a large number of birds roost on the roof.

Outlet blockages in siphonic systems were briefly discussed by Wright *et al* in 2006. The researchers revealed, from test rig experiments, pipework pressures were between 50% and 210% lower when one outlet was blocked in a two outlet rig.

Tests undertaken by Arthur and Wright (2007) discussed the importance of the siphonic system components and the priming process involved for each. Experimental work on four different discharge terminations was discussed, as well as the effect each configuration have on the system's ability to prime. They established, in some instances, that a submerged downpipe of 380mm can extend priming times by up to 20seconds or 60% of that of an *'idealised'* system. This increased the gutter depths rapidly, with the development of rapid full-bore flow at the base of the discharge pipe.

However, they also found that a submerged terminal restricted the exit of air from the system.

Recently, Lucke and Beecham (2009) investigated negative pressures within system pipework and the effects of cavitation. This research concluded that negative pressures generated within the downpipes can be regulated by injecting a controlled quantity of air into the pipe.

2.4 Design codes

Many countries have not identified design considerations needed for a fully operational siphonic drainage system within their respective roof drainage byelaw design standards. In 2000, a European Standard EN 12056-3:2000 *'Gravity drainage inside buildings'* was published by the CEN Task Group TC 165/WG21/TG3 as the replacement for BS 6367 *'Code of Practice for Drainage of Roofs and Paved Areas'*. Limited design and installation techniques for siphonic systems were given.

However, the German Engineers Association (VDI, 2000) published a detailed drainage design manual. Published in two languages, German and English, the design guide was the first design manual for siphonic systems to be published. Details were given for design principles, maintenance instructions and calculation procedures.

In 2004, a UK Siphonic Roof Drainage Association was formed, using DTI funding. This association identified the need for a British Standard covering design, principles and installation for roof drainage systems. As such, in 2007 a new British Standard was published, BS8490 *'Guide to siphonic roof drainage systems'*. This standard provides relatively detailed design guidance, while still referring to BSEN 12056-3 for rainfall data. The BS8490 standard has been published based upon the findings from the research undertaken by others.

In 2006, a year before publication of the British Standard for siphonic roof drainage systems, the *'American Society of Plumbing Engineers'* published a comprehensive 3rd draft of a Siphonic Roof Drainage Design code. This provided a detailed review of how to achieve an optimal siphonic system design. Also in America, ASME A112.6.9-2005 was published; a five page document, which limited its recommendations to basic design and calculation methods (ASME, 2005).

2.5. Siphonic rainwater system operation

2.5.1 Hydraulic design principles

For design purposes, flow conditions within the siphonic pipework are assumed as full-bore, following instantaneous priming, thus allowing the application of steady-state hydraulic theory via Bernoulli's equation. This allows the total energy of the fluid to be represented by three elements: firstly, the energy associated with internal pressure, secondly, the kinetic energy and finally the potential energy.

Bernoulli's equation:

$$\left(p_1 + \frac{1}{2}\rho V_1^2 + \rho g z_1\right) - \left(p_2 + \frac{1}{2}\rho V_2^2 + \rho g z_2\right) = \Delta E_{12} \qquad (2.1)$$

For typical hydraulic applications, Equation (2.1) is often rewritten in terms of pressure head *'h'* (h = p/ρg). This is often used as the basis for most industry-based computer simulation models.

$$\left(h_1 + \frac{V_1^2}{2g} + z_1\right) - \left(h_2 + \frac{V_2^2}{2g} + z_2\right) = \Delta H_{12} \qquad (2.2)$$

where, 'ΔH_{12}' is the head loss between points 1 and 2.

It is interesting to note that the Bernoulli equation offers only averaged flow conditions within the siphonic system. As such, it does not offer information regarding turbulent pressure fluctuations within the flow. Further, it does not account for flow curvature on local pressures within fittings. The effects of bends on flow produces a pressure profile across the bend, with the pressure being lower on the inside than on the outside - where the pressure calculated is thought of as the mean pressure along the centerline of the bend (May, 2004).

Note the volumetric flow rate as *'Q'* and the pipe cross-sectional area as *'A'*, Equation (2.2) may then be written as:

$$\left(h_1 + \frac{\alpha_1 Q_1^2}{2g A_1^2} + z_1\right) - \left(h_2 + \frac{\alpha_2 Q_2^2}{2g A_2^2} + z_2\right) = \Delta H_{12} \qquad (2.3)$$

Assuming the siphonic system is full-bore (at its maximum capacity), rewriting Equation (2.3) for the total head loss between an outlet and the point of discharge from the system:

$$H_T = \Delta Z + h_I - h_E - \frac{V_E^2}{2g} \qquad (2.4)$$

It should be noted that the depth above a siphonic outlet (in its gutter) is generally very small in comparison to the height of the building. For this reason it is generally omitted when using the Bernoulli equation for calculating flow conditions within the pipework. If the pressure values in the system are based on, and calculated using, atmospheric pressure as the datum, the value of 'h_I' can be assumed to be atmospheric and equal to zero.

The head loss 'ΔH' can also be separated into two components:

$$\Delta H = \Delta H_p + \Delta H_f \qquad (2.5)$$

where, 'ΔH_p' is the loss due to the hydraulic resistance of the pipe walls and 'ΔH_f' additional losses due to fittings.

2.5.2 Frictional head losses

The Colebrook-White equation is the most commonly used equation for frictional losses as it has been tested and validated by a range of flow conditions and pipe materials (May, 2004). Where any dispute lies for the values of head loss, BSEN 12056-3 states that it shall be used.

For siphonic theory, the Colebrook-White equation for frictional losses in 100% full-bore pipes is written.

$$i_F = \left(\frac{V^2}{8gd_p}\right)\left\{\log_{10}\left[\frac{k_p}{3710d_p} + \frac{1.755v}{\sqrt{(gi_Fd_p^3)}}\right]\right\}^2 \qquad (2.6)$$

i.e. an iterative method of solution is required to establish the head loss gradient, 'i_F'. Depending on the surface of the pipe walls, the effects of irregular bends or joints and

the distance between the roughness parameter of same size pipe joints, k_P, will vary. When pipes are initially installed, the pipes may be very smooth, whereas in time the pipes may become rougher due to ageing and scratching of the material (May, 2004).

The local head loss, 'Δh_L' (m) can be calculated, when a siphonic system is full-bore, from.

$$\Delta H_L = K\frac{V^2}{2g} \tag{2.7}$$

where, '*K*' is a non-dimensional head loss coefficient. Coefficients for bends, junctions, and reducers can be found in Idelchik (1986) and Miller (1990).

2.5.3 Design rainfall intensity

Generally, siphonic roof drainage systems are designed to cope with steady-state pressures associated with a design storm, normally specified as a steady-state rainfall intensity (Arthur and Wright, 2001). Specification of this rainfall intensity depends on three factors; duration of the storm event, '*Return Period*' and geographical location (BS EN12056-3, 2000). The return period indicates the duration between recurrences of a specific event, e.g. a 1 in 30 year event. As such, the system may never operate as designed. If the design threshold is exceeded, the system will fail unless the excess water can be drained elsewhere. The choice of return period should be selected based on the design life of the building, the roof construction and the acceptable level of risk to the structure and its contents (BS 8490, 2007).

Meteorological data is normally presented in the form of '*two minute events*', the two minutes represent a time of concentration, i.e. the time for the roof catchment runoff to reach the outlet. The probability, 'P_r' of exceeding the design rainfall event during the lifetime of the building can be established from:

$$P_r = 1 - \left[1 - \left(\frac{1}{T}\right)\right]^{L_y} \tag{2.8}$$

when, '*T*' is the return period of the statistical rainfall event in years, and 'L_y' the design life of the building in years.

The value of 'P_r' can be 0.0 (assured safety against all storm events) to 1.0 (absolute certainty that the rainfall intensity will be exceeded in a given year). Despite the importance of the determination of rainfall intensity, in practice, some specialists design siphonic systems based on a pre-defined specific rainfall intensity that remains unchanged irrespective of geographical region.

2.5.4 Two-phase flow

Much research has been aimed at highlighting air entrainment in siphonic rainwater systems, where unwanted air can have serious consequences for operation, potentially resulting in system failure (May, 1995, Arthur *et al*, 2005). Water aeration is effectively two-phase flow, where many factors potentially control the air entrainment into a siphonic system (May 1995).

Quantifying air entrainment is difficult. Arthur *et al*. (2005) showed that even under a laboratory experimental arrangement, determining the air entrainment can be complex. In 1979, Wylie and Streeter had initially stated accurate simulation models or two-phase flow models are less likely to be reliable than single phase models.

Two-phase flow energy losses were investigated by Lockhart and Martinelli (1949). They found that two-phase flows had greater energy losses than single mixtures of air or water. This was based on the fact that, with air, the cross-sectional area of the water reduces and results in a loss in friction.

In response to rainfall events below the design intensity, there will be five flow configurations depending upon the rainfall profile (Alves, 1954). A typical rainfall event may develop as the curve in Figure 2.1 indicates. It is interesting to note, a time delay will always be present in siphonic systems, as indicated. This allows for gutters to fill from roof runoff etc, and means the drainage system will follow the intermittent trend line in Figure 2.1. In Figure 2.2, the letters *'a to e'* represent the flow phases the system will pass through, either by priming or unpriming. It has been observed from tests with a 50% water flow capacity at phase 3 that *'bubble flow'* develops, suggesting that a 60% water volume should be considered safe as a lower limit for bubble flow, Johri (1988) (UV systems 1995).

To date Arthur and Swaffield (1999) and Lucke and Beecham (2010) have attempted to control and measure the air in siphonic systems. Arthur and Swaffield (1999) discussed the issues relating to the presence of air in the pipework, as it will change the systems operating pressure, velocity and pipework friction losses.

Two-phase flows were again confirmed as complex by May and Escarameia (1996). They considered the importance of air bubbles in two-phase mixtures whilst traveling from high pressure to low pressure regions. They also considered the choice of system friction factors in initial design calculations, as these will greatly affect system performance.

In 1996, May and Escarameia investigated air concentrations in water flow utilizing a void-fraction meter. They discovered that when a system reached its maximum capacity, the air concentration at the end of the discharge pipe was less than 1%. This 1% was assumed to arise from air bubbles taken from the turbulent inflow from the gutter and air being squeezed from the water in the lower pressure regions.

The behavior of two-phase flow and how it should be considered in the designing of the siphonic system has always been an area of great debate (Öngoren and Materna, 2006). Claims have been made that some designers make allowances for two-phase flow when designing and sizing the systems, May (2004). May discussed how the air water mixture will have a lower density than water. Additionally, May suggested that this is a realistic option and systems should be able to operate in this state, as most storms will be lower than the design storm.

2.5.5 System balancing

The balancing of a siphonic system is critical for efficient operation. Balancing requires runoff to each outlet to match the associated *'branch'* capacity. If this balancing is incorrect, one of two things may occur. Firstly, an outlet with a lower design capacity may either divert rainwater to other outlets or may introduce gutter overtopping. Secondly, outlets demonstrating spare capacity may increase swirl which will entrain excess air that can restrict or interrupt priming and reduce overall capacity (May, 2004 and BS8490, 2007). However, by pipework rerouting or via changes in the design, balancing can still be achieved (Snoad, 2009).

Although every effort should be made to ensure a system is balanced, operational characteristics do allow for a minor degree of imbalance. Subtracting the total head loss along each flow path from the available head defines the outlets residual head. It is recommended by HR Wallingford (May and Escarameia, 1996) and the British Standard 8490:2007 that the maximum residual head difference between outlets should not exceed 1.0m or 10% of the available head.

2.5.6 System priming speed

In order for a siphonic drainage network to fulfill its function, the system must operate as both a two-phase conventional system when the volumetric runoff falls below the design capacity - and as a full-bore system, when conditions for priming are met. With no allowance for water storage within the gutters or pipework (BS8490:2008), when the volumetric runoff rate is exceeded, gutter overtopping or potential water ingress to the building may occur. Transition between the two flow conditions should occur quickly, so noise and vibration are avoided and to prevent a build-up of water in the gutter. It is recommended a siphonic system should prime quickly, within 60seconds (BS8490:2007). A reasonable estimation of the filling time, 'T_F', may be found from:

$$T_F = \frac{1.2V_p}{Q_{in}} \qquad (2.9)$$

when, 'V_p' is the volume of the collector pipe and 'Q_{in}' is the flow rate entering collector pipe during priming.

For a system to prime properly, gutter water depths should steadily increase, submerging the baffle plate gradually. Water flow through the system will increase correspondingly. Pipe pressures at this early stage will be equal, or close to, ambient atmospheric. Water will flow down the vertical tailpipe and into the horizontal collection pipe in a sub-critical state. As the rainfall event develops, and the gutter depth increases, flow velocity will increase in the collection pipe causing supercritical flow conditions to develop and form a hydraulic jump slightly downstream towards the downpipe (Arthur and Swaffield, 2001(a)).

Whilst the sub-critical water depth downstream of the hydraulic jump is less than the diameter of the pipe, the flow in the tailpipe will remain annular. As the flow rate in the

system increases, the sub-critical depth downstream of the jump will increase respectively. At the transitional stage, with increasing flow rate, the water will reach the pipe soffit. The collector pipe then runs full-bore. At this stage, a pocket of air becomes trapped between the hydraulic jump and the upstream end of the collector pipe. When the water reaches the top of the downpipe, this develops into a solid column. Once full, the downpipe will cause pressures upstream to fall also. This de-pressurization creates an increase in water flow into the system, resulting in full-bore flow upstream of the collection pipe. Trapped air in the collection pipe then moves at velocity, and travels through the downpipe causing slight re-pressurization until it discharges from the system. Once the air pocket has been discharged, the system is fully primed (Arthur and Swaffield, 2001(a)).

2.5.7 Sub-atmospheric pressures

Siphonic rainwater systems have been found to fail from sub-atmospheric pressures generated within the pipework, where negative pressures have surpassed the pipe buckling limits. Bowler and Arthur (1999) recognized that frequent siphonic failures were caused by pipe implosion. May *et al* (1996) concurred with this. Bowler and Arthur (1999) stated, at that time, that there were no recognized international design standards for pipework operating under negative pressures. They suggested when considering internal negative pressures generated by the system, pipe elasticity needs consideration.

It is interesting to note that by applying the energy equation for designing siphonic systems, an incorrect design and calculation fault will occur for buildings taller than 15metres. The theoretical pressure, therefore, would be lower than absolute zero pressure (-101.3kPa). May (1995) questioned this, as these negative pressures are not possible because the water flow will break into cavities before the pressure is even reached. Pipe pressure rating concerns were then investigated by May and Escarameia (1996) where they highlighted pipe ratings are supplied for positive pressures, whereas negative pressure information is not always available. May and Escarameia discussed how, under positive pressures, pipes will deform symmetrically, while pipes under negative pressures are subjected to compressive forces that magnify any pipe material deformities that can lead to system failure - suggesting pipe materials and fittings should be positive and negative pressure tested to ensure system integrity.

Other sources, e.g. Arthur *et al*. (2001), Loro (2004), Arthur and Wright, (2007) and design manuals VDI (2000), ASPE (2006) and BS8490 (2007) offer guidance to limiting internal pipe pressures.

2.5.8 Cavitation

The physical limit for negative pressure within a siphonic system is the vapour pressure of water. When the local pressure in water falls below the vaporization point, bubbles will develop and cavitation can occur. Problems arise when the cavities travel downstream and meet areas of high pressures, such as pipe bends and junctions. May (1995) and ASPE (2006) both agree that cavitation occurs more at bends and sudden transition of pipe sizes than at any other point within the system. BS8490: 2007 recommends against the use of a 90º elbow at the top of the discharge pipe as it is not suitable due to the risk of cavitation. Two 45º bends should instead be installed. Lucke and Beecham (2009) found that substituting the 90º bend at the top of the discharge pipe significantly reduced any cavitation, but also increased test rig flow capacity by ~18%.

Additionally, the creation of vapor bubbles and potential implosion of bubbles may result in pipe vibration and noise, which can impact the integrity of the piping, hangers and joints (ASPE, 2006).

The potential for cavitation in a system may be determined from calculating the cavitation index, 'σ' :

$$\sigma = \frac{2_g\,(h - h_{vp})}{V^2} \qquad (2.10)$$

when, 'h' is the mean static pressure head and 'h_{vp}' is the vapor pressure of the water (m). If the cavitation index value, 'σ', in Equation (2.10) is less than the limiting values for the fittings and the pipework that have been used within the system, cavitation will begin (BS8490: 2007). If the hydraulic equation gives a smaller value than 1.5, the danger is flow will break the cavitation and the designed system capacity will not be achieved (VDI, 2000). BS8490 also highlights a cavitation index of less than σ = 1.5 to 2.0, depending on pipe fittings, will increase the intensity of damage caused by cavitation.

Considering these factors, it was suggested by May (2004) that a typical cavitation value of $\sigma_1 = 1.5$ is appropriate, where serious effects occurs at 20% less than this. Substituting this value into Equation (2.10) gives the following relationship between flow velocity and the minimum allowable value of pressure head, 'h_{min}' (relative to vacuum), in a siphonic system (May, 2004):

$$h_{min} = 0.061V2 + h_{vp} \quad (2.11)$$

when, 'h' and 'h_{vp}' is the head of water (m) and 'V' is the mean velocity (m/s).

2.6 Supplying the rainwater system

2.6.1 General

Even in the original BRS 1958 digest 116 *'Roof drainage'*, choice of appropriate rainfall intensity was recognized as crucial. Bramhall (2005) highlighted that a misinterpretation of the suggestions given in the digest could introduce error in the choice of design rainfall event.

An important statement was also presented, and relevant to this research, i.e. '*to some extent also the duration of rainfall peaks is important: if the gutter is almost empty to start with, a sharp peak lasting only a minute or two might be accommodated…'* it was noted that peak intensities occur more in summer with lower winds speeds than in the winter months, allowing the rainfall to drop vertically and reduce the loads onto pitched roofs.

The more recent design guide CP 308:1974 was amended and developed as the British Standard Code of Practice for Drainage of Roofs and Paved Areas (BS6367: 1983). New information was added on geographical locations, improved gutter capacity equations and resistance factors for extensive gutter lengths. The guide, however, could be seen as being flawed - the meteorological data was taken from a 1975 report by the Natural Environment Council (Bramhall, 2005). At the start of the design standard, rainfall intensities with a magnitude of 75mm/hr were regarded as being satisfactory. No reference to the use or guidance towards siphonic drainage system was given at this time within a British Standard or Building Research Digest. Then in 1988 the Institute of Plumbers published a design guide that was based and referenced towards the procedures given in BS6367.

2.6.2 Siphonic rainwater system gutters

May and Escarameia (1996) identified that gutter sizing procedures in BS6367:1983 could be used for gutters feeding siphonic drainage systems. They also discovered gutter water levels are typically higher when outlets have leaf-guards in position, and that guards have little effect on system capacity. In 1999, Bramhall and Saul compared measured gutter depths taken from their siphonic rig to the calculated values given in BS6367:1983. They established that the calculated values were similar to these measured, thus indicating the accuracy of the guidelines.

Although, siphonic outlet baffles come in many designs, they may be categorized as either a plate-type or an inverted cup-type with perforated holes. Regardless of design and geometry, the principles are the same; where the baffle is there to restrict and inhibit the entrainment of air into the connecting tailpipe feeding the siphonic system. In 1996, May and Escarameia found that the baffle design of numerous outlets had little effect on system capacity.

In 1998, Bramhall and Saul determined that outlet positions within the gutter affect performance. They determined that 45mm water depth coverage was necessary for the system to reach maximum capacity for their test. They also analyzed the suction effect in the pipe on gutter water depths. Outlet tests investigated by Wright *et al*. (2002) required a 90mm and 130mm water depth, for a complete atmospheric seal in the system, while allowing the system to run siphonically at 5.9l/s and 7.8l/s respectively. Further, May (2004) recommended a generalized 10% safety factor to be included to allow for an increased water depth were it is thought there is the possibility of debris accumulating at the outlets.

2.7 Siphonic outlet

2.7.1 Classes of siphonic outlets

Many manufacturers currently exist within the siphonic rainwater market, each providing different outlet designs. These may be broadly categorized as incorporating flat baffles or inverted cups in various materials and with the option of square or round form. However, current outlet designs are fundamentally similar, each consisting of a bowl or sump, an air baffle and a leaf-guard. The outlet bowl depth will typically vary where shallow bowls require less space requirements below the roof or gutter. May and

Escarameia (1996) believe that a deeper bowl prevents the entrainment of air into the pipework, while suggesting performance also relies on air baffle design.

Generally, there are two baffle designs. These have been illustrated in Figure 2.3 (a & b). The first type, and commonly found in the UK, is a solid flat plate elevated from the gutter sole to allow rainwater to enter the sump through a circumferential inlet between the plate and the bowl sides. The inlet also prevents water swirl above the plate, which otherwise causes air entrainment.

The second baffle type, an inverted perforated cup, sits directly above the centre line of the sump and the open end of the tailpipe. May and Escarameia (1996) viewed this baffle design as having two distinct functions. Firstly, the baffle increases the water depth within the bowl at low flow rates; ultimately restricting air entrainment. Secondly, the design disrupts the likelihood of vortices forming, thus restricting water reciprocating within the bowl.

Studies on plate-type baffles are rare but have shown that sudden transitions from two-phase part-full flow to full-bore flow and vice versa can occur, while the inverted perforated cup allows a gradual transition through the development of full-bore flow (May, 1996). This also implies that as gutter levels decrease this baffle will allow for gradual entrainment of air back into the system, thereby reducing pipework pressure fluctuations

2.7.2 Outlet blockages cause and effect

It is interesting to note that experiments undertaken by Wright *et al* (2006) found, on their two outlet siphonic rig at Heriot-Watt University, when one outlet was blocked prior to the simulation of a rainfall event, the system acted as a single outlet system. System flows were reduced and pipework pressures significantly more negative than when the system was operating at its fully primed capacity. They also measured system capacity as being lower with one outlet blocked, but the capacity of the open outlet was higher than when the rig had both outlets open. The data also correlated with theory that suggests system pressures would be lower when an outlet is blocked. This means that should a system already operate at low pressures and a blockage occurs, system cavitation or pipe implosion could result (Arthur *et al*, 2007).

Outlet blockages are potentially the main cause of system failures (Arthur *et al*. 2005 and May *et al*, 1996). Investigations by May (1996) into the efficiency of leaf-guards for preventing debris entering the system indicated that debris collected around the perimeter. As a consequence, gutter water levels did rise. One of the key benefits siphonic systems offer, depending on gutter design, is flow redistribution between outlets draining the same gutter if one does become blocked. UV systems (1996) recommends, and encourages, siphonic outlets be approximately 0.5metres from vertical walls and not less than 1.5metres from intersecting walls - thus reducing the outlets chances of being covered in detritus that the wind blows into corners of roofs. During the initial installation phases, some specialists, such as Geberit, write into their contract clauses that the installer will be responsible for preventing the entry of detritus into pipework and outlets. Their contracts can also state that the leaf-guard should be fitted as soon as possible during the installation phase (Geberit, 2010).

Periodic maintenance, cleaning and routine inspections - in line with general good practice - should be carried out to prevent outlets from clogging (Geberit, 2010). Detritus blockages generally consist of biological growth, wind blown matter, possible construction waste from installation and materials dropped by birds. If an outlet does become blocked and the system capacity decreases, gutter overtopping is also possible. Bowler and Arthur (1999) suggests outlets should be inspected at least 6 times a year, while BS8490:2007 suggests 4 times per year, for the first year, after which a programme of maintenance should be undertaken with the final decisions on maintenance being the responsibility of the owner.

2.8 In service performance

A large number of siphonic systems have been installed within the UK, where the majority of installations appear to operate satisfactorily, but while some have not. May (1996) defined a system failure as an incident where a building has suffered from internal flooding from the siphonic system due to gutter overtopping, pipe collapse, leaks at connections or a lack of water tightness between the outlet and the gutter of the roof layer.

Arthur and Swaffield (2000) presented findings of site monitoring of - the National Archives of Scotland Document Repository building in Edinburgh. At the time, the monitoring arrangement was simplistic and novel, but results were limited. The

recording period of 40 days had 12 rainfall events where three caused system de-pressurization. In general, results indicated that the system, at that stage, was working well under the design rainfall intensity. Four years before, Escarameia and Swaffield (1999) also began monitoring roof gutter performances from two different sites. Swaffield, in addition, produced an unsteady flow program *'GUTTER'* which was used to simulate chosen recorded storms. They established that wind direction at the sites had little effect on the percentage runoff, that the monitoring arrangement was suitable for the task, that the systems monitored were adequate for the needs and that the numerical simulations compared well with site measurements.

2.9 Summary

This Chapter has discussed literature from the early developments of siphonic system concepts through to current research. Additionally, shortfalls in siphonic rainwater research have been highlighted. The important hydraulic research that has been undertaken by others has been identified, indicating the relationship between the roof gutters and the siphonic system. Further, relationships have been highlighted based on empirical investigations, and site monitoring and theoretical studies.

Chapter 3
Rainwater modelling techniques

3.1 Introduction

This Chapter discusses theoretical and fundamental mathematics used in computer-based siphonic rainwater simulation techniques established in both industry and academia. Topics covered include: steady state hydraulics; unsteady flow solutions; and associated boundary conditions. As discussed in Chapter 2, a rainwater system, due to the natural variation in precipitation, exhibits unsteady flow characteristics. There is therefore a prerequisite for an accurate simulation model to assess system performance.

3.2 Simulation techniques

3.2.1 Industry models

In the UK, the majority of industry-based siphonic simulation software packages assume the system flows 100% full. This assumption allows fundamental hydraulic principles to be used. This allows use of Bernoulli's equation to determine relationships between pressure, velocity and energy loss. Interestingly, May (1996) did find only one industry-based package which allowed for air-water mixtures of up to 40% air content.

Using Bernoulli's Equation (3.1) deems system design capacity to be directly dependent on inflow density, where a sudden change in air quantity will cause a sudden pressure change; and as a result, system capacity will be reduced. Also, as the models use steady state theory, they are incapable of predicting system priming and hence, the full range of system performance characteristics.

$$\left(H + \frac{Q^2}{2gA^2} + z\right)_{Point\ X} - \left(H + \frac{Q^2}{2gA^2} + z\right)_{Point\ Y} = \Delta H_{X,Y} = \frac{kv^2}{2g} \qquad (3.1)$$

The Colebrook-White relationship in Equation (3.2) is typically used in industry to calculate energy losses. Pipe wall frictional losses are calculated with an assumed pipe roughness 'k_s'. Losses at bends and other fittings can be established using Equation (3.3). Although these equations are well recognised they should be used with caution,

as they will perform poorly in situations where water contains air (Idelchik, 1987). This disadvantage may lead to installed systems creating noise and vibration.

$$\frac{1}{\sqrt{2gDi}} = -\frac{2.0A}{Q}\log_{10}\left(\frac{k_S}{3.71D} + \frac{2.51v}{D\sqrt{2gDi}}\right) \quad (3.2)$$

$$\Delta H_F = \frac{KQ^2}{2gA^2} \quad (3.3)$$

May (1996) also found other plausible causes of design inaccuracies, where one package was able to calculate system hydraulics and provide a detailed output summary, but where the user was required to interpret and where necessary, modify the results. Another program adapted the design automatically, whilst also producing costs and bills of quantities, however this program offered less information on flow conditions. Some manufacturers programs are based only on one type of outlet and pipe, whilst other programs allow for different loss coefficients (May, 1996). Another did not consider individual fitting losses, but compensated by adjusting the 'k_s' value for pipe wall frictional losses.

Beyond that presented above, it is difficult to collect information on operating characteristics of manufacturers' simulation models. The use of steady-state techniques limits application, and therefore means that the impact of varying rainfall events on system performance can only be addressed via models capable of simulating unsteady flow conditions.

The following discusses more sophisticated techniques of simulating varying and unsteady flow via research developed models.

3.2.2 Research driven simulation models

Several research driven numerical models now exist at Heriot-Watt University. The first was '*GUTTER*', then '*SIPHONET*', '*SIPHONET 2*' and now, '*ROOFNET*', all of which can simulate elements of a roof drainage system.

ROOFNET allows the input of data which describes the aspects of an installation. This includes the details of the rainfall event, the roof size, area to be drained and details of the supporting gutters along with pipework design and size. A fundamental kinematic

wave approach is used to model the flow of rainfall from the roof surface to the gutter. And based on the Method of Characteristics technique and the equations of one-dimensional flow, the model simulates gutter runoff to the outlet, where it then enters the siphonic system (Arthur & Wright(a), 2005). The siphonic system is also modelled based on the Method of Characteristics technique. Data outputs include depths, velocities and flow rates.

A more dynamic model does exist in the form of '*SIPHONET2'* which can simulate the priming of the siphonic system in detail, however numerical stability problems and longer computational simulation run times restrict model applicability (Wright *et al*, 2006).

3.2.3 Simulation model fundamentals

Addressing time dependency of rainfall events on free surface flow conditions, and dealing with consequences of climate change, with increased rainfall intensities and durations, requires simulation software that is capable of modelling unsteady flows. The St. Venant equations defined in this Section describe both full-bore and partially filled pipe flow conditions.

Simulating the movement of hydraulic jumps is a necessary element in a system, and as such, the MacCormack solution technique, discussed in Section 3.4.2, is deemed most suitable to calculate initial free surface flow conditions. The MacCormack technique relies on the hyperbolic nature of the governing equations. This technique is a non-centred, two-step finite-difference scheme that is second-order accurate in time and space. The St. Venant equations of continuity and momentum are also used to model the initial pressurised flow, with the necessary introduction of the Preissmann slot technique. However, as the vertical downpipe begins to fill and the system starts to depressurise the MacCormack technique is replaced by the Method of Characteristics technique for the governing equations of full-bore flow (Wright *et al*, 2006).

Either solution technique requires boundary conditions for the model to proceed. These are typically derived from a relationship between pressure and flow rate.

3.3 The St. Venant equations

All methods devised to analyse unsteady flow start with the continuity and momentum equations. The continuity and momentum equations are together called the St.Venant equations, and were first used by the French scientist in the 18th Century. A variety of numerical techniques are available to solve these equations, some specific to certain conditions and circumstances. Most require an amount of computational power.

3.3.1 Unsteady free surface flow

With varying flow depths and system inflows, each resulting from the temporal variation of the precipitation event, such conditions require computational methods to resolve the St. Venant equations.

The continuity and momentum equations applicable to varied unsteady flow are:

$$\frac{\partial u}{\partial x} + \frac{1}{A}\left(\frac{\partial A}{\partial t} + u\frac{\partial A}{\partial x}\right) - \frac{q}{A} = 0 \qquad (3.4)$$

and

$$g\frac{\partial h}{\partial x} + \left(\frac{\partial u}{\partial t} + u\frac{\partial u}{\partial t}\right) + g(S - S_0) + \frac{uq}{A} = 0 \qquad (3.5)$$

For the momentum equation, the friction slope *'S'* is typically defined by the Chezy or Manning equations for open channels, while it is normal practice to use the more accurate Colebrook-White formula for channels or partially filled pipes when flow depths or diameter is less than a metre long. The frictional slope is:

$$S = \frac{n^2 u_P |u_P|}{h_P^{4/3}} \qquad (3.6)$$

When the channel is wide the hydraulic mean depth, *'A/P'*, tends to depth *'h'*. Substitution into the momentum equation generates an expression:

$$g\frac{h_S - h_R}{2\Delta x} + \frac{u_P - u_C}{\Delta t} + u_C\frac{u_S - u_R}{2\Delta x} + g\left(\frac{n^2 u_P |u_P|}{h_P^{4/3}} - S_0\right) = 0 \qquad (3.7)$$

The equations of continuity and momentum can be solved by the Method of Characteristics (a technique described in Section 3.4.1), where an *'x-t'* grid is used. The stability of numerical modelling is paramount, especially in finite difference schemes. For the Method of Characteristics, stability is established via the Courant criterion. This links the internodel time and step sizes to flow velocity and wave speed:

$$\Delta t \leq \frac{\Delta x}{(u+c)_{max}} \tag{3.8}$$

Using the *'max'* means that the attenuation of a wave within a pipe or channel will give values of the denominator in the Courant criterion that will vary at any one time along the length of the flow.

3.3.2 Simplification of the transient equations

It should be remembered that equations presented here are set with no restrictions upon the fluid type (beyond homogeneous and Newtonian nature). This means that the equations can be applied to liquid or gas flows and to both full-bore and free surface flows. For the analysis of unsteady flow, a reduced version of the momentum and continuity equations are:

Equation of momentum

In velocity head terms:

$$L_1 = V\frac{\partial V}{\partial x} + \frac{\partial V}{\partial t} + g\frac{\partial H}{\partial x} + \frac{fV|V|}{2m} = 0 \tag{3.9}$$

or

in velocity pressure terms:

$$L_1 = V\frac{\partial V}{\partial x} + \frac{\partial V}{\partial t} + \frac{1}{\rho}\frac{\partial p}{\partial x} - g\sin\alpha + \frac{fV|V|}{2m} = 0 \tag{3.10}$$

Equation of continuity

In velocity head terms:

$$L_2 = \rho c^2 \frac{\partial V}{\partial x} + V\rho g\left[\frac{\partial H}{\partial x} + \sin\alpha\right] + \rho g \frac{\partial H}{\partial t} = 0 \qquad (3.11)$$

or

in velocity pressure terms:

$$L_2 = \rho c^2 \frac{\partial V}{\partial x} + V\frac{\partial p}{\partial x} + \frac{\partial p}{\partial t} = 0 \qquad (3.12)$$

These are a pair of quasi linear hyperbolic partial differential equations, and as such are not directly solvable. The Method of Characteristics allows these equations to be transformed into a pair of total differential equations that are suitable for solution by finite difference methods (Swaffield and Boldy, 1993).

3.4 Historical development of the Method of Characteristics

A mathematical method in which unsteady flow could be analysed was addressed in 1750 by French mathematicians who established the now well known equations of continuity and momentum, referred to as the St. Venant equations. The term *'Method of Characteristics'* was first used by Monge in 1789, and used graphical methods to solve the St. Venant equations (McDougall, 1995). This approach was particularly suited to free surface flows and open channel fluid flow, however, although the friction factor had by this stage been introduced, the approach offered graphical errors and was laborious by nature of the process.

The Method of Characteristics solution has been available as a mathematical technique since the 1850s, when Riemann developed a numerical technique by which the St. Venant equations could be transformed into a pair of total differential equations and solved by finite difference techniques. Massau, in 1900, utilised this method to analyse open channel flow, followed much later by Lamoen, in 1947, who used this technique in the analysis of pressure transients.

The Method of Characteristics technique was little used, until the 1960s. Following the presentation of many papers discussing the application of the Method of Characteristics, with finite difference techniques, especially that by Mary Lister (1960), this approach was established as the accepted technique for numerical modelling of unsteady fluid flow where it found wide application, not only in the study of channel flows, but also in supersonic airflows and general fluid mechanics applications, particularly waterhammer. In the early 1970s, this approach was widely accepted in Europe by Fox (1968), Evanelisti (1969) and Swaffield (1970). The development of computing technology in the 1970s and 1980s enhanced the use and applicability of this technique and allowed the development of large and complex network models (Fox, 1989, Jack, 1997).

3.4.1 The Method of Characteristics

The St.Venant equations are derived from the equations for momentum and continuity, and may be shown as a pair of quasi–linear hyperbolic partial differential equations that can be transformed into a pair of total derivative equations solve by a finite difference scheme (Swaffield and Boldy, 1993, Fox, 1989).

Once the total derivative equations are linked to finite difference techniques, the equations may be suitably expressed such that relationships cast in terms of velocity and wave propagation speed and set against time and distance variables may be combined with the definition of boundary conditions to allow the prediction of system pressure and velocity variables. This technique, is illustrated in Figure 3.1. It shows a typical grid representative of the scheme used for the calculation of the propagation of pressure transients throughout a pipe. Note that this figure represents both time, in the Y-axis, and distance in the X-axis.

The condition at point *'P'* in the grid is based on the conditions upstream and downstream, one time step in the past, and requires the definition of the characteristic slopes as a foundation for the calculation. The straight lines shown in Figure 3.1 between *'A'* and *'P'* and *'B'* and *'P'* should be curved, however, it has been shown that because of the short time steps, a straight line approximation may be used as it introduces little error into the calculation. From the grid in Figure 3.1, *'R'* and *'S'* represent points where the condition is known by interpolation where *P* is the condition to be calculated. The characteristic lines between *'R'* and *'P'* and *'S'* and *'P'* represent

equations used to calculate the condition at point *'P'*. The line of communication formed by the characteristic slopes allows information regarding velocity and wave and hence pressure, to be propagated throughout the system (Swaffield and Boldy, 1993). This technique however, has been found to give anomalies when used to represent the free surface flow conditions found in the collector pipe of siphonic systems, and as such been used for full-bore flow and gutter conditions only. A more suitably-based scheme, the MacCormack technique, has produced a more reliable solution for system modelling in these pipework sections.

3.4.2 The MacCormack technique

The second order nature of the MacCormack (1971) technique generates oscillations in the area of the hydraulic jump which effectively have no real meaning and as such are numerical anomalies. A commonly-used method of resolving this is to add an artificial viscosity to the solution (Jameson *et al*, 1981). It is interesting to note that the St. Venant equations derived for free surface flows when utilized with the Preissmann slot technique means that the equations can essentially be applied to short periods of pressurisation of full-bore.

The solution is calculated via a two-step predictor-corrector process. Illustrated in Figure 3.2, and described firstly by expressing the governing Equation (3.9) and (3.11) in vector form:

$$\frac{\partial U}{\partial t} + \frac{\partial F}{\partial x} = S \tag{3.13}$$

where

$$U = \begin{bmatrix} A \\ Q \end{bmatrix}; \quad F = \begin{bmatrix} Q \\ \frac{Q^2}{A} + gI_1 \end{bmatrix}; \quad S = \begin{bmatrix} 0 \\ gA(S_0 - S_f) \end{bmatrix} \tag{3.14}$$

By alternating the forward and backward expressions in the predictor and corrector steps, the solution allows for the wave travelling through the system in any direction to be expressed.

Using the finite difference Equations (3.15) to (3.17), a general expression (3.18) can be established. At this stage the variable *'ε'* can be set to 0 for a forward representation or 1 for a backward difference.

Forward difference:

$$y'(x_0) = \frac{y(x_0+\Delta x)-y(x_0)}{\Delta x} + Neglected\ terms \tag{3.15}$$

Backward difference:

$$y'(x_0) = -\frac{y(x_0-\Delta x)-y(x_0)}{\Delta x} + Neglected\ terms \tag{3.16}$$

The rate of change of the variable with time will then be:

$$\frac{dy}{dt} = \frac{y(x_{o,t+\Delta t})-y(x_{0,t})}{\Delta t} \tag{3.17}$$

and

$$U_P^1 = U_c - \frac{\Delta t}{\Delta x}[(1-\varepsilon)F_s - (1-2\varepsilon)F_c - \varepsilon F_R] + \Delta t H_c \tag{3.18}$$

Equation 3.18 can also be used to find *'h'* and *'Q'* at a node in time *'t+ Δt'*. The resulting values are termed as predictor values at each node and are to be used to establish the predictor values of *'U'*, *'F'*, *'H'* to be used with the St Venant equations. This process is repeated for all nodes along the full distance.

After establishing all the predictor values, they can then be used in the corrector step. The values of *'h'* and *'Q'* once again can be determined for nodes *'2'* to *'N'* by introducing the predictor values into the finite difference expressions (3.15), (3.10) and (3.17) to obtain a general numerical expression.

$$U_P = 0.5(U_C + U_P^1) - \frac{\Delta t}{2\Delta x}[\varepsilon F_S^1 + (1-2\varepsilon)F_P^1 + (\varepsilon-1)F_R^1] + 0.5\Delta t H_P^1 \tag{3.19}$$

Once again the values of *'ε'* can be set to *'0'*, for a forward representation of the spatial derivatives or as 1 for a backward differences. Note that mean values of *'U'* and

'U1','F' and *'F1'* and *'H1'* can be used. From Figure 3.2, it is clear that this technique requires a boundary equation once it has reached its limited number of time steps. Boundary conditions are discussed in Section 3.5

3.4.3 Modelling system priming

Modelling a siphonic system at the transitional stage to full-bore flow in the horizontal pipework may be achieved using Equations (3.20) to (3.23) (and as illustrated in Figure 3.3). This procedure requires the flow-rate at which full-bore flow develops, the location in the pipe where this begins, and the quantity of air upstream of the hydraulic jump.

Depth immediately downstream of first bend is calculated by:

$$H_g = \frac{Q^2}{2_g A^2} - \frac{Q^2}{2_g A_c^2} \tag{3.20}$$

calculation of the upstream depth is expressed by:

$$f(H) = 1 - \frac{Q}{CA_n\sqrt{R_n S_0}} = 0 \tag{3.21}$$

and

$$\rho A_1 \left(g\overline{H}_1 + \frac{Q^2}{A_1^2}\right) = \rho A_2 \left(g\overline{H}_2 + \frac{Q^2}{A_2^2}\right) \tag{3.22}$$

The location of the hydraulic jump within the horizontal pipe can be calculated from:

$$\Delta x H_e - H_j = \int_{H_e}^{H_j} \frac{1 - Q^2 T/gA^3}{S_o - Q^2/A^2 RG^2} dH \tag{3.23}$$

These hydraulic expressions can now be represented using the quasi-linear hyperbolic partial differential equations expressed in terms of two variables–discharge and pressure head. These can then be solved using the Method of Characteristics technique.

3.4.4 Modelling system depressurisation

As the siphonic system depressurises and the downpipe starts to fill, the Method of Characteristics solution technique of the governing equations is again suitable. The technique is illustrated in Figure 3.4 and can be used by manipulating the governing Equations (3.4) and (3.5) to give two total derivative equations.

The C^-characteristics

$$\frac{dV}{dt} + \frac{g}{c}\frac{dH}{dt} + \frac{g}{c}V \sin S_0 + \frac{f}{2m} = 0 \qquad \text{when} \quad \frac{dx}{dt} = V - c, \tag{3.24}$$

and

C^+ characteristic

$$\frac{dV}{dt} - \frac{g}{c} - \frac{dH}{dt} - \frac{g}{c}V \sin S_0 + \frac{f}{2m} = 0 \quad \text{when} \quad \frac{dx}{dt} = V + c. \tag{3.25}$$

Equations (3.24) and (3.25) then form the basis for a finite difference solution. This gives two expressions which can be solved simultaneously for *'V'* and *'H'*. Referring to points *'R'*, *'S'* and *'P'* in Figure 3.4, the expressions will be:

$$V_P = V_R - \left(\frac{g}{C_R}\right)(H_P - H_R) - g\left(S_{f_R} - S_0\right)\Delta t, \tag{3.26}$$

and

$$V_P = V_s + \left(\frac{g}{C_S}\right)(H_P - H_S) - g\left(S_{f_S} - S_0\right)\Delta t. \tag{3.27}$$

3.5 System boundary conditions

Either solution technique (the Method of Characteristics or the MacCormack solution) requires definitions of the condition at system boundaries. The technique is illustrated in Figure 3.5. Boundaries which make up a siphonic system within free surface flow and full-bore flow are outlined below:

3.5.1 Free surface flow boundary conditions

System entry

The available C^-characteristic, in subcritical flow, can be solved with a weir expression relating inflow to gutter water depth. A volumetric balance of roof gutter inflow and the gutter outflow during the proceeding time step results in the gutter depth. Alternatively, if at system entry supercritical flow conditions form, no characteristics are available, and necessary to assume normal flow (Wright *et al*, 2006).

Two pipe junction

This covers 90^o bends and changes in pipe diameter. For pipe connections, these may be treated as a single pipe length, with the condition determined by the upstream pipe characteristic of C^+ and the downstream C^-characteristic. This ensures the smooth progress of hydraulic jumps upstream (Wright *et al*, 2006).

T-piece pipe junction

Flow at this boundary will always be subcritical. Three characteristic equations are available and are solved with the junction continuity equation with an empirical expression. This expression relates junction depth to through flow and diameter of the pipe downstream (Wright *et al*, 2006).

Horizontal to vertical pipework connection

The flow from the discharge end of the last horizontal pipe will remain as free surface. For subcritical flow, the available C^+ characteristic can be solved with the critical depth equation, whilst the supercritical conditions can be calculated using the two available characteristics (Wright *et al*, 2006).

System exit

As the flow conditions within the discharge downpipe will be annular, the system exit can be determined using simple annular flow, where no boundary condition is required (Wright *et al*, 2006).

3.5.2 Full-bore flow boundary conditions

System entry

The available C^- characteristic can be solved with expressions relating gutter depth, air entrainment content in the inflow, inlet section losses and the standing hydrostatic head at the base of the entry section (Wright *et al*, 2006).

Blocked system entry

The boundary condition is similar as the unblocked condition previously described, where a blocked outlet now requires a percentage blockage of an open outlet (Wright *et al*, 2006). This is further described in Chapter 7.

Two pipe junction

This relates to either 90° bends or pipe diameter changes. An expression which relates a junction head loss to junction flow will solve the upstream characteristic available, C^+, and the downstream C^- characteristic (Wright *et al*, 2006).

T-piece pipe junction

The upstream pipes offer two available C^+ characteristics, and a downstream C^- characteristic. These can be solved with an expression of junction head loss to junction through flow (Wright *et al*, 2006).

Horizontal to vertical pipework connection

The exit of the last horizontal pipe (C^+ characteristic) will be solved with an C^-available at the downpipe entry (Wright *et al*, 2006).

System exit

The system exit which has a final C^+ characteristic is solved by an expression of head loss to water flow (Wright *et al*, 2006).

3.6 Simulation model

Presently ROOFNET lacks suitable outlet loss coefficients to simulate partial blockages due to detritus accumulation. The siphonic outlet terms used are:

Open outlet

$$\frac{K \times V \times V}{2 \times g} \tag{3.28}$$

Partial blockage

$$\frac{(K+\%) \times V \times V}{2 \times g} \tag{3.29}$$

where the *'%'* is a percentage of the open outlet due to a blockage. An objective of this research is to empirically derive outlet loss coefficients and to define *'K'*.

3.7 Summary

This Chapter has discussed industrial and research based simulation techniques used for designing and assessing siphonic rainwater systems. It has highlight how many industry models are based on the assumption of instantaneous full-bore flow throughout the system and how research models improve upon this by having the capability to also simulate unsteady flow through the rainwater system. The history and development of the Method of Characteristics and the MacCormack technique has been detailed. This Chapter has also provided a background to the boundary equations with a particular focus onto the outlet.

Chapter 4

Siphonic rainwater drainage site investigations

4.1 Introduction

This Chapter presents the methodological approach and findings of an 18-month study of detritus accumulation at two siphonic roof drainage sites in Scotland. The apparatus and recording software set-up is explained, and findings (that are based on an analysis of digital images and weather station data) are discussed. The study also examines corresponding pressure and gutter depth data recorded during periods of significant rainfall.

4.2 Purpose of site monitoring

The on-site monitoring had three aims. Firstly, to determine detritus materials and quantities typically found at siphonic outlets, and how these accumulations are affected by different environmental parameters. The second, to investigate the effect of outlet accumulation on roof drainage performance, through the monitoring of roof gutters and system pipework. And the third, to inform laboratory testing discussed in Chapter 5.

A suitable methodology to achieve the three aims was established, where an automated site monitoring arrangement recording an operational siphonic rainwater system and weather parameters in two geographically different locations.

4.3 Sites monitored

4.3.1 Site selection criteria

Site selection was considered from two aspects; a technical and practical requirement. Site criteria requirements essentially were:

i. geographical location;

ii. typical weather conditions;

iii. siphonic system size;

iv. access to the system.

Following careful inspection to assess site conditions, two locations were chosen. One site was located in Edinburgh and a second in Glasgow. These cities are on the opposing coasts of Scotland, east and west respectively, and are ideally located to examine different weather parameters and the effects on outlet accumulation. This study has restricted operational monitoring to two siphonic sites, as these offer an array of environmental variables required for the research.

4.3.2 Description of sites

The locations monitored were: site 1, the National Records of Scotland Document Repository building located in a semi-urban environment in Edinburgh and site 2, Glasgow Rangers Football Club Stadium *'Ibrox'* situated in central Glasgow.

4.3.3 Site 1-National Records of Scotland

Thomas Thomson House, built in 1994, and generally known as the National Records of Scotland Document Repository (NRS), is owned and maintained by the Scottish Government and is located approximately three miles from Edinburgh City centre. The layout of the site, and positioning of the building, is shown in Figure 4.1(a). It can be seen that the site is surrounded by grassed areas to the west and south, with car parks and access roads close to the structure. Within the grassed areas there are a scattering of approximately 30 trees, the closest being five meters from the building. There are no structures directly adjacent to the building to shelter the site. It is also typical to see a large number of birds roosting on the building. The building comprises two roofs in a *'T'* shape layout. The roof selected, see Figure 4.1(a), for this monitoring study, is approximately 2094m^2 of polished aluminium, and is drained by five independent siphonic systems via box gutters.

To give a detailed representation of detritus accumulation, two different systems were monitored. System 1, see Figure 4.1(b) is a two outlet plate-type baffle system on the west side of the roof serving an area of 607m^2 with a design capacity of 75mm/hr. This system was chosen as the index outlet (outlet furthest from discharge pipe) has a history

of blocking and water pooling in the gutter, while the primary outlet (outlet closest to discharge pipe) has not.

A second system was monitored on the east side of the main roof, as presented in Figure 4.1(c). This single outlet system drains a 311m^2 roof section and has a design capacity of 75mm/hr. From facilities management records, this system has never experienced difficulty with accumulation at the outlet. Each system has 50mm ID stainless steel pipework. Galvanised box gutters, 200mm high by 360mm wide are installed throughout.

The scheduled cleaning of the gutters had just changed as monitoring began, from twice-yearly to once per annum.

4.3.4 Site 2-Ibrox stadium

The site layout, and positioning and orientation of Ibrox stadium, is shown in Figure 4.2(a). It can be seen that the site is surrounded by car parking spaces and as such is not sheltered by other buildings or trees. The stadium comprises four main stands with two seated corner stands. Three of the main stands use traditional gravity roof drainage systems. The fourth stand, *'the main stand'* is a category B listed building and is served by a siphonic roof drainage system. The main stand alone has been monitored.

The main stand has a tin clad roof of approximate area 5200m^2, served by two mirrored siphonic systems. Each drains half the roof area (2600m^2). The west system was chosen for the monitoring programme. There is no scheduled cleaning of the gutters. Instead outlets are cleaned on inspection of the roof or when entrance to the roof void is required. Figure 4.2(b) illustrates the siphonic arrangement.

Seven cup-type baffles connect the valley gutter via HDPE pipework to a single 160mm (ID) downpipe that travels through the attached stairwell. Each of the seven outlets sits in an individual valley gutter, or *'bay'*, and drains an area of 371.4m^2. Bay 1 was selected as the outlet at which detritus accumulation would be monitored (based on information from the facilities management team).

4.4 Monitoring equipment

4.4.1 Monitoring arrangements overview

The recording arrangement comprised digital web-cameras in weather-protected casements installed at chosen siphonic outlets to capture images of detritus accumulation at predefined time intervals. A fully-equipped weather station, which recorded rainfall, temperature/humidity and wind velocity/direction was installed, along with gutter depth sensors and pipe pressure transducers to record siphonic system operation.

4.4.2 Camera criteria

Initially, a range of web-cameras were evaluated against essential criteria to ensure a reliable source of quality images throughout the recording period. Many cameras were found to be unreliable in feasibility tests. Factors requiring consideration were that the cameras:

i. must be weather resistant;

ii. offer a reliable feed of images;

iii. work on a continuous snap shot arrangement;

iv. offer a high quality resolution;

v. could be positioned approximately 50metres from the recording PC and record without cable lengths affecting image quality.

It was established through laboratory testing that a rewired 1.3mega pixel camera could transfer quality images approximately 50metres over Cat5e cable to USB RJ45 ethernet adaptor connectors without additional power supply, while a higher resolution camera could only transfer quality images over a much shorter cable length before image distortion or camera freezing would occur. This rewiring allowed 50metre distances to be achieved between the camera and the data-acquisition PC. Camera stands for each site were manufactured for each gutter geometry and special care given to the camera angles to optimise the best possible view of the outlet.

4.4.3 Camera recording

Initially, camera trials at the National Records building recorded on a continuous minutely-rate to establish whether such a recording rate was necessary. However, it was found that this rate was memory-intensive. A reassessment found recording on a two minute time lapse sequence lost no image information. This also saved on memory space. Once recorded in this way, the sequence of images could be viewed. Due to the nature and purpose of each building, camera lights were not permitted, therefore daylight images only could be analysed.

Image recording was established through a combination of the camera's specific software driver and the freeware *'DORGEM'* recording program. A precise date and time, yielding file names of the format: Camera_YYYY_MM_DD_HH_MM_SS.jpg was given to each image. This filename format provided an effective and efficient basis for finding specific photographs for any given time, and allowed mapping to the corresponding weather station data and siphonic system responses. It should be noted that some image files were corrupt due to lens condensation, rainwater on the lens, or in some cases *'Force Majeure'*.

The jpeg recording format was adopted as this gave the smallest format available with the DORGEM program without loosing image clarity. Using the jpeg format also increased processing speed, as images stored are already compressed.

4.4.4 Weather and drainage apparatus

Three individual pieces of apparatus made up the weather station. These recorded five weather related parameters:

i. precipitation;

ii. relative humidity and temperature;

iii. wind direction and velocity.

A TR-525 M aluminium tipping bucket rain gauge with a resolution of 0.1mm was installed with an accuracy of 1.0%. The relative humidity/temperature sensor used was

a NOVUS RHT-DM with an accuracy of ±1.5%. The traditional cup or vane anemometer was replaced with a *'Windsonic'* by Gill Instruments, an ultrasonic wind sensor for both direction and velocity (with an accuracy of ±2% for the wind velocity and ±30° for wind direction). This allowed a greater accuracy of results than the cup or vanemometer. These three individual pieces of apparatus were attached to a two metre tall aluminium pole on tripod legs, bolted to a timber plinth and weighted down when positioned on each site.

Pipework pressures were monitored using Sensor techniques BTE 6000 series foil faced stainless steel pressure transducers. Gutter depths were recorded using capacitance-type depth sensors.

All apparatus was cabled to an Agilent U2300A USB Modular Multifunction data Acquisition Card in a modified Harmond Instrument Box. All apparatus was calibrated before being fixed and established on site. The acquisition system was controlled and recorded via a Dell Optiplex with an Intel Pentium 4 800MHz FSB processor with a 40GB hard drive running on Microsoft 2007.

A specifically written recording program, *'RAINFALL'*, was developed for this research that was capable of simultaneously monitoring several pieces of apparatus. The weather station apparatus was arranged to record on a ten minute time lapse sequence while the rain gauge worked independently.

This gauge worked once a rainfall event began; additionally, as the rainfall intensity exceeded 5mm/hr, the programme started recording from the pressure transducers and gutter depth sensors, with the DORGEM program running independently in the background. This established the system as fully self-automated.

It is worth noting that the monitoring system was not designed to capture incidences of *'wash and sudden-blockage'* that might prompt near-instantaneous pressure surges in the pipework; rather it was designed to monitor the accumulation, over time, of detritus at the outlets and the effect of the resultant blockage on system performance.

4.4.5 Apparatus calibration

The cameras required fine focus adjustments once installed on-site. All weather station apparatus required calibration, except the rain gauge which was purchased with the manufacturers' calibration. Operational checks were then performed on the temperature, humidity, windsonic and rain gauge sensors to guarantee acceptable results. The water depth capacitance sensors and the pressure transducers each required calibration.

4.4.6 Summary of recording procedure

The operation of data recording for each site, when a rainfall event occurs, is as follows:

i. rainfall event occurs;

ii. rain gauge starts to record;

iii. above 5mm/hr, pressure transducers and depth sensors record;

iv. rainfall event ends;

v. apparatus continues to record roof surface run-off;

vi. end of recording.

The temperature/humidity and windsonic readings were continuously recorded on a ten minute time lapse in parallel with the rest of the recording apparatus. The two sites, due to system scales, had different pressure and depth recording run-on times. A period of five minutes over-run was chosen for the National Records, and ten minutes for Ibrox, to allow sufficient time for the water in the gutter, including the furthest upstream section, to flow into the outlet. Initial tests carried out to establish the time taken for rainfall, at the upstream section of the roof to flow to the outlet, were based on BS EN 12056:3 however it was found this time needed amending to allow for gutter flow.

The National Records site in Edinburgh allowed convenient data retrieval on a weekly basis. Site 2, Ibrox stadium in Glasgow, required a more automated arrangement, whereby once a week, the recorded data would transfer to an online data-holding site *'dropbox'*, thus allowing data download on an office based PC.

4.5 Site instrumentation

4.5.1 National Records building

The galvanised box gutters serving both systems at the National Records building have two cameras installed at two of the three outlets. These outlets will be termed outlet 1 and outlet 2 hereinafter, with locations presented in Figure 4.3(a). This allowed a view for each of the siphonic outlets and leaf-guards. The PC workstations were located within the roof void of the main building. A Logitech E3500 and Mikomi 7115, each at 1.3MP (34 and 36metres respectively from the PC) were installed at outlet 1. The east system, outlet 2, also used a Mikomi 7117 and Logitech C250, 1.3MPs at 23 and 25metres respectively from PC2.

To measure water depths in the gutters, sensors were installed at the siphonic outlet, see Figures 4.3(b & c). In total, four water depth sensors were installed across the two systems monitored.

The four pressure transducers used, three for system 1 (VPT1, VPT2 and VPT3) and one for system 2 (VPT4), were each securely fixed and bracketed to the steel pipe using a specially manufactured clamp. Figures 4.3(b & c) present these positions. System 1 had sensor VPT3 installed in the tailpipe of outlet 1 to indicate when this length of pipe primed, while transducer VPT2 would indicate complete collector pipe priming. The final sensor, transducer VPT1 was installed at the top of the discharge pipe to record the maximum sub-atmospheric pressures for the complete system. On the east side, system 2 had one pressure transducer, as this was a single outlet system, installed at the top of the discharge pipe.

The weather station was secured to the roof of the west stairwell, as Figure 4.3(a) indicates. Data collection began on the 9th March 2010 followed quickly by a scheduled gutter clean on 11th March, with end date for analysis taken to the 1st October 2011. This coincided to give a full year's data collection from Ibrox.

4.5.2 Ibrox stadium

Figure 4.4(a) presents the two camera locations for bay 1, at outlet 1. Even though this is a valley gutter and the outlet is recessed into the inclined contributing roof, two cameras were installed to record opposing angles. A Mikomi 7117 and a Philips SP2000, 1.3MP, each 38metres from the PC were installed.

Throughout the bay 1 valley gutter, five depth sensors were installed, with one at the outlet that was built into the camera support stand, two on the opposite side of the gutter and two at opposing gutter ends. The sensors directly opposite the outlet and at the gutter ends allowed a gutter depth profile to be created for a given rainfall event. Figure 4.4(b) indicates the location of these sensors. Each sensor had a robust support stand built and clamped onto the edge of the overhanging roof cladding. In total, four pressure transducers were installed to monitor the siphonic system, see Figure 4.4(b). In terms of detritus effects VPT1, is the most critical. The remaining transducers allowed for flow profiles of the system in operation. Additionally, the camera images recorded at outlet 1 can be directly related to the results from VPT1.

Due to the roof design, no anchor points could be established for the weather station. Instead, this was positioned on the flat roof of the stairwell leading into the stand, as presented in Figure 4.4(a). This stairwell also housed the data recording equipment and PC.

Data was collected from 09th September 2010 until 1st October 2011.

4.5.3 Absent site data

Despite attempts to ensure the integrity of the image capture system, there were nonetheless times during this monitoring period where images, and sometimes pressure and depth data also, were not available from both sites. These events were caused by extreme weather conditions (3rd week December 2010) were abnormal snow storms severely damaged the recording apparatus, and again for both sites, a loss of power occurred late January 2011.

4.6 Data collection results

4.6.1 Evaluating detritus accumulations

Processing data for recorded environmental parameters required several relatively straightforward, but time-intensive, steps. The site data recorded has been evaluated in two ways. The first reviewed weather parameters alone, while the second analysed precipitation and physical parameters.

4.6.2 Image analysis

First, an excel sheet was created that indicated date, detritus quantity/value, mm/hr (precipitation), temperature (°c), wind speed (m/s) and wind direction. The weather data parameters were then converted using calibration equations established before site installation. The two minute time lapse images for each camera were then assessed. Detritus quantification values were graphed and dates of interest noted from all measured variables. It should be noted that events described here are for intensity values of 5mm/hr or greater, (the minimum threshold for recording).

4.6.3 Summary of analysis procedure

The analysis procedure used to understand the effect environmental parameters had on detritus accumulation at outlets was:

i. set up excel sheet for detritus, temperature, wind and precipitation;

ii. convert weather station results into usable values;

iii. assign value to each detritus image;

iv. graph detritus daily accumulation;

v. analyse detritus accumulation graph, along with images, temperature and precipitation data for dates of interest.

4.7 National Records building

4.7.1 General

A summary of all recorded storms is presented in Table 4.1. A summary of detritus levels reached for systems 1 and 2 is presented in Figures 4.5(a & b).

4.7.2 Blockage classification

As the aim of the study was to examine the type and rate of detritus build-up at the outlet over time, it was necessary to analyse the images captured and to identify trends in the extent of accumulation. To achieve this, images were allocated a blockage *'coverage'* classification. All site images from March 2010 to October 2011 have been analysed individually and allocated to one of seven categories.

This was achieved by establishing a boundary between the blockage steps and assigning a dimensionless value (from 0 to 6), see Figure 4.6(a to g). It should be noted here, that the assigned number is based on a mean detritus level taken from the images of both cameras recording at the outlet. This practice of assigning a figure to identify an objects appearance is termed the *'universal numbering technique'* (Aeini and Mahmoudi, 2010). For this research, a *'0'* represents a clean outlet, whilst progressively increasing to the worst case scenario of *'very extreme'* with an assigned value of *'6'*. Although the original intention had been to analyse images using a specially written computer program that would differentiate between areas of leaf-guard that were clear and those that were blocked, it soon became evident that the restrictions imposed by the system gutters, that resulted in angled camera views rather than direct, meant images had to be analysed individually. Although time-intensive, this method in assigning coverage classification, did allow for automatic cross-reference and validation.

Further, this categorisation of images allowed for the building of an accumulation profile for pattern analysis when mapped to measured environmental parameters. During the task of building the detritus accumulation profile, typical materials found at the outlet were recorded.

4.7.3 Data analysis

It will be appreciated that with no prior knowledge of how detritus might accumulate in the gutter or at the outlet, it was difficult to hypothesise any relationship between prevailing weather conditions and changes in the level of accumulation. However, with regard to performance of the system, it was anticipated before commencement of the test programme, that detritus levels would build over time, that they would be influenced by both *'heavy'* and *'prolonged'* rainfall events, and potentially also by extended periods of dry weather, and that levels would not decrease until such times as gutter cleaning was undertaken by the facilities management team.

The recorded images were evaluated in two ways. The first examines site weather influences on detritus accumulation. A detritus graphical grid of +/ -1 has been superimposed over the detritus accumulation profile. This indicates whether detritus has been added since the previous day; represented by +1. If the detritus level has reduced, this is presented by -1. This overlay identifies the effects of not only precipitation, but temperature. Points of interest have been highlighted with circled numbers on each Figure and termed *'case points'* in the following Sections. It should be noted here that the term *'case point'* is taken to mean scenarios whereby either detritus has moved or changed due to an environmental parameter or where the weather has been constant over a period of time (i.e. warm, no rain) but with no effect on accumulation.

The second analysis involved plotting the total accumulation profile for outlet coverage against daily cumulative rainfall (mm). Following this, incidents of significant detritus categorisation change were highlighted with circled letters on each Figure, and also termed *'case points'*. For this analysis, *'case point'* refer to a time when detritus has changed due to either one, or a combination of, environmental parameters.

4.7.4 NRS, system 1-west: weather affects on accumulations

Case 1, presented in Figure 4.7(a) and Table 4.2, occurred after a number of light rainfall events and a slight build-up of detritus. The analysis then begins from the 11th May 2010 where, in this time, six days of no rain occurred but detritus levels increased from *'light'* to *'heavy'*. After this, 18 rainfall events washed detritus to the outlet, but with insufficient influence to change the detritus categorisation level. Following Case 1, Case 2 covered 43 days of dry weather with an average daily temperature of 16.7°c (±3.1^{o}c), with a scattering of six random wet days, all of which had no influence on the detritus build-up.

For Case 3, ten rainfall events occurred on a single day. From image analysis it was clear the detritus accumulation had risen to an *'extreme'* level. A period of 103 dry days then followed, Case 4, which subsequently included 20 days of 48 rather random rainfall events that had no influence on detritus levels. Some detritus was washed through the system after three rainfall events, Case 5, and on the 1st November, had three rainfall events saw the detritus level decrease to a *'heavy'* category. In Case 6, the accumulation decreased further after a rainfall event appeared to wash detritus through the system. This occurred after seven prior rainfall events covering an 8 day period.

Case 7, a dry weather period of five days with average daily temperatures of 2.9°c (±1.2°c), had no substantial influence on the detritus accumulation. Following this (Case 8), from 21st November, two days of rainfall with eight events caused the detritus to increase again to *'heavy'*.

After gutter cleaning and re-installation of the equipment on the 27th January 2011, four rainfall events occurred over a five day period which resulted in a moderate change to the outlet accumulation. However, on the 3rd February 2011, 24 events on this day alone encouraged most detritus within the gutter and on the roof to collect at the outlet, this is Case 9. This changed the detritus categorisation from *'clean'* to *'light'*. Case 10, four days later, after a single heavy rainfall event washed more detritus to the outlet.

For Case 11, a 28 day nominally dry period of average daily temperature 12.7°c (±2.5°c) with a scattering of six rainfall events, ended on the 10th March with 25 events on this single day. These events had no influence on the detritus build-up, which remained at a *'moderate'* level. From the 14th March, minor changes occurred after two major rainfall events, that occurred on the 23rd May 2011 and on the 29th May. Case 12 occurred 36 days after repair of the computer (from power outages), where 62 events had occurred and after two rainfall events, detritus levels increased to *'moderate/heavy'*. Case 13 saw 16 rainfall events where the detritus was washed to the outlet.

In Case 14, an *'extreme'* to *'very extreme'* level change occurred after four rainfall events, where the second event washed more detritus to the leaf-guard. The final case remained at a *'very extreme'* detritus level for 100 days; at this level 33 rainfall events occurred.

4.7.5 NRS, system 1-west: analysis

The accumulation build-up profile was mapped against each weather parameter measured. Figures 4.7(b to e) indicate rainfall, temperature, wind direction and velocity respectively. From the Figures, it is difficult to find a relationship between detritus build-up and temperature, wind direction and velocity alone. Relationships between rainfall and detritus accumulation can, however, be seen in Figure 4.7(b). The following text discusses *'cases'* highlighted on the rainfall Figure whilst also analysing in detail three incidents of greater detritus movement (as indicated). Table 4.3 indicates each case point in detail, highlighting the intensity and the pre and post gutter depths,

while Table 4.4 gives an insight to the environmental conditions. Pipework pressures are tabulated in Table 4.5

Only three days after installation of the recording equipment, on the 8th March 2010, a scheduled gutter cleaning took place. This was fortuitous as it resulted in the identification of a benchmark *'ideal'* condition. The first incident of significant detritus movement, see Figure 4.7(b), started on the 22nd May 2010 when an event of 5.92mm/hr increased the blockage categorisation to '*heavy'*. Approximately four white feathers, birch leaves, and black solidified sediment were observed. Gutter pooling did not occur on this occasion as the water was still able to pass through the detritus build-up. Prior to this, the detritus had built-up on four occasions. On the 20th July, an event with an average intensity of 6.65mm/hr increased the build-up to an '*extreme'* level; after which gutter depths remained at 71mm. Figures 4.8(a & b) illustrate data recorded from the siphonic system on the 20th July 2010. These indicate pressures as quite steady at around -0.22 mH20. A sudden depressurisation occurs 20minutes from commencement of the event in response to an increase in rainfall intensity. It can also be seen, Figure 4.8(b), gutter depths steadily rose to 71mm.

An event of 5.97mm/hr at 18:19:50, Case F, washed detritus through the system resulting in detritus levels decreasing. An event which followed on the 15th November washed more detritus from the outlet, however water still remained within the gutter at a depth of 72mm. Case H, an event with an average intensity of 5.76mm/hr, washed detritus to the outlet and resulted in gutter water settling at a depth of 79mm. Images indicated that yellow/orange beech leaves and an exceptional quantity of solidified sediment had remained at the outlet. This is interesting as the start of November is the end of the fledgling period for the birds, a period when molting occurs. A dip in temperature, Figure 4.7(c), also occurred at the same time (and almost in the same profile) as the detritus.

Figure 4.7(d) presents the wind direction recorded for the entire length of the monitoring period with the detritus profile for system 1 overlaid. It can be seen that the wind is effectively southerly. Further, no direct relationship or pattern appears with regard to detritus accumulation.

Cases I, J and K all saw the detritus levels increase with typical weather parameters for the site while Case L, had an rainfall event of 5.19mm/hr, resulting in detritus being swept to the outlet where the gutter depths settled at 74mm. Figure 4.9(a) illustrates the rainfall profile against the system pressure. As can be seen, the pressure begins to peak 102seconds after the commencement of the event and 96seconds after the rainfall peak. Subsequently gutter levels were at a maximum.

Another event which influenced accumulation occurred on the 19th June 2011 with a maximum intensity of 9.02mm/hr after which the build-up increased to a *'very extreme'* level. Several gutter overtopping events followed until the monitoring period ended.

4.7.6 NRS, system 2-east: weather affects on accumulations

Figure 4.10(a) presents the detritus accumulation profile for the monitoring period plotted with daily accumulations for outlet 2. Data for each case point has been tabulated in Table 4.6.

Case 1, with frequent low level rainfall intensities since installation of the monitoring system on the 8th March 2010, shows detritus levels grow to a *'heavy'* category very quickly. Following this, the wash effect of a rainfall event transported detritus to the leaf-guard, raising the accumulation to an *'extreme'* level, Case 2.

For Case 3, minor changes in detritus levels occurred between the 8th May and 9th July 2010. During this time 21 rainfall events were recorded that had little influence on detritus. Directly after this, the detritus accumulation increased on the 10th July 2010 after two rainfall events. These events caused a wash effect within the gutter, resulting in a detritus increase to *'very extreme'*; Case 4.

The detritus held at a *'very extreme'* level for 15 days during which time the gutter was subjected to 30 rainfall events, resulting in gutter overtopping several times, Case 5. For Case 6, after some gutter overtopping, some detritus became loose and transferred through the system, resulting in the water depth dropping and the detritus decreasing to *'extreme'*. After this, a period of 124 days saw gutter water pooling, Case 7. During this time, no change in detritus levels occurred. Interestingly, 69 scatterings of rainfall events occurred, but not with intensities that caused system failure. Gutter cleaning took place on the 21st January 2011 and the re-installation of the equipment on the 27th

January 2011 after abnormal storm events. Case 9 saw 24 rainfall events increase detritus levels to a *'moderate/heavy'* category. Case 10 then saw 37 days and 29 rainfall events which had no affect on the detritus accumulation levels.

Case 11 involved no significant weather events that influenced the detritus levels at outlet 2. However, 20 rainfall events on the 23rd May and 25 rainfall events on the 29th May 2011 stood out as extreme rainfall periods. As was similar for outlet 1 on the west side of the roof, no changes occurred at the outlet. Some detritus did accumulate at the outlet but not to such a significant level that would increase the detritus categorisation.

Following this, Case 12 saw detritus levels increase to *'extreme'*. This took 13 days (10 of which were dry) and 15 events. On 10th June, after three rainfall events, the detritus levels grew to *'heavy'*, where the third rainfall event of the day caused the greatest change in detritus levels. Case 13, after 11 rainfall events and considerable water settling time, it was noted the detritus levels had grown to a *'very extreme'* level. Case 14 highlights this, where the detritus remained at the outlet at a *'very extreme'* level for 100 days without movement. Monitoring finished on the 30th September 2011.

4.7.7 NRS, system 2-east: analysis

The accumulation profile was cast against each weather parameter measured. Again from measured environmental parameters, no relationship exists between detritus build-up and temperature, wind direction and velocity. It can be seen however that rainfall relationships with detritus accumulation appear in Figure 4.10(b). Taking rainfall as the primary weather parameter, the following text discusses *'cases'* highlighted on the rainfall Figure whilst also looking at two significant detritus movement incidents. Each case has been tabulated, with gutter depths before and after shown in Table 4.7, and environmental parameter conditions in Table 4.8. The response of the siphonic system can be seen in Table 4.5. As noted no temperature relationships have been established, see Figure 4.10(c).

The first significant incident of detritus movement began on the 4th May 2010 following an event of average intensity of 5.88mm/hr that left the gutter level at 55mm and the detritus category as *'heavy'*. Prior to this, Cases A, B and C had seen rapidly changes in detritus following the wash from minor rainfall events. On the 9th July, a 13.6mm/hr rainfall event left gutter water depths at 78.3mm. This event, Figure 4.11(b), resulted in

the system depressurising and gutter depths increasing as indicated. This resulted in detritus levels altering to '*very extreme'*. Detritus consisted of approximately three white feathers and an excessive amount of black solidified sediment. This was followed by an event on the 26th July which saw the detritus return to '*extreme*'. Gutter overtopping occurred frequently after this.

The second area of interest, Figure 4.10(b), occurred over a 14 day period when the 7th June saw an event of average rainfall intensity of 5.66mm/hr increase detritus levels to *'heavy'*. Images indicated a copious amount of black sediment had accumulated. On 9th June, this level changed to *'extreme'*. The event (Figure 4.12(a)), lasted for 9.44minutes with an average rainfall intensity of 6.78mm/hr. This washed detritus to the outlet, with gutters pooling at 71mm depth. Following this, the gutter overtopped frequently until the end of the monitoring period. Once again, no apparent relationship was established with other weather parameters.

4.7.8 NRS conclusions

Based on the preceding text, the following conclusions may be drawn:

i. detritus accumulation generally increased during April/May and decreased during the August/ September months;

ii. detritus accumulation grew marginally faster to '*v.extreme'* at outlet 1 as compared to outlet 2;

iii. from the shaded blocks on Figures 4.7(b) and 4.10(b), it has been shown that detritus can and does rapidly increase over a relatively short period of time. Generally detritus levels increased from sustained rainfall events rather than a single event. However, in cases where detritus reached the heaviest category, heavy rainfall events prompted the accumulation change;

iv. although leaves, feathers and twigs were present, the majority of the accumulation at the two outlets is presented by emulsification or solidification of dust, dirt and organic matter;

v. that there exists a link between the frequency of heavier rainfall events and an increase in accumulation category;

vi. that there exists a link between higher intensity rainfall events and an increase in detritus levels;

vii. that detritus accumulation can, and does, build with only relatively low intensity rainfall events but that notably high intensity rainfall events do seem to result in a direct and significant increase in detritus level;

viii. that there is no evidence of a link between detritus classification and temperature (for either system). The same is true for wind velocity and direction;

ix. that, as substantiated by the data gathered, the local climate may be best described as *'mild and wet'*, with a propensity for *'drizzle'*. For most of the monitoring period, the daily accumulation of rainfall was relatively low i.e. below 10mm depth;

x. that sub-atmospheric pressure for each siphonic system was recorded, implying self-cleansing velocities were achieved;

xi. that gutter overtopping has occurred. These occurrences have generally resulted from standing gutter water, indicating the extent of blockages at the monitored siphonic outlet were significant.

4.8 Ibrox stadium

4.8.1 General

Table 4.9 presents a summary of the events which occurred during the monitoring period, with Figure 4.13 highlighting the number of times each detritus category was reached.

4.8.2 Blockage classification

Analysis of the recorded images required the same method as described in Section 4.7.3. From this, five distinct stages of accumulation, were identified, Figure 4.14 (a to e). Each detritus quantification image has been assigned a dimensionless value from 0 to 4 and analysed in the same manner as site 1. A different detritus scale has been established at Ibrox due to the low levels of detritus that accumulate in comparison to the National Records building. Also, unlike the National Records building, Ibrox has no

scheduled gutter cleaning, although detritus quantities were quite light at the start of the monitoring period.

4.8.3 Ibrox, weather affects on accumulations

The total accumulation build-up at the outlet can be seen in Figure 4.15(a). Table 4.10 gives further case point information.

After installation of the recording equipment on the 7th September 2010, no change in detritus accumulation occurred until the 19th September (Case 1) where six low intensity events on this single day washed detritus to the outlet, causing the accumulation level to increase to *'moderate'*. Case 2 resulted from four rainfall events on a single day, increasing the detritus build-up again. Case 3 then consisted of five events which increased the detritus to a *'heavy'* category.

For Case 4, the detritus maintained a *'heavy'* category level for 13 days at an average daily temperature of ±3.1°c, even with eight rainfall events occurring during this time. Two events on the 18th October washed some detritus through the system, resulting in the accumulation dropping to a *'moderate/heavy'* category. Case 6, saw the accumulation remain at the *'moderate/heavy'* category until the 29th October.

After equipment re-installation on the 26th January 2011 following the snow disruption, 10 events occurred over a 14 day period which had no effect on the outlet accumulation; however on the 24th February 2011, a computer failure and power failure affected the recording of information. This was rectified by the 7th of March 2011. Then for 63 days the detritus remained at a consistent level, after which on the 10th May, the build-up increased to a *'heavy'* category, Case 9. The following case, Case 10, saw levels stabilise for two weeks. Case 11 had three events on a single day which resulted in the detritus decreasing. Levels then dropped further, Case 12, and then settled to a light category on the 1st June 2011, Case 13. Case 14 saw the *'light'* level stay consistent until the 24th June 2011. Then on the 25th June, the detritus levels increased to a *'moderate'* level, Case 15. Then for 48 days the levels remained as *'moderate'* until the 14th August 2011, Case 16.

The final Case (17) occurred on the 15th August when detritus levels again increased to a *'moderate heavy'* category and remained so for 47 days until the end of the monitoring period.

4.8.4 Ibrox: analysis

The accumulation profile has been cast against each weather parameter measured; however there appears no sound correlation between the two. Figures 4.15(b & c) indicate precipitation and temperature plotted against the detritus accumulation profile. As indicated in Figure 4.15(b), relationships between rainfall and detritus accumulation appear. Taking rainfall as the primary weather parameter, the following discusses *'cases'* highlighted on the rainfall figure whilst also assessing two incidents of interest. Each case point has been detailed further in Table 4.11, showing gutter depths before, during and after the event. Table 4.12 highlights the associated environmental conditions at the time of the event with system responses presented in Table 4.13.

Analysing precipitation, Figure 4.15(b), as a primary weather parameter, the first stages of notable detritus movement began on the 19th and 23rd September, where at each date the levels increased. Following this, on 3rd October 2010, an event of average intensity 5.36mm/hr washed detritus to the outlet, increasing the accumulation level to *'heavy'* and causing gutter pooling of 35mm depth. A second event, Figure 4.16(a & b), on the 18th October of 9.92mm/hr intensity then removed detritus from the outlet. Gutter depths after the event settled at 38mm with a gradual trickle through the remaining detritus. Following this, an event of 10.34mm/hr on the 29th October at 18:36:24 (with a maximum intensity 19.89mm/hr), see Figure 4.17, washed further detritus from the outlet, resulting in levels reducing to a *'moderate'* level and a gutter depth of 28mm.

On the 10th May 2011, see Figure 4.15(b), detritus was flushed from the roof to the outlet increasing the accumulation to a *'moderate heavy'* level. Detritus consisted of small twigs and sediment. This was quickly followed by a reduction in detritus (Case G) with a rainfall event of 42.67mm/hr, and was further reduced on the 2nd June where the outlet had accumulated a marginal amount of twigs and a small quantity of black sediment that kept gutter depths at 28mm depth. On the 26th June, a rainfall event of intensity 38mm/hr increased the accumulation to a *'moderate'* category. Detritus accumulation stayed relatively steady for the remainder of this monitoring period.

4.8.5 Ibrox conclusions

Based on the preceding text, the following conclusions may be drawn:

i. site images indicated greater accumulation quantities occurred in September/October 2010 and at the end of April and start of May 2011;

ii. from the recorded images, it has been found that typical detritus build-up was minimal at the monitored outlet. It has been concluded that five stages of blockages exist, where the maximum stage (stage five) remains marginal in relation to outlet coverage. However the images did indicate that even though leaves, feathers and twigs were present, a greater proportion of the accumulation resulted from emulsification or solidification of dust, dirt and organic matter;

iii. gutter wash-through or detritus displacement can, and does, occur, however due to the small detritus quantities and camera angles, causes are difficult to identify;

iv. it is difficult to draw conclusive data from detritus classification mapped against temperature. Similar inconclusive data occurs when the detritus profile is mapped to wind direction and velocity. It was established that the wind also came from the south similar to site 1;

v. the siphonic system never failed during the monitoring period, with pressure responses to rainfall events indicating sub-atmospheric flow is possible.

4.9 General site findings

The conclusions of the work in this Chapter may be briefly summarised as follows:

i. examination of images captured from site, revealed that, although leaves, feathers and twigs were present, the majority of the accumulation at the monitored outlets is emulsified or solidified dust, dirt and/or organic matter;

ii. it is difficult to draw any sound conclusion from the detritus classification mapping with temperature;

iii. it is difficult to draw any conclusive relationship between detritus classification and wind direction and velocity;

iv. although difficult to establish holistically, there does seem to exist a relationship between a larger number of rainfall events and an overall increase in category of detritus accumulation.;

v. outlet wash-through or detritus displacement can, and does, occur;

vi. the data suggests that detritus accumulation can, and does, build with only relatively low intensity rainfall events.

Further, it has been observed that operational problems and system failures do occur but only from restricted outlets which has led to gutter overtopping. Site 1 results suggest that the siphonic systems are not maintained to levels required to limit occurrences of system failure. Site 2 did not fail during the monitoring period, suggesting it is adequately sized and detritus levels do not interfere with system operation.

4.10 Summary of chapter

This Chapter has presented findings of an 18month monitoring programme of detritus accumulation and its consequences on system operation at two installed siphonic rainwater drainage sites in Scotland. The aim was to investigate detritus types and build-up rates, to establish whether connections between local weather and accumulation exist, and to evaluate the consequences of blockages on system performance. Site data has informed laboratory investigations reported in Chapter 5. Further, an indication of the theoretical impact on system operation is examined using the ROOFNET simulation model in Chapter 7.

Chapter 5

Siphonic outlet loss coefficient experimental investigations

5.1 Introduction

Chapter 4 identified typical detritus quantities and types found at the outlets of two geographically different siphonic system sites. This Chapter presents system performance data that have been established using a partially-blocked single outlet laboratory test rig. This will enable derivation of an outlet loss coefficient from relationships between measured variables, including flow-rate, gutter depth, system pressure and outlet blockage. This Chapter describes the methodology developed and apparatus used to establish these experimental results.

5.2 Basic characteristics of an operating outlet

Siphonic outlets comprise of a leaf-guard, an internal baffle and a sump (May *et al*, 1996). All manufactured designs are either plate-type baffle or inverted cup-type. Both types of baffle reduce the ingress of air into the system in similar ways. For the outlet to perform satisfactorily at low flows up to its design capacity, the outlet allows gutter water to flow freely through the openings into the siphonic system whereby the system behaves as a conventional system (allowing the free passage of rainwater and entrained air). At higher rates of flow, when design capacities are reached and water depths around the outlets are sufficient to cut off the air supply into the pipework, the flow will become full-bore i.e. 100% water.

5.3 Outline test methodology

This Chapter establishes a foundation for determination of an outlet loss coefficient for two different outlet types. Detritus quantities and types established from site investigations have informed these experiments. To obtain loss coefficient values, an experimental rig was designed to BS8490:2007, and flouricine added to the water to enhance visibility. Two datasets were established; the first where real detritus was used at the leaf-guard and also at the baffle, and the second where synthetic infills were used (each based on percentage coverage). This allowed comparisons between actual detritus

accumulation and a controlled percentage blockage. Two variables were measured i.e. pressure within the discharge pipe and gutter water depth. The outlets were subject to flow-rates from 1.0l/s to 9.0l/s (the maximum theoretical capacity) set at 1.0l/s intervals (Section 5.5 describes the experimental test rig).

The recording procedure was identical for each test set. The procedure adopted was: set the required flow-rate, position blockage, bleed air release valve, re-run flow-rate, run recording software (discussed in detail in Section 5.7.7).

5.4 Outlets tested

Figure 5.1(a) indicates the design and dimensioning of the plate-baffle, Outlet *'A'*, where the rainwater enters the system through 8of 45mm by 25mm openings between the aluminum alloy plate and the shallow 18mm sump. An aluminum alloy plastic-coated leaf-guard slots over the plate. This plate-type outlet is used at the National Records building.

Outlet B, the inverted aluminum cup-baffle is shown in Figure 5.1(b) and illustrates how the baffle sits in a 65mm deep sump, elevated 15mm from the sump base. The vertical side of the cup has 30 perforations, each 15mm in diameter (3 rows of 10 holes). The roof of the inverted cup has seven rectangular slots. A plastic leaf-guard protects this outlet with similar dimensional characteristics to the plate-type baffle. This outlet type is installed at Ibrox stadium.

5.5 Overview of apparatus

5.5.1 Description of the drainage rig

All experiments were carried out on a test rig installed in the University's drainage laboratory, see Figure 5.2(a). The configuration of the laboratory rig was based on recommendations given in BS8490:2007 and comprised one transparent vertical Polyvinyl Chloride (PVC) pipe of 4.0metres length with an external diameter of 50mm and internal diameter 43mm (BS3505) connected to a galvanised gutter of 2.0m by 0.6m by 0.6m. The gutter length is defined as the distance between each end (which is zero flow) that is a stop end. The defining feature of the gutter flow is the run-off which will enter the pipe, meaning the length of the gutter causes the rate of flow to steadily increase from zero flow to the exit point at the outlet.

Transparent PVC was installed to enable visual observation and digital camera image capture. The discharge pipe was supported using a scaffolding rig and pipe clamps connected to threaded steel hangers. The upper end of the discharge pipe was fitted directly to the outlet which in turn was centrally positioned in the gutter sole.

A submersible radial flow pump capable of delivering a maximum flow-rate of approximately 17l/s was used to elevate the water to the rig from a holding reservoir of capacity 2200 litres. The water was routed via two PVC Class E 75mm rear-feed pipes in order to provide a uniform inflow, see Figure 5.2(b), to the mock roof surface. Each feed was fitted with an independent magnetic flow meter.

Sensor technics foil faced BTE6000 diaphragm transducers with a range of ± 10mH20 water gauge were used. Pressures were measured in two locations. One transducer (VPT1) was positioned ten internal pipe diameters below the base of the outlet connection, while VPT2 was positioned a further ten pipe diameters below. Rubber tubing connected the transducer to pressure tappings on the discharge pipe. An *'air release valve'* was fitted, as shown in Figure 5.2(c) to allow the escape of trapped water.

Four capacitance type depth sensors (with a maximum recording depth of 270mm) were installed along the centreline of the galvanised box gutter as Figure 5.2(d) indicates. Depth sensors (DS1 and DS2) were positioned 150mm from the centre of the outlet to ensure results would not be affected by vortex flow. Depth sensors DS3 and DS4 were positioned 150mm from each opposing end of the gutter. All apparatus was connected to a PC-based data acquisition system recording at a sampling rate of 500Hz.

5.5.2 Criteria for transducer selection

In order to achieve accurate pressure recordings, the selection of transducer type was matched against pre-defined criteria that included: range, sensitivity, frequency response, accuracy, linearity and hysteresis. In more detail:

i. range should match expected pressures;

ii. sensitivity, i.e. the ratio of change in transducer output to a change in the input, should be high;

iii. frequency response, i.e. the range of frequencies over which the transducer can give an accurate response, should be good;

iv. accuracy, i.e. how close the output of the transducer is to the actual value, should be high;

v. linearity, i.e. the closeness of a calibration curve or output of a transducer to a straight line, should be accurate. Transducers are specified as being linear but from experience and knowledge, some deviation from linear, particularly at extreme ends of the range, is known to occur.

5.5.3 Calibration

A pressure across the foil face of the transducer diaphragm causes a change in electrical resistance and consequently output voltage. This relationship is linear.

Calibration of each transducer was hence undertaken using a static pressure applied to the sensor to produce an output voltage (V). The capacitance depth sensors were calibrated in a similar manner, whereby the probes were submerged in premeasured depths of water. This also resulted in a linear relationship between output voltage (V) and water depth (mm).

All transducers used yielded an r^2 of 1, see Figure 5.3(a), as did (effectively) the four depth sensors as presented in Figures 5.3(b to e).

5.6 Outlet obstructions

5.6.1 Test parameters

Two data sets for each outlet were established. The first involved *'real'* detritus and the second, manufactured *'percentage coverage'* barriers. From recorded site images, two types of detritus accumulation are known to exist, the first is detritus accumulation at the leaf-guard and the second, unavoidable accumulation that occurs at the baffle. Thus, collectively, four test sets were undertaken:

1. different quantities of detritus placed at leaf-guard;

2. different quantities of detritus placed at baffle;

3. different sizes of synthetic barrier at the leaf-guard, where each was sized as a percentage of the open area of the leaf-guard;

4. different sizes of synthetic barrier infills at the baffle, where each was sized as a percentage of the open area of the baffle.

Test set 1 involved representative detritus material of varying quantities as determined from analysis of site images from the National Records building and Ibrox. Detritus included leaves, twigs and feathers. Nine quantities were tested, ranging from 130g to 220g. The detritus was positioned around the leaf-guard before each test.

Test set 2 involved the same selection and quantities of detritus (as for test set 1) placed inside the leaf-guard and around the baffle.

Test set 3 involved locating manufactured PVC hollow disks (hoops), cut to represent percentage coverage, around each leaf-guard.

Test set 4 involved inserting manufactured infills into the baffle opening, where these represented a percentage closure of the outlet.

5.6.2 Detritus tests

Site testing, discussed in Chapter 4, allowed a determination of detritus materials typically found at siphonic outlets. Four material types were identified and have informed laboratory experiments. These were:

i. leaves;

ii. twigs;

iii. feathers;

iv. solidified or emulsified sediment.

The following text details typical characteristics for each material.

5.6.3 Leaf accumulation

Leaf types observed at the National Records building outlets have been established as beech and birch. The beech leaf was the most prevalent. These leaves are pointed oval in shape (typically between 4cm by 9cm) and were found to display varying degrees of moisture content and colour. Although leaf accumulation was significant, quantification and mass could not be achieved from image analysis. Ibrox outlets accumulated minimal leaf accumulation which could not be identified because of the prevalent solidified sediment.

5.6.4 Twigs

Twigs were approximately 1cm to 3cm in length, with outlet accumulations never consisting of more than 2 twigs at any one time.

5.6.5 Feathers

The National Records building has always experienced some problems with roosting birds, observed as feral pigeons and gulls (Herring Gull and Black Back Gull). Feathers from both gulls (the species could not be identified) and feral pigeons were observed at the siphonic outlets. The number of feathers varied during the course of the year, from none to a maximum of five. At Ibrox, a maximum of two feathers, at any given time, were observed during the monitoring period.

The two species of gulls are known to occupy dense colonies on the flat roof of the National Records building. The larger population belongs to the Herring Gull; a large gull between 55cm and 67cm long and weighing 0.750kg to 1.25kg with a wing span of 130cm to 158cm. A few Black Back gulls have also been seen at the National Records building. These are larger in size than the Herring gull at around 64cm to 78cm long, with a wingspan of 150cm to 170cm and bodyweight of 1.1kg to 2.3kg. The Herring gull has also been observed at Ibrox, roosting on the sloping tin roof where the structural support penetrates the roof cladding.

The facilities management team at the National Records building have tried to limit flocks roosting by installing bird control spikes and netting to cover ledges below the overhanging gutters and other potential nesting locations. This may have reduced the accumulation of droppings on and around the building.

5.6.6 Sediment accumulation

Emulsified sediment is extensive and most prevalent at the outlets of the National Records building (mainly due to the channelling effect of the gutters) but also forms the greater proportion of blockages at Ibrox. This accumulation consists primarily of granular material and organic breakdown of leaves. The sediment was observed to act as a binding agent for other detritus in the gutter. This was unquantifiable from recorded images.

5.7 Experimental procedure

5.7.1 Preliminary detritus test methodology

Initially, laboratory tests involved scattering detritus in the gutter. However it was found that without a binding agent (provided on site by the emulsified sediment) the detritus would suspend and pass through the leaf-guard. Figures 5.4(a & b), respectively, highlight the detritus before and after the accumulation test. Although it was not possible to quantify the detritus that passed through the system, the detritus ultimately had no affect on system pressures.

5.7.2 Detritus test methodology amended

As such, a substitute binding agent was found to be necessary. This additional material needed to be:

i. unobtrusive;

ii. impervious;

iii. non-degradable.

To correspond with the criteria listed, and to avoid the difficulties of suspended detritus, a nylon-meshed netting material was used. The mesh net, when filled with the quantified detritus (a '*Gabion*' concept), restrained the materials whilst ensuring continued buoyancy.

5.7.3 Test set 1: detritus blockages at leaf-guard

As discussed above, detritus materials found onsite included leaves, twigs and feathers. However the accumulation quantities (based on images) ranged quite considerably during the monitoring period. Unfortunately, determination of representative quantities could not be accurately achieved.

Preliminary experiments hence began with limited detritus quantities in order to obtain a threshold where system responses exhibited change; this was set at 130g. Subsequently, from this transitional quantity, nine tests ranging through 130g to 220g were undertaken with reference to site accumulation. The smallest quantity (130g) reflects a *'moderate'* category of detritus (from the accumulation profiles). The largest quantity tested (220g) reflects *'very extreme'* detritus coverage. For each test, the filled nylon mesh was wrapped around the leaf-guard in an evenly distributed manner.

5.7.4 Test set 2: detritus blockages at baffle

From images recorded at sites, materials collected at the siphonic baffle were known to be akin to those at the leaf-guard. During initial tests it was established that detritus quantities again (i.e. as in test 1) only affected system responses at 130g. Once filled, the mesh nets were placed directly at the baffle, behind the leaf-guard.

5.7.5 Test set 3: synthetic leaf-guard blockages

Synthetic barrier *'hoops'* were manufactured from 160mm diameter PVC plastic pipe and fitted around the leaf-guard. Each hoop was accurately manufactured to represent a specific percentage blockage of the fitted leaf-guard.

The barrier heights were increased to 61.6mm (level with the vertical side of the guard). The arrangement for the plate-baffle leaf-guard is presented in Figure 5.5 and also in Table 5.1. This indicates the combinations used in progressively increasing the leaf-guard coverage. For the cup-type baffle (outlet B), Figure 5.6 and Table 5.2 present the test references for each percentage coverage.

5.7.6 Test set 4: baffle blockage

To introduce a synthetic baffle blockage for each outlet, polystyrene foam was fabricated to represent predetermined percentage blockages.

The plate-baffle employs straightening vanes encircling the opening perimeter of the discharge pipe, see Figure 5.7. Between these vanes, eight channels guide water through the opening. Collectively, six tests were undertaken as referenced in Table 5.3. Each test required the positioning of manufactured synthetic infills within the channels.

The cup-baffle, see Figure 5.8, has three rows of 10, circular perforations encircling the vertical sides with seven slots in the '*roof*'. Table 5.4 presents the representative percentage coverage for each of the seven tests. Manufactured foam was applied to simulate base and roof perforation infills while tape was adopted for vertical coverage.

5.7.7 The tests

The recording sequence was as follows; the required water flow-rate was set and the blockages positioned; the data acquisition programme was then run for an initial period of 25seconds and the supply flow started. Tests were run for a period of about four minutes after which the pump was stopped, although data were recorded until the water had been completely drained from the gutter. Each test was undertaken three times for the purposes of repeatability. In total, 1352 tests were undertaken.

5.7.8 Experimental test observations

A digital camera mounted at an inclined angle on the gutter was used to observe vortex flow at the outlet. At one point during testing, the camera was positioned directly above the outlet. The images and video capture clearly indicated the variation in vortex formation and water depths for each of the two different outlets. It was observed that water flow would encircle the plate-baffle perimeter, while for the cup-baffle, the flow must first fill the sump before a vortex forms.

5.8 Experimental results

5.8.1 General

Figures 5.9(a & b) present typical voltage outputs recorded by the data logging system, as well as the corresponding pressure and gutter depth measurements for outlet *'A'* at 5l/s. These Figures clearly indicate the cyclical response of the system even when no blockage is applied.

5.8.2 Initial outlet findings – no blockages

The most suitable way of reading all open outlet responses is from the pressure and depth data summarised in Tables 5.5(a & b). These present results for the plate-type and cup-type baffles when tested with no blockage barriers.

Each outlet tested with 1l/s to 3l/s displayed no influence on system pressures or depths, therefore the system behaved as a conventional system. Vortex formation began at 4l/s for each outlet. Figures 5.10(a & b), for outlets *'A'* and *'B'* respectively, present a summary of results when no barriers are fitted. For each outlet; it was observed that flow-rates beneath 5.0l/s offered no consistent pressure changes. At and above this flow-rate, cyclical responses were noted, and solely for the plate-baffle, a high-frequency noise was generated during testing. No noise occurred with outlet *'B'* at this early stage. Table 5.5(a & b) results indicate;

i. baffle *'A'* generated 37% less negative pressure than the cup baffle. Justification is given to Outlet *'B'* bearing a greater sump volumetric capacity;

ii. in particular for outlet *'A'*, a high degree of swirl was exhibited at the leaf-guard perimeter;

iii. at the same flow-rate, some swirl started with the cup baffle.

It is interesting to note that, at 6l/s for each outlet, a point of change occurred where an increase of negative pressure was attained. At 7l/s, outlet *'A'* again created a higher frequency noise. The cup-baffle created no noise throughout the test; postulated to be due to the operational design and specific component layout whereby all flow-rates beneath the design capacity allow air to steadily enter the system through the perforations.

At 8l/s, a larger change in vortex swirl at the outlets was observed, principally outlet *'A'*. At this flow-rate, the high frequency noise so apparent for the previous tests appeared lesser in intensity. This is attributed to air being restricted from entering the discharge pipe. At 9l/s, there was smooth operation with no noise. As a result the plate outlet behaved as siphonic theory would suggest with phasing of the flow, while outlet *'B'* exhibited laminar flow consistent with its theoretical design.

Ultimately, comparing test results has undoubtedly indicated differences in operation at different flow-rates. The following Section discusses results for blockage tests. It should be noted that flow-rates beneath 5l/s have not been included here due to the large amounts of air that are drawn into the system.

Note, this is not a comparative study between outlet design and operation, but a description of responses only within the context of this research study. The results are not to be interpreted as suggesting one outlet design is better or worse than the other.

5.8.3 Outlet A – tests with blockages

Figure 5.11(a) presents test results for *'hoops'* positioned at the leaf-guard. It was observed that blockage percentages of up to 82% have negligible effect on outlet performance and system pressure. Above 82%, it is clear that pressures generally decrease. Figure 5.11(b) also highlights this change where gutter depths, have increased. Figure 5.11(c) presents data for pressure changes when detritus is positioned at the leaf-guard. It is quite noticeable from Figure 5.11(c & d) that after 184g, considerable pressure changes occur at all flow-rates. Also, at 210g all pressure trends altered once more.

When the pressure results for detritus and synthetic blockages are compared, see Figure 5.11(e), there is a marginal overlap of data points at maximum system capacity.

Figure 5.12(a) presents the results for synthetic infill blockages at the baffle. It can be seen that as the percentage blockage increases, so too does the corresponding negative pressure. Figure 5.12(b) highlights the increase in gutter depths as blockage is increased. Visual observations confirmed lower quantities of air entrainment with larger percentage blockages at 6l/s and above. At lower percentages, air was

continually present. Figure 5.12(c) presents results for detritus positioned at the baffle where pressure changes were seen to be minimal. This may be attributed to the quantity and detritus layout in regards to the open area of the baffle. From visual observations and from Figure 5.12(d), it is known that water penetrated the baffle and still generated gutter water depths that rose quickly. Similar flow conditions were observed with detritus at the leaf-guard, where gutter depths increased quickly. Frequently, the overtopping level was approached with varying quantities of air entrained into the downpipe. Figure 5.12(e) shows a comparison of results for synthetic and *'detritus'* blockages.

5.8.4 Outlet B – tests with blockages

Figure 5.13(a) presents the synthetic barrier results for outlet *'B'*; the cup-baffle. Figure 5.13(b) indicates the rapid rise in gutter depths in response to the rapid suction of generated in the system at 75% blockage. Figure 5.13(c) indicates the results when various detritus quantities are positioned at the leaf-guard. It can be seen that system pressures varied only slightly. Figure 5.13(d) shows how, at design capacity, various detritus quantities have only marginal effect on the system response. This would imply that there is a limited amount of water passing into the pipework; confirmed by visual observations and gutter depth recordings (which increased proportionately to supply flow-rate). Figure 5.13(e) shows a comparison of results for synthetic and *'detritus'* blockage.

Figure 5.14(a) presents the findings for synthetic infills at the baffle. It can be seen from this graph that at a 93% blockage, an irregularity, whereby pressures rise to atmospheric occurs. This was due to the barriers restricting not only the air intake, but also water. Figure 5.14(c) presents the test results for detritus placed behind the leaf-guard and in front of the baffle. It is interesting to note from Figure 5.14(c & d), that changes occur at 184g.

Figure 5.14(e) shows a comparison of results for synthetic and *'detritus'* blockage.

5.9 Test data summary

This Chapter has presented details of laboratory investigations, and a discussion of results. Tests for outlet *'B'* (cup baffle) indicated that performances generally change at around 45% and at any applied blockage for outlet *'A'*. A potential reason between the performances of the outlets may be attributed to their design. Secondly, it is apparent a relationship exists between the outlet, the design and the scale of blockage as a function of supply flow-rate. All of the data collated is presented in Chapter 6 where a detailed analysis is undertaken and outlet loss coefficients derived.

Chapter 6
Derivation of outlet loss coefficients

6.1 Introduction

Laboratory testing was conducted to investigate outlet losses under various blockage conditions. It is important to identify, at this stage, the four different test sets for each siphonic outlet. Firstly, different quantities of detritus were placed at the leaf-guard. Secondly, different quantities of detritus were placed at the baffle. Thirdly, different sizes of synthetic hoops were added at the leaf-guard, with each barrier introducing percentage coverage. Finally, different sizes of synthetic barrier infills at the baffle were added, also sized on a percentage coverage.

This Chapter now discusses development of empirical outlet loss coefficients for open and partially blocked outlets derived from these laboratory investigations.

6.2 Test rig hydraulics

The total head loss within a siphonic system comprises of outlet loss, friction loss and fittings loss. The following analysis of experimental results is based on the conservation of mass, momentum and energy (in the form of Bernoulli's theory). The calculation procedures presented are therefore based on steady and uniform flow only; this means the discharge and flow depth in each segment of the laboratory rig were constant with respect to time and distance. Also, since a single downpipe has been tested, the average velocity throughout is considered to be constant.

In installed siphonic roof drainage systems, the flow at each outlet is variable, thus flow conditions are not truly steady or uniform until full-bore flow is achieved. However, since the methods used in siphonic drainage design are based on peak discharges and steady flow, it is conservative practice to use this steady uniform flow assumption.

Bernoulli's equation states that the total head *'h'* along a streamline remains constant. To analyse the flow in the test pipe, the Bernoulli equation can be applied along a

streamline from point 1 on the surface of the gutter to point 2 at the top of the discharge pipe, where:

$$\frac{P_1}{\rho g} + \frac{u_1^2}{2g} + z_1 = h = \frac{P_2}{\rho g} + \frac{u_2^2}{2g} + z_2 \qquad (6.1)$$

To calculate total head *'h'* at the gutter, P_1 = 0 (as this is atmospheric), and as the gutter water is moving very slowly compared to that in the pipe, then $u_1 = 0$.

Considering energy conservation and allowing for head loss due to friction, the total head will change. Equation (6.1) hence now includes head loss due to friction, 'h_f'.

$$\frac{P_1}{\rho g} + \frac{V_1^2}{2g} + z_1 = \frac{P_2}{\rho g} + \frac{V_2^2}{2g} + z_2 + h_f \qquad (6.2)$$

6.3 Energy losses

The siphonic outlet head loss will depend on its geometry. This loss is expressed as a velocity head, reduced by a correction factor, known as the outlet loss coefficient *'K'*. Although it is typically reported as constant, it can vary with flow. Typically, values are for near or full-flow conditions.

The energy loss is expressed as:

$$H = \frac{K\left(V_2^2 - V_1^2\right)}{2g} \qquad (6.3)$$

However, the actual depth of the approaching water ponds at the entrance, this velocity head is usually considered to be negligible. So the used expression becomes:

$$H = \frac{KV^2}{2g} \qquad (6.4)$$

6.4 Outlet loss coefficient calculation procedure

6.4.1 General

The following Sections describe how the experimental data was used to derive an outlet loss coefficient for each test undertaken.

6.4.2 Downpipe velocity

An approximation of pipework velocity is necessary to derive the outlet loss coefficient. Converting the measured pipe pressure to velocity at the top of the discharge pipe was undertaken as described below:

The flow 'Q' at any section is defined as the volume of water passing that section per unit of time, expressed as:

$$Q = VA \tag{6.5}$$

When the discharge is constant, the flow is said to be continuous and therefore.

$$Q = V_1 A_1 = V_2 A_2 = \ldots \tag{6.6}$$

where the subscripts designate different pipe locations. This equation is known as the flow continuity equation, where velocity for full-bore flow is:

$$V_1 = \frac{Q}{A} = \frac{Q}{\left(\frac{\pi D^2}{4}\right)} \tag{6.7}$$

However, these expressions are for pipes flowing full, (in this investigation, 9l/s). For the other flow-rates (8l/s and smaller), the velocity may be calculated by dividing the reduced flow-rate by the maximum value. This therefore represents a proportional value of full-flow (ACPA, 2007).

$$\frac{Flowrate}{Flowrate_{full\ bore}} \tag{6.8}$$

However this expression can only be applied when the outlet is open (free of blockage). Thus, Equation (6.9) is used also:

$$\frac{pressure}{pressure_{full\ bore}} \tag{6.9}$$

After calculating proportional values, the velocity for the test undertaken was calculated.

6.4.3 Head losses

It is necessary to have a straight forward and practical method of determining head loss coefficient for a siphonic system. A two-step procedure of estimating the total head loss has been used: Firstly the pressure drop at the outlet, based on an energy loss value due to the straight piping section and exit, was calculated. This contribution was then subtracted from the total head loss in such a way that the remaining value expresses only the outlet friction loss.

Based on the recommendations in BS8490:2007, the head losses 'Δh_o' due to the outlet is determined from:

$$\Delta h_o = H_B - \Delta h_f - \frac{V^2}{2g} \qquad (6.10)$$

when, 'H_B' is the vertical height of the pipe (m), and 'Δh_f' is the frictional head loss over the total length of the discharge pipe.

The roughness friction factors 'K_p' for the straight pipe sections are determined using the Colebrook-White equation, Equation (3.2). The value of 'K_p' is then used to calculate the frictional head loss 'Δh_f' over the total length of the discharge pipe.

Thus, the energy at the inlet and the loss coefficient, '*K*' of the outlet can be established from:

$$K = \frac{2g\Delta h_o}{V^2} \qquad (6.11)$$

The results of each test set are tabulated, one table per test set, see Tables 6.1 to 6.8, showing for each: supply flow rate, outlet coverage and the calculated outlet loss coefficient.

6.5 Results

6.5.1 General

From calculated results, a loss coefficient of 1.4 at system design capacity was established for each outlet design. Loss coefficients calculated here incorporate blockages (where noted) and also the head loss of the outlet.

6.5.2 Discussion of results

It can be seen from Tables 6.1 to 6.8 that at full-bore flow (9l/s), the loss coefficients derived for both outlets are the same, 1.4. Even at 8l/s and 7l/s the calculated results for each outlet remain very similar. However at lower flowrates (6l/s and 5l/s) discrepancies appear between results. Further, the coefficients are substantially larger at the lower flowrates, resulting in a larger energy loss. This confirms the thoughts of Arthur and Swaffield (1999c) which stated the presence of air will affect system pressures, velocity and friction losses.

It can be seen that, typically, loss coefficients for full-bore flow conditions rise with an increase in blockage coverage. However in some instances the calculated losses decrease with a higher blockage. This is attributed to a lack of water being permitted to penetrate the outlet barrier and thus restricting the water flow and sub-atmospheric pressures. Also, for both outlets, the loss coefficients became completely independent for values less than 7l/s as the air to water quantities influence the unpredictability of the results.

It can be seen that when the outlet entrance is not submerged (at lower flow-rates and with blockages) the loss coefficients are usually somewhat higher, but because of the many unknowns entering into determination of water flow, the values tabulated for the full-bore flow conditions of 9l/s for each outlet type can be used for submerged or un-submerged cases.

6.6 Comparison of theoretical values to derived

As discussed in Section 3.6, the existing expression for outlet losses in the simulation model comprise of two independent constants, these are:

$$K = 1.2 + (blockage\ percentage) \qquad (6.12)$$

where 1.2 is a typical culvert entrance loss. In general this theory is logical, however the 1.2 is a recommended value for culverts alone and the percentage blockage at the outlet is based on the outlet coverage allowing for free passage of rainwater.

These data have been plotted; see Figure (6.1 to 6.4), as a total energy loss coefficient at the outlet against outlet coverage, on each graph a range of black data points has been plotted for the theoretical blockage losses, that indicate a black steadily increasing trend, in comparison to the experimentally derived losses. It is clear a discrepancy appears between the derived and existing values at comparable blockage coverage. Further, the existing method uses a standard 1.2 for an open outlet then adds a percentage blockage: this combination gives a consistent incline of data points, while the empirically derived loss coefficients clearly indicate a different pattern. This pattern tails off, representing the effect entrainment of air has on outlet performance.

This restriction of water flow through the outlet when a blockage is applied means that, while the existing method appears logical; it does in fact assume a higher blockage loss than was experimentally derived.

6.7 Summary

Empirically derived loss coefficients established from a laboratory environment have been discussed within this Chapter. The loss coefficients derived have given a divergence of output, from existing values currently used in the simulation model.

Chapter 7
Model simulation with site data

7.1 Introduction

Site investigations have informed laboratory testing to derive empirical loss coefficients for open and partially blocked outlets. This Chapter deals with simulating the outlet loss coefficient in a Method of Characteristics based numerical model.

Laboratory tests were based on an analysis of digital images and weather station data recorded from sites and positioned within the context of enhancing representation of the outlet loss coefficient. Site images provided information on typical detritus that accumulates at siphonic outlets. Laboratory experiments involved inserting various detritus materials or synthetic percentage blockages at the siphonic outlet to simulate how accumulation affects performance. Pipework pressure and gutter depths were recorded. Loss coefficients where then calculated.

An indication of the impact upon performance, assessed using the simulation software, is presented within this Chapter.

7.2 Detritus accumulations

One of the key benefits of siphonic systems is that of flow distribution between outlets draining the same gutter if one becomes blocked. Unfortunately, the gutters at the National Records building do not have this design feature, since the two-outlet system (West) has a separator plate between each gutter. As such, it may potentially have been fortuitous to have one gutter supplying both outlets, where flow distribution may potentially have lowered the risk of gutter overtopping.

Images also reported that blockages do frequently occur and established that although leaves, feathers and twigs were present, the majority of the accumulation at the two outlets is presented by emulsification or solidification of dust, dirt and organic matter.

7.3 Cases of detritus movement

Chapter 4 presented the findings of the onsite monitoring program at two siphonic roof drainage sites in Scotland. The aims of the site monitoring were to establish the type and rate of detritus build-up at outlets over time. Further, the study recorded, via pressure transducers and gutter depth sensors, the corresponding pressure transients and gutter depths during a period of significant rainfall and/or priming. Chapter 4 also noted how site location, weather parameters and maintenance schedules affect detritus accumulations. Also that detritus can and does build-up rapidly, and that detritus wash through and outlet displacement can occur in different circumstances.

As presented in Figures 4.7(b) and 4.10(b), detritus accumulation profile graphs for each monitored outlet have been established based on the recorded site images. These accumulation graphs were then mapped to weather recorded data, i.e. rainfall, air temperature, wind direction and velocity. A full analysis was carried out on circumstances of interest, where detritus classification changed significantly. These *'incidents'* are presented in Figures 7.1 to 7.4, which indicate the rainfall intensity values for the short duration periods of time as highlighted in bold on Figures 4.7(b) and 4.10(b). Figures 7.1(a & b) present data for a classification change 1 to 4, for the dates 11th May 2010 until 24th May 2010 (14 days inclusive), Figure 7.2(a & b) for a classification change 2 to 6, for dates 10th June 2011 until 24th June 2011 (15 days inclusive) and Figure 7.3(a & b) presents a classification change 3 to 6, for dates 5th June until 22nd June 2011 (18 days inclusive).

Further, Figure 7.4 presents the findings for a period of possible wash through or displacement for System 1-West for a classification change 5 to 3, for dates 1st November until 16th November 2010 (16 days inclusive).

The analysis of the results indicated:

i. detritus can and does accumulate relatively quickly;

ii. higher intensity rainfall events do appear to increase detritus levels;

iii. generally, a larger number of rainfall events do appear to increase accumulation;

iv. gutter wash through or displacement does occur;

v. blockages can affect system operation, where gutter overtopping has occurred.

The site findings then informed the laboratory experiments that followed.

7.4 Outlet loss coefficient findings

The influence of blockage at a siphonic outlet is known to substantially alter the pressure response of the system, where the relationship is dependent upon the extent of coverage. Much of the theory on outlet losses assumes a constant flow relationship in relation to losses and percentage blockage with no variation. However, the flow rate in the system will constantly change with percentage blockage.

It was established that the total head loss within a siphonic system comprises of outlet loss, friction loss and fittings loss. The analysis of experimental results undertaken was based on the conservation of mass, momentum and energy (in the form of Bernoulli's theory). As such the calculation procedures were based on steady and uniform flow only, this means the discharge and flow depth in each segment of the laboratory rig were constant with respect to time and distance. It should be noted however, that in actual siphonic roof drainage systems, the flow is variable. This means flow conditions are not truly steady or uniform until full-bore flow is achieved.

Laboratory experiments comprised four blockage test sets, where either a blockage (synthetic or detritus) was positioned at the leaf-guard or baffle and supplied with a pre-set flow-rate. Pipe pressures and gutter depths were recorded. Test results confirmed that blockages do alter system pressures. However, empirically derived loss coefficients (from these laboratory investigations) indicated a divergence of system responses from the original concept of applying a standard 1.2 *'K'* value then adding a percentage blockage. As the theoretical energy loss at the outlet displays a linear relationship with blockage increase, the loss coefficients derived show a declining curve. Also, and possibly more important, at the larger percentage blockages, the theoretical losses continue on the straight slope, but the derived losses tend to atmospheric pressure, indicating the systems response to the suction of air and a restriction of water. This implies that the existing method would over estimate the energy loss at the outlet and thereby impose a lower water intake than would actually occur.

7.5 Site data

The data established from site have clearly indicated the extent of blockage at any given siphonic outlet may be significant. This is particularly true at the National Records building. Images have indicated outlet blockages generally consisted of leaves, feathers and twigs with the majority of the accumulation presented by emulsification or solidification of dust, dirt and organic matter. As such, to establish further the effect a blockage has on system operation, a chosen rainfall event and its influence on system 1-West has been compared to output results from a numerical model.

7.6 Simulation

As discussed, the Method of Characteristics approach has been recognised as a suitable technique by which to address unsteady flow conditions such as those that exist within a siphonic system. The ROOFNET model in which the outlet loss coefficients may be used was part of an application of the method of characteristics technique to siphonic analysis developed at Heriot Watt University. The model was set up with the design and specification of the National Records building System 1-West, as presented in Figure 4.1(b) with a 10 minute rainfall event with a 5 year return period (the recommended return period for a city based commercial property). Rather than using an average steady rainfall intensity, a more representative rainfall event has been used, with a 50% summer profile (symmetrical and single peaked), Figure 7.5. This '*bell-shape'* rainfall intensity is presented in the flood studies report and is recommended by the Wallingford Procedure.

7.7 Results and discussion

The site investigations have indicated accumulation extent at an outlet may be significant enough to affect system operation. Simulation output, Figure 7.6, compares both pipe pressures and throughflow rates for the downpipe of the system when the index outlet is completely unobstructed and when a significant blockage is presented. This highlights how the pipe pressure is notably lower when the blockage loss is imposed, in this case altering the peak negative pressure from -3.6mH20 to -5.6mH20. At the same time it can be seen that the pipe flow through is around 1.1l/sec less. Thus the simulation output illustrates how the restriction imposed at the outlet reduced the rainwater throughflow, but subsequently increases the negative pressure. This scenario creates a set of circumstances that could pose considerable risk to the integrity of the system and potentially the building.

As can be seen from Figure 7.5, the 10 minute design storm used in the model peaks at 300 seconds at 130mm/hr. Reviewing the recorded data from site, and finding a similar rainfall intensity as that used in the model, an example of a rainfall event with a peak intensity of approximately 150mm/hr (for a short duration) was identified and shown in Figure 7.7.

It should be noted that there is standing water in the gutter (as established from images) prior to this rainfall event. Generally, a detritus build-up will have a degree of porosity (allowing some water to pass naturally into the system) which is frequently an insufficient head for this to reduce levels significantly. This combination of reduced capacity, as illustrated in Figure 7.6, and depth of standing gutter water quickly results in an increased reduction of water throughflow into the system, and also significant gutter overtopping.

7.8 Summary of chapter findings

Although the data discussed in this text have focused on System 1 at the National Records building, Edinburgh, it is possible to draw wider conclusions.

It has been found that a design storm and rainfall intensity recorded from site cannot be directly matched, however it is possible to assess the operation of an installed system by matching, as closely as possible, event based peak intensities. Further, this Chapter highlights the need for a periodic maintenance regime. Also, the extent of detritus build-up at siphonic system outlets may be important to building owners and facility managers in planning scheduled gutter cleaning. The measured shift of loss coefficients and flow performance (post-installation) may be an important aspect for consideration with designers.

7.9 Concluding remarks

This Chapter has effectively brought the outcomes of the proceeding Chapters to a conclusion. An example of a rainfall event recorded from the National Records building has been mapped to simulation model predictions using a symmetrical single peaked summer rainfall profile. Results have also shown how an outlet blockage alters system performance, thereby altering system working capacity.

Chapter 8
Conclusions and recommendations for further work

8.1 Summary

Commonly, loss coefficients are provided by manufacturers for siphonic outlets. This allows design and simulation of the system. However, investigations into detritus accumulation at outlets and the impacts upon the loss coefficient are uncommon. This thesis was addressing this issue as described below:

Chapters 1 and 2 provided an introduction to the basic concept of siphonic rainwater drainage systems, discussing the causes of system failure and how the climate may affect system operation. A literature review charted early developments of siphonic system concepts through to current research. Hydraulic principles were also outlined.

Industrial and research-based modelling techniques used for designing and assessing siphonic systems were discussed in Chapter 3. This highlighted how many industry models are based on assuming instantaneous full-bore steady flow throughout the system and how research models can simulate unsteady flow. The history and development of the Method of Characteristics and the MacCormack technique was outlined.

To gather information on the extent and impact of blockages on siphonic outlets, monitoring equipment was installed at two sites, Chapter 4. Cameras monitored detritus accumulations over time, while a fully-equipped weather station, capable of monitoring temperature, wind direction/ velocity and rainfall allowed a mapping of weather conditions to recorded images. Images also indicated the materials that typically accumulate, and this informed the laboratory experiments.

Chapter 5 described the laboratory experiments undertaken with the aim of deriving loss coefficients for each outlet-type. It discussed the test rig and measuring apparatus.

Results were analysed and discussed. Reasons for different system responses between the two outlets where given.

The derivation of outlet loss coefficients were described in Chapter 6. Head loss coefficients were expressed as experimental values based on flow velocity and pressure loss. Resulting outlet loss coefficients where also compared with those used in the numerical simulation model.

Chapter 7 reported simulation results for one siphonic system at the National Records building, Edinburgh. Overall the results show how a blockage alters the performance of the system through impact on the '*operational'* loss coefficient of the outlet. The degree of blockage clearly indicated the change in working capacity of the system.

8.2 Conclusions

This research has focused on representation of fundamental outlet loss coefficients for open or partially blocked siphonic outlets. The thesis has shown:

i. detritus accumulation can, and does, occur with only relatively low intensity rainfall events;

ii. high intensity rainfall events do result in a direct increase in detritus accumulation. Although not necessarily common, there is nonetheless clear evidence of a gutter wash effect;

iii. although difficult to establish categorically, there does seem to exist a relationship between a larger number of rainfall events and an overall increase in detritus accumulation;

iv. gutter wash through or detritus displacement can, and does, occur. Without continuous monitoring of a greater proportion of the gutter system, it is difficult to tell whether a reduction in detritus is due to wash through or to displacement, however this finding is significant;

v. from the monitored pipework pressures, it has been shown that each siphonic system has become depressurised during operation, this ability indicates self-cleansing velocities are achievable;

vi. from the camera images, it has been shown that better maintenance of gutter outlets is necessary to prevent system failure;

vii. it was established that each outlet tested in the laboratory is substantially different in terms of operating characteristics and response to blockages;

viii. the laboratory apparatus has been found to provide accurate results in determination of loss coefficients;

ix. empirically derived loss coefficients are both significant and critical within the numerical simulation model.

8.3 Recommendations for further work

The aim of the work discussed herein was to examine how weather parameters contribute to the performance of siphonic roof drainage systems by studying the type and rate of detritus build-up at outlets over time. This work has shown that a number of variables do exist which influence detritus build-up. Numerical modeling of outlet loss coefficients has been undertaken using a Method of Characteristics based simulation model.

There are, however, six areas where it is felt further work may prove useful:

Firstly, two outlet-types were examined; it is felt similar tests could be conducted with other outlet-types. This would allow further data gathering for each test situation, which in turn would allow the simulation program to model a wider range of systems.

Secondly, the site monitoring considered mostly technical and environmental aspects, but consideration could be given to the influence of birds roosting on outlet accumulation. It is suggested that a full bird season could be monitored to highlight the effect the breeding cycles have on detritus accumulation.

Thirdly, each siphonic site monitored had a different baffle type from the other. It is suggested that for a direct comparison and understanding of siphonic operation, similar baffle type installations could be monitored.

Fourthly, the current study was undertaken for an 18month period. It is suggested that a much longer period of monitoring be undertaken to attribute and categorize environmental parameters to detritus accumulation.

Fifth, laboratory testing was undertaken with steady flow intensities and blockages. It is suggested that variable flow and blockages be tested, as this may represent site conditions more realistically. These tests could then possibly derive variable loss coefficients rather than constant losses derived within.

Finally, incorporation of UKCP09 precipitation data to the simulation model would allow a system assessment for predicted climate change.

8.4 General

This final Chapter has summarised the site results, laboratory investigations and simulation results. The Chapter has also discussed the aims and objectives as outlined in Chapter 1 and has presented conclusions and recommendations for further work.

References

American concrete pipe association,. (ACPA). 2007. *'Concrete pipe design manual'*.

Aeini, F, & Mahmoudi, F,. 2010. *'Classification and numbering of posterior teeth in bitewing dental images'*. 3rd International Conference on Advanced Computer Theory and Engineering (ICACTE).

Alves, G, E,. 1954. *'Concurrent liquid-gas flow in a pipeline contractor'*. Chemical engineer prog. 50.449.

American society of plumbing engineers, Design Standards Committee, Working committee 45, *'Siphonic roof drainage Draft 3'*. January 2006.

Arthur, S, Swaffield, J, A, & May, R, W, P,. 1998. *'Priming of a siphonic rainwater drainage system'*. Proceedings of Water Supply and Drainage for Buildings CIB W62 1998. Rotterdam. Netherlands.

Arthur, S, & Swaffield, J, A,. 1999. *'Numerical modelling or siphonic rainwater drainage systems – the role of air in the system'*. Proceedings of 8th International Conference on Urban Drainage, 1999, IWA Sydney, Australia.

Arthur, S, & Swaffield, J, A,. 2000. *'Onsite evaluation of an installed siphonic roof drainage system'*. Proceedings of Water Supply and Drainage for Buildings CIB W62 2000. Rio de Janeiro, Brazil.

Arthur, S, & Wright, G, B,. 2001. *'Siphonic roof drainage system analysis utilising unsteady flow theory'*. Building and Environment **36**(2001); 939-948.

Arthur, S, & Swaffield, J, A,. 2001. *'Siphonic roof drainage: current understanding'*. Urban water **3**(2001); 43-52.

Arthur, S, & Swaffield, J, A,. 2001(a). *'Siphonic roof drainage system analysis utilising unsteady flow theory'*. Building and Environment **36**(2001); 939-948.

Arthur, S, Wright, G, B, & Swaffield, J, A,. 2005. *'Operational performance of siphonic roof' drainage systems'*. Building and Environment **40**(2005); 788-796.

Arthur, S, & Wright, G, B,. 2005. *'Recent and future advances in roof drainage design and performance'*. Building Services Engineering Research and Technology **26**(2005); 337.

Arthur, S, & Wright, G, B,. 2007. *'Siphonic roof drainage systems-priming focused design'*. Building and Environment **42**(2007); 2421-2431.

Bowler, R, & Arthur, S,. 1999. *'Siphonic roof rainwater drainage – design considerations'*. Proceedings of Water Supply and Drainage for Buildings CIB W62 1999. Edinburgh, Scotland.

Bramhall, M, A, & Saul, A, J,. 1998. *'Examination of the performance of siphonic rainwater outlets'*. Proceedings of Water Supply and Drainage for Buildings CIB W62 1998. Rotterdam, Netherlands.

Bramhall, M, A,. 2005. *'The Performance of siphonic rainwater outlets within gutters'*. PhD Thesis, University of Sheffield, England.

Bramhall, M, A, & Saul, A, J,. 1999. *'The hydraulic performance of siphonic rainwater outlets relative to their location within a gutter'*. Proceedings of Water Supply and Drainage for Buildings CIB W62 1999. Edinburgh, Scotland.

British European Standard, BSEN12056-3:2000. *'Gravity drainage systems inside buildings: roof drainage, layout and calculation'*. UK: British Standards Institution: UK.

British Standard, BS8490:2007. *'Guide to siphonic roof drainage systems'*. British Standards Publishing Limited: UK.

British Standard, BS6367:1983. *'Code of practice for drainage of roofs and paved areas'*. British Standards Publishing Limited: UK.

British Standards Institution (BSI). CP 308:1974. *'Drainage of roofs and paved areas'*.

Building research station digest. 116:1958. *'Roof drainage'*.

Escarameia, M, & Swaffield, J, A,. 1999. *'Prototype monitoring and numerical simulation of roof gutter systems'*. Proceedings of International conference on urban storm drainage, Sydney, Australia.

Evangelisti, G,. 1969. *'Waterhammer analysis by the method of characteristics'*. L'Energia Ellectrica Vol **10**(1969); no. 10-12.

Fox, J, A,. 1968. *'The use of the digital computer in the solution of waterhammer problems'* Proceedings I.C.E. (39).

Fox, J, A,. 1989. *'Transient flow in pipes, open channels and sewers'*. Ellis Horwood.

Fullflow accessed 2011.
http://www.fullflow.com/pages/research-development/

Geberit,. 2010. *'System specification clauses'*. Geberit Pluvia system.

Idelchik, I, E,. 1986. *'Handbook of hydraulic resistance'*. Hemisphere Publishing Corporation, Washington.

Jack, L, B,. 1997. *'An investigation and analysis of the air pressure regime within building drainage vent systems'*. PhD. Thesis, Heriot-Watt University, Edinburgh.

Jameson, A, Schmidt E, Turkel E. 1981. *'Numerical solutions of the Euler equations by finite volume methods using Rungu-Kutta time stepping schemes'*. Proceedings of AIAA 14th fluid and plasma dynamics conference, Palo Alto, USA.

Lister, M,. 1960. *'Numerical solutions of hyperbolic partial differential equations by the method of characteristics'*. In: Ralston, A, Wilf, H,S,. editors. Numerical Methods for Digital Computers, Wiley, New York.

Lockhart, R, W, Martinelli, R, C,. 1949. *'Proposed correlation of data for Isothermal two-phase, two component flow in pipes'*. Chemical Engineering Progress, **45**(1949) no.1.

LORO, 2004. *'Siphonic Roof Drainage Systems'*. LORO-DRAINJET* Drainage system technical manual.

Lucke, T, & Beecham, S,. 2009. *'Cavitation, aeration and negative pressures in siphonic roof drainage systems'*. Building Services Engineering Research and Technology **30**(2009); 2, 103-119.

Lucke, T, & Beecham, S,. 2010. *'Capacity loss in siphonic roof drainage systems due to aeration'*. Building Research and Information **38**(2010); 2, 206-217.

MacCormack R, W,. 1971. *'Numerical solution of the interaction of a shock wave with laminar boundary layer'*. Proceedings of 2nd International Conference on Numerical Methods in Fluid Dynamics, 1971, Berlin, Germany.

May, R, W, P,. 1995. *'Design of conventional and siphonic roof drainage systems'*. Proceedings of Public Health Services in Buildings – Water Supply, Quality and Drainage, IWEM, London.

May, R, W, P & Escarameia, M,. 1996. *'Performance of siphonic drainage systems for roof gutters'*. Report SR463 Wallingford: HR Wallingford.

May, R, W, P,. 2003. *'Manual for the design of roof drainage systems – a guide to the use of European Standards BS EN 12056-3:2000'*. Report SR620 HR Wallingford.

May, R, W, P,. 2004, *'Design criteria for siphonic roof drainage systems'*. Report SR 654 HR Wallingford.

McDougall, J, A,. 1995. *'Mathematical modelling of solid transport in defective building drainage systems'*. PhD. Thesis, Heriot-Watt University, Edinburgh.

Miller, D, S,. 1990. *'Internal Flow Systems'*. BHR Group, Cranfield, England 2nd Edition.

Öngoren, A, & Materna R,. 2006. *'Multi-phase flow characteristics of siphonic roof drainage system under part load conditions'*. Proceedings of Water Supply and Drainage for Buildings CIB W62 2006. Taipei, Taiwan.

Slater, J, A, Cockerham, G, & Williams, P, D,. 1999. *'Loss factors in siphonic roof drainage'*. Proceedings of Water Supply and Drainage for Buildings CIB W62 1999. Edinburgh, Scotland.

Snoad, P,. 2009. *'Syphonic roof drainage – how does it work'*. Technical manual siphonic roof drainage explained.

Sommerhein, P,. 1999. *'Design parameters for roof drainage systems'*. Proceedings of Water Supply and Drainage for Buildings CIB W62 1999. Edinburgh, Scotland.

Swaffield, J, A, & Boldy, A, P,. 1993. *'Pressure surge in pipe and duct systems'*. Aldershot: Avebury Technical, Aldershot: Ashgate Publiching Ltd.

Swaffield, J, A, Escarameia, M, & Campbell, D, P,. 1998. *'Unsteady roof gutter flow: Development and application of simulation'*. Building Services Engineering Research and Technology **20**(1998); 1, 29-39.

Swaffield, J, A, & Campbell, D, P,. June 2003. *'Evaluation of the dynamic balancing of siphonic roof rainwater drainage networks'*. (EPSRC Grant Reference: GR/M66424/01).

UV systems, 2005. *'Manual for roof drainage'*

UV systems accessed 2011.
http://www.uv-system.com/background.html

Verein Deutscher Ingenieure (VDI) 2000. *'Roof drainage with siphonic systems'*. (3806); German Institute of Engineers Siphonic Roof Design Manual.

Wearing, M,. 2005. *'Siphonic roof drainage'*. Metal gutter manufacturers association– Information data leaflet, November 2005.

Wright, G, B, Swaffield, J, A, & Arthur, S,. 2002. *'The performance characteristics of multi-outlet siphonic roof drainage systems'*. Building Services Engineering Research and Technology **23**(2002); 3, 127-141.

Wright, G, B, Arthur, S, & Swaffield, J, A,. 2006. *'Numerical simulation of the dynamic operation of multi-outlet siphonic roof drainage systems'*. Building and Environment **41** (2006); 1279-1290.

Wylie, E, B, & Streeter, V, L,. 1979. *'Fluid mechanics'*. 7th Edition McGraw Hill, New York.

Illustrations for Chapter 1.

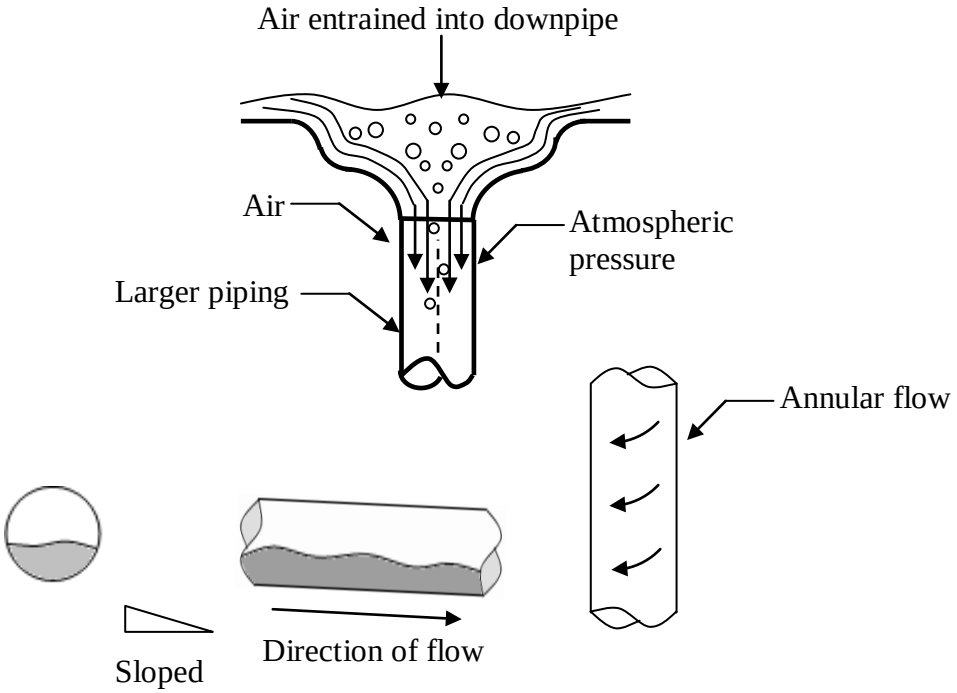

Figure 1.1(a) Conventional gravity system.

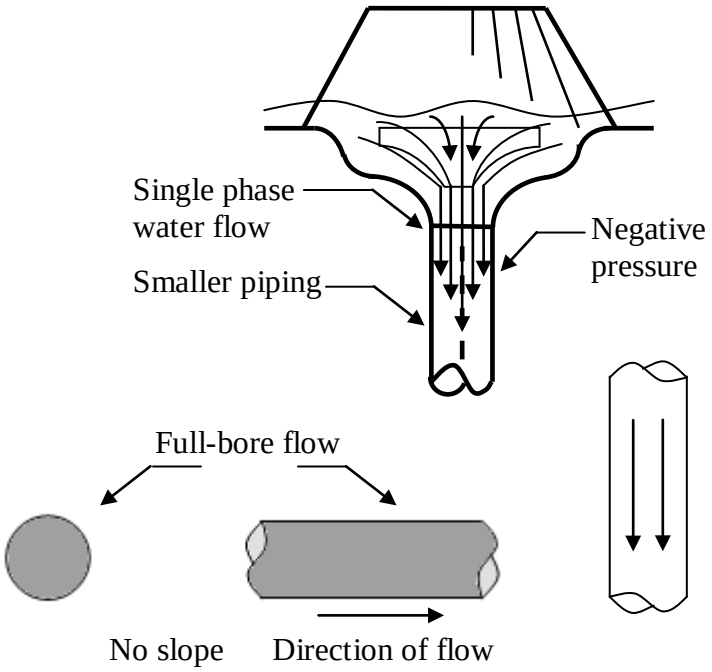

Figure 1.1(b) Siphonic roof drainage system.

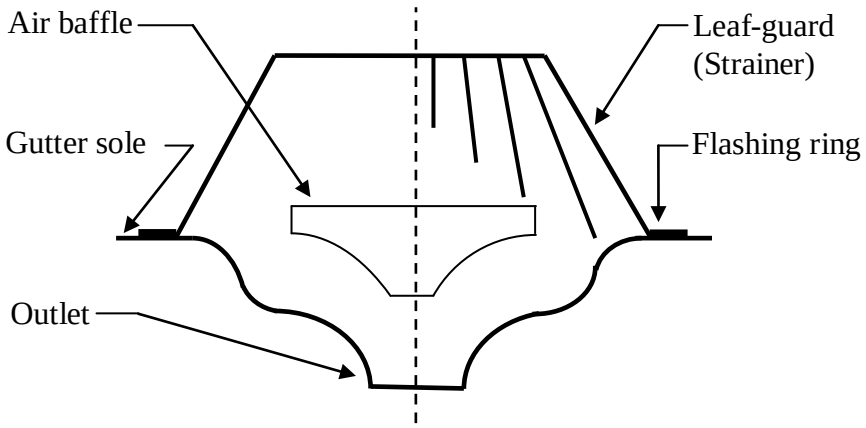

Figure 1.2 Typical siphonic roof outlet design.

Illustrations for Chapter 2.

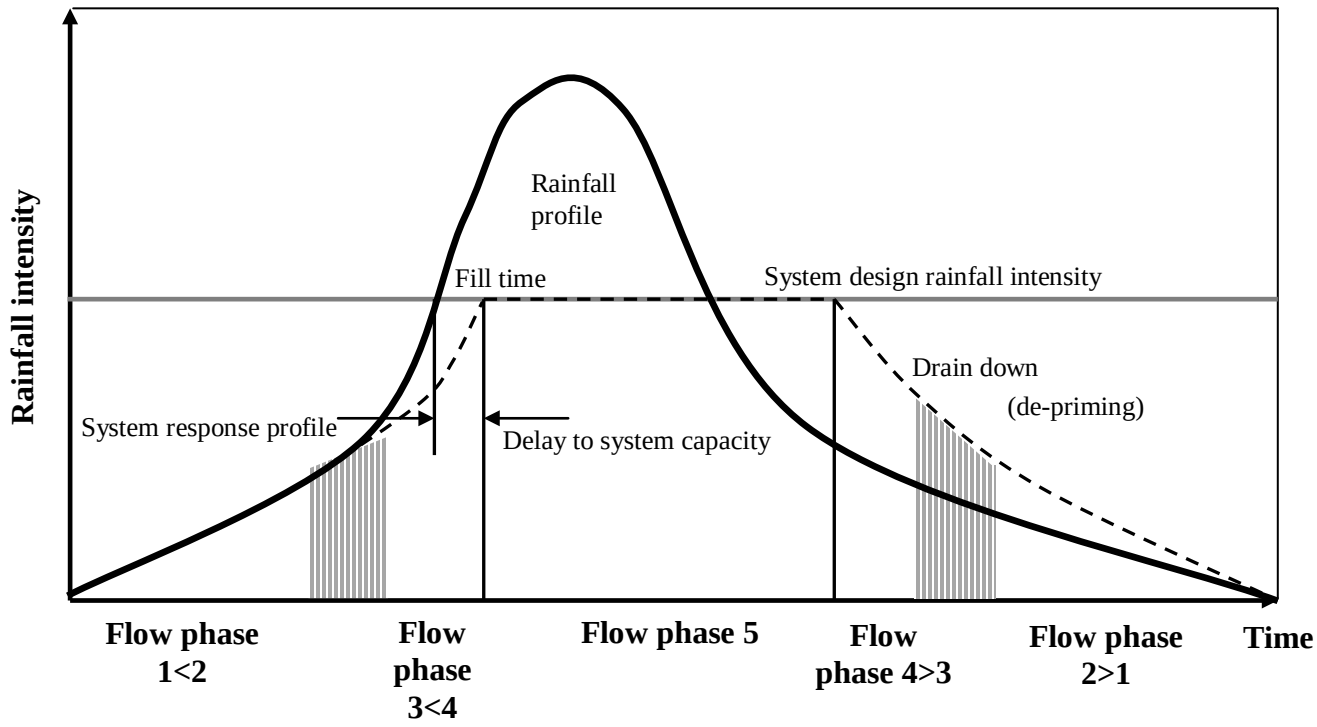

Figure 2.1 Typical system self-priming profile (UV-System 2008, annotations by author).

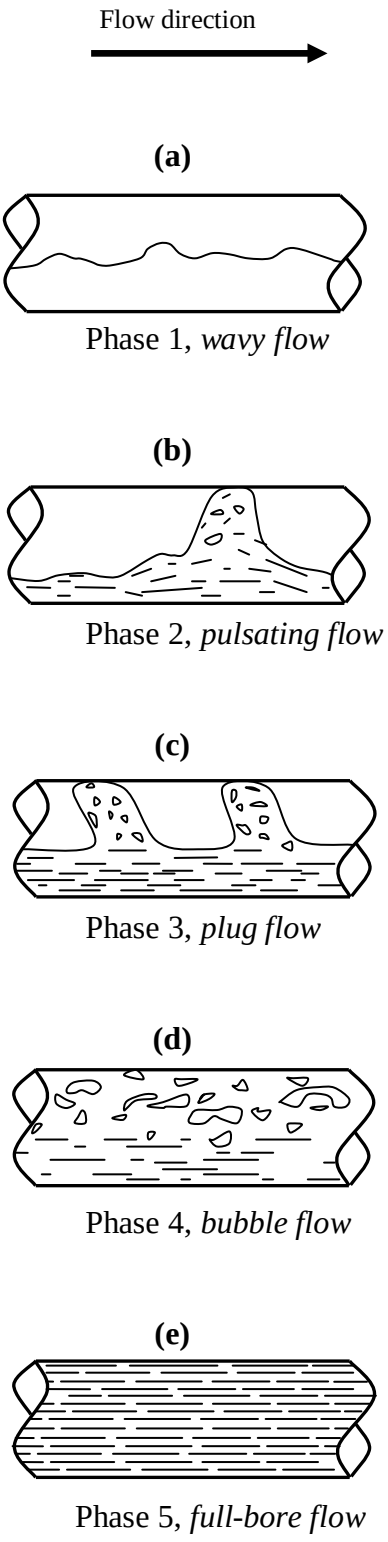

Figure 2.2(a to e) Flow development in horizontal-pipe (UV-Systems, 2008).

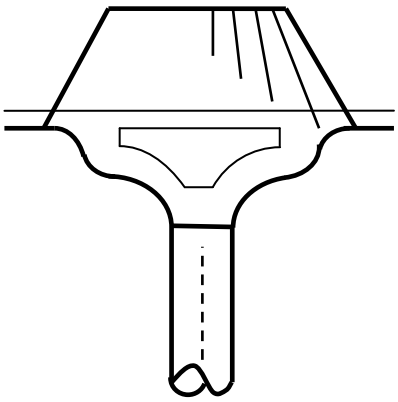

(a)

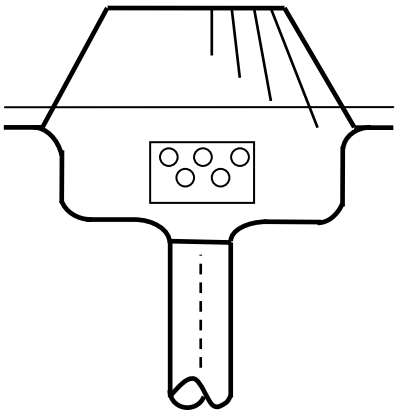

(b)

Figure 2.3(a&b) Plate and cup-baffle respectively.

Illustrations for Chapter 3.

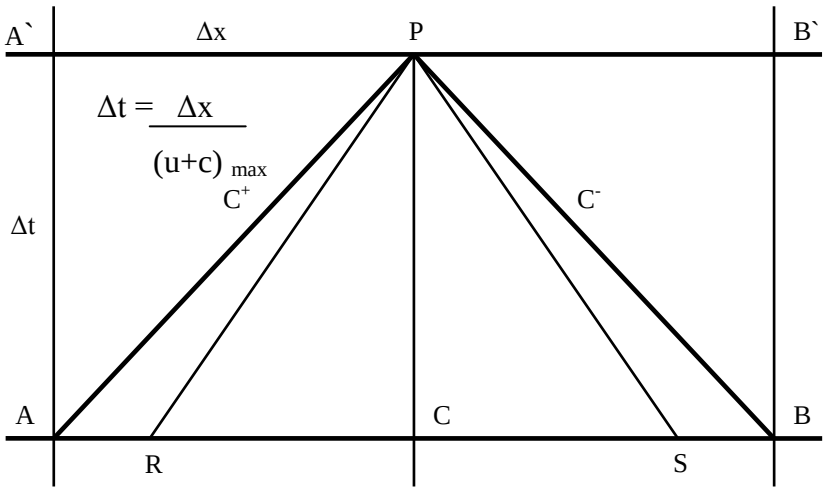

Figure 3.1 Method of Characteristics grid approach to pressure transient modelling.

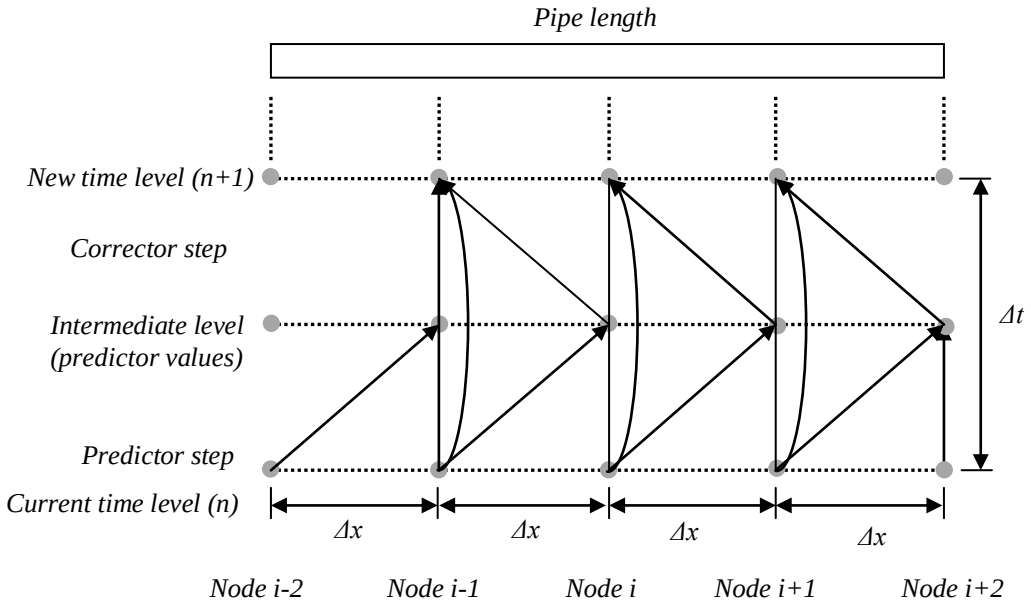

Denotes:

Pipe node

Information route (data from one node passed to another node)

Figure 3.2 The MacCormack solution method.

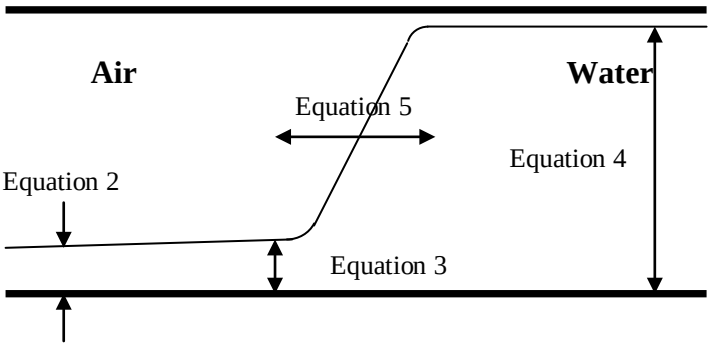

Figure 3.3 Hydraulic jump that forms at the upstream end of the system (Arthur and Swaffield, 1999).

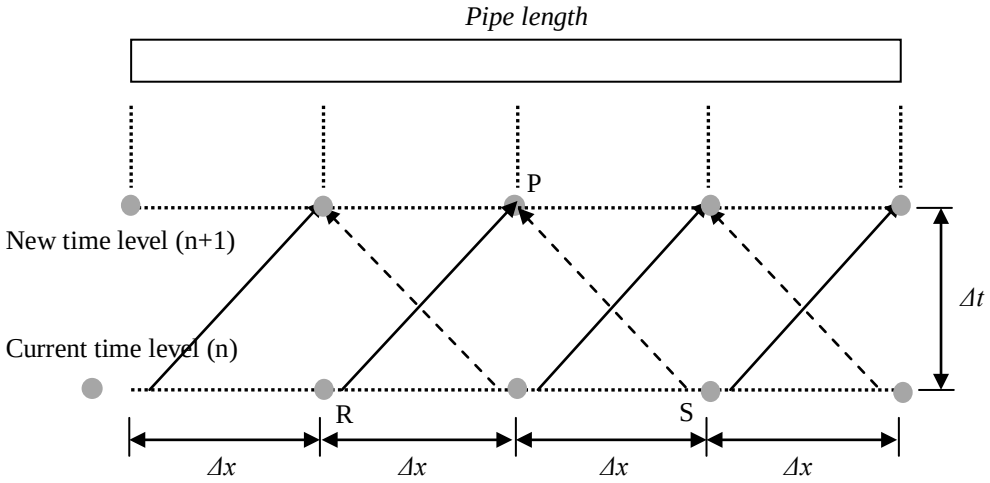

Denotes:

Pipe node

C^+ characteristic (downstream information route from one time level to the next time level)

C^- characteristic (upstream information route from one time level to the next time level)

Figure 3.4 Method of Characteristics applied to full-bore flow conditions (Wright *et al*, 2006).

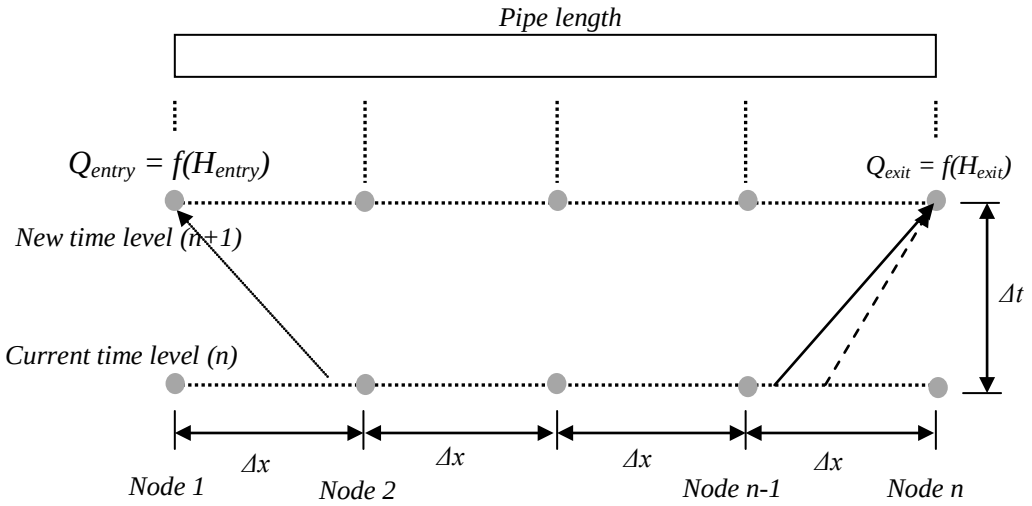

Denotes:

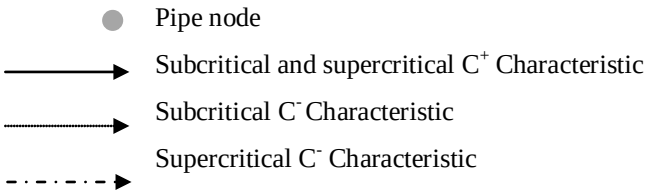

Figure 3.5 Boundary solution using either the MacCormack method or the Method of Characteristics.

Illustrations for Chapter 4.

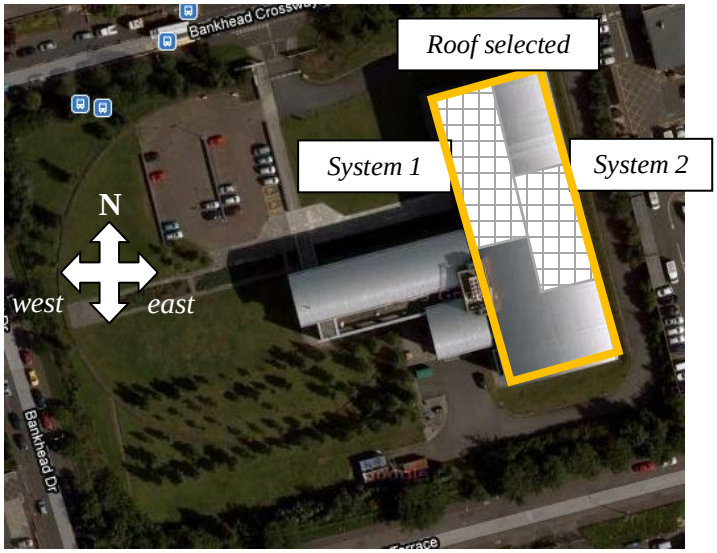

Figure 4.1(a) NRS site layout, showing coverage of siphonic systems (Google earth).

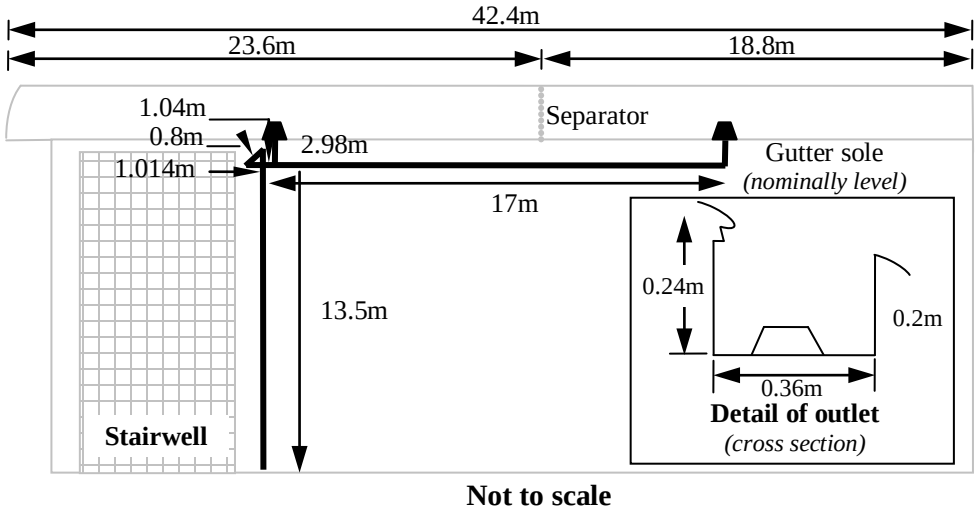

Figure 4.1(b) NRS, System 1-West elevation.

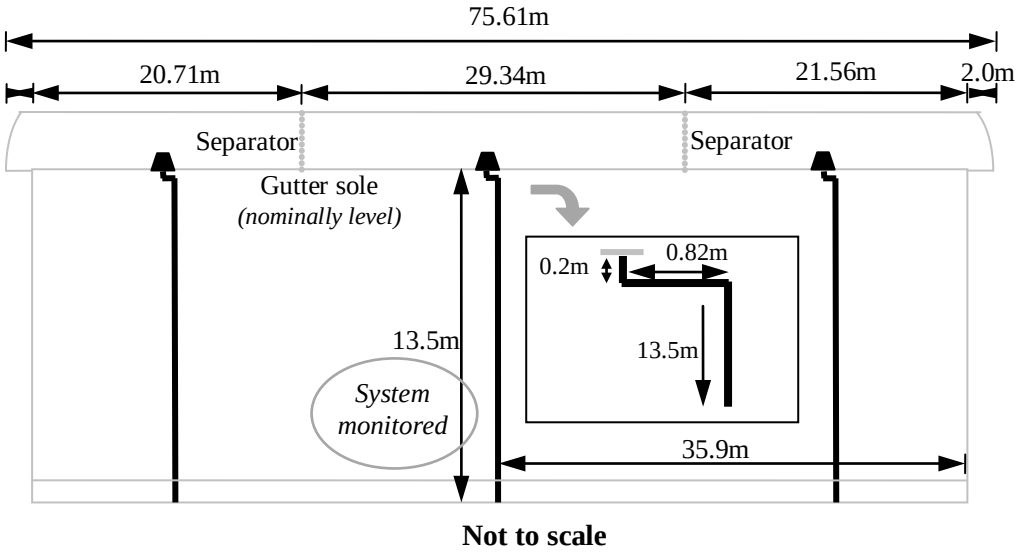

Figure 4.1(c) NRS, System 2-East elevation.

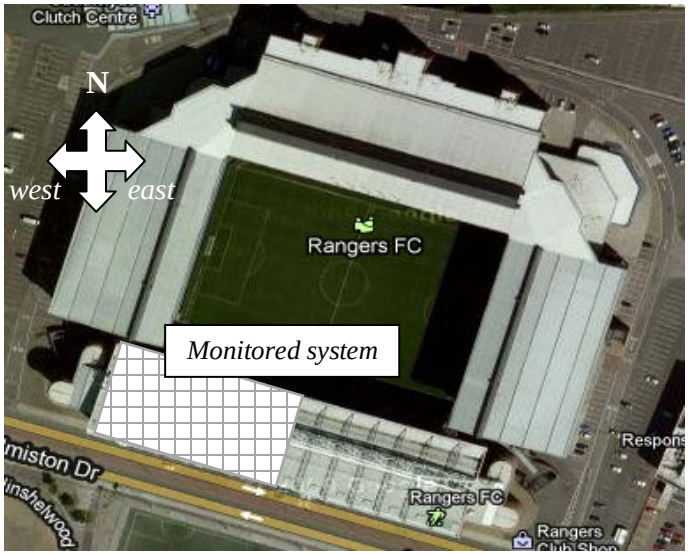

Figure 4.2(a) Ibrox stadium site layout, showing coverage of siphonic system (Google earth).

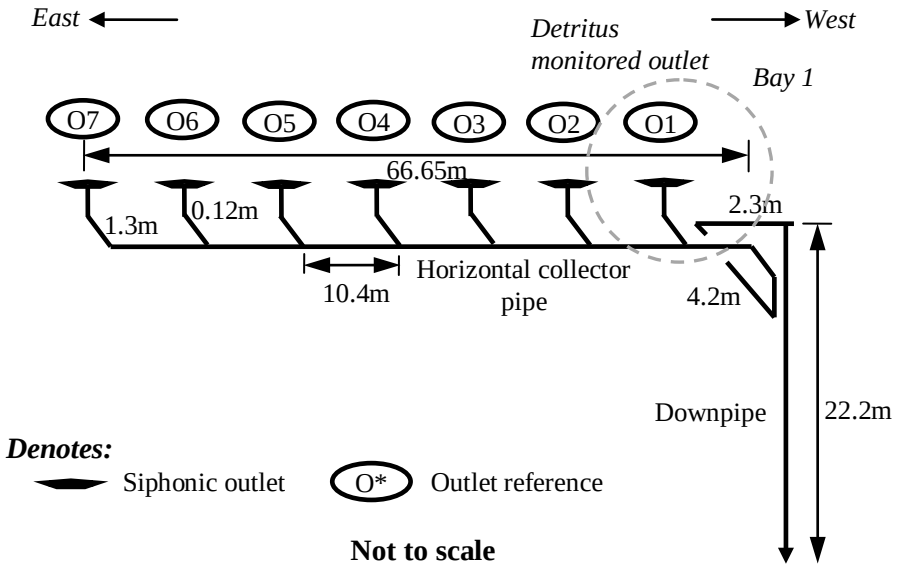

Figure 4.2(b) Ibrox stadium, schematic.

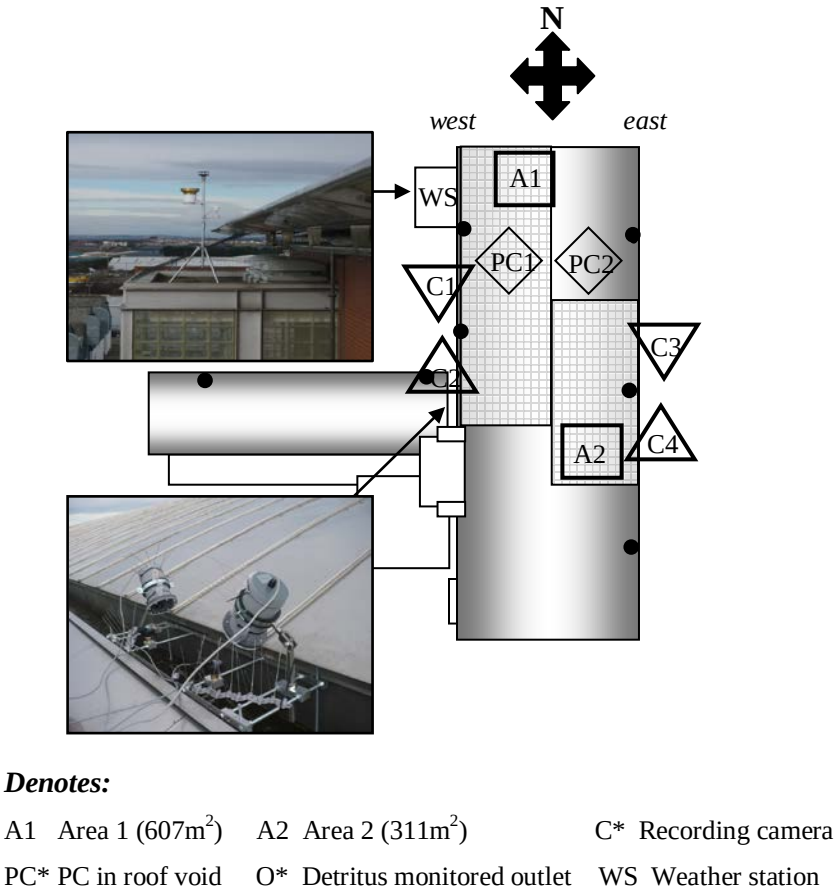

Figure 4.3(a) NRS, layout of monitored areas.

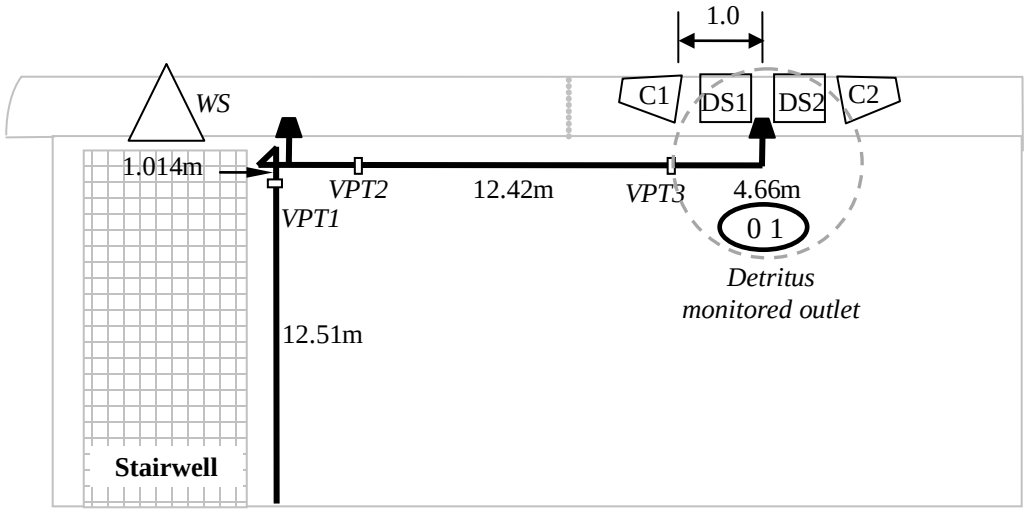

Denotes: **Not to scale**

01	Detritus monitored outlet	VPT*	Pressure transducer
DS*	Depth sensor	C*	Recording cameras
WS	Weather station		

Figure 4.3(b) NRS, System 1-West: Instrumentation.

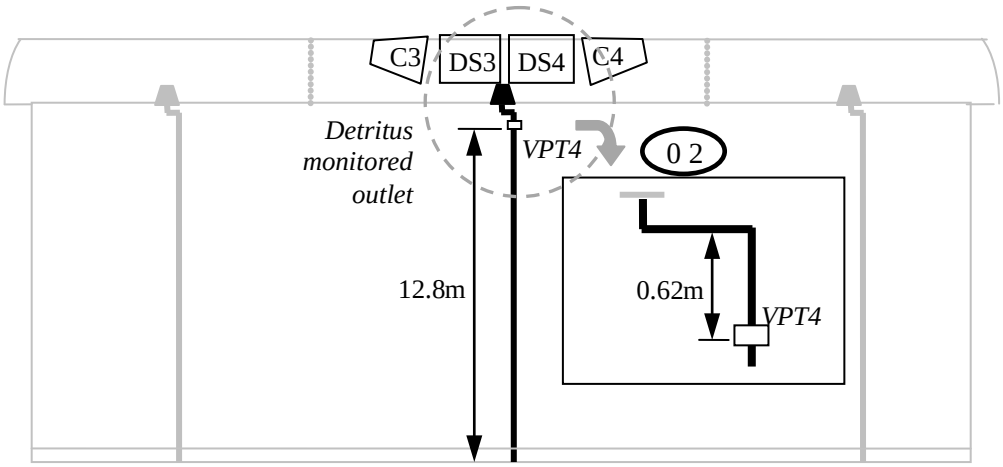

Denotes: **Not to scale**

02	Detritus monitored outlet	VPT*	Pressure transducer
DS*	Depth sensor	C*	Recording cameras

Figure 4.3(c) NRS, System 2-East: Instrumentation.

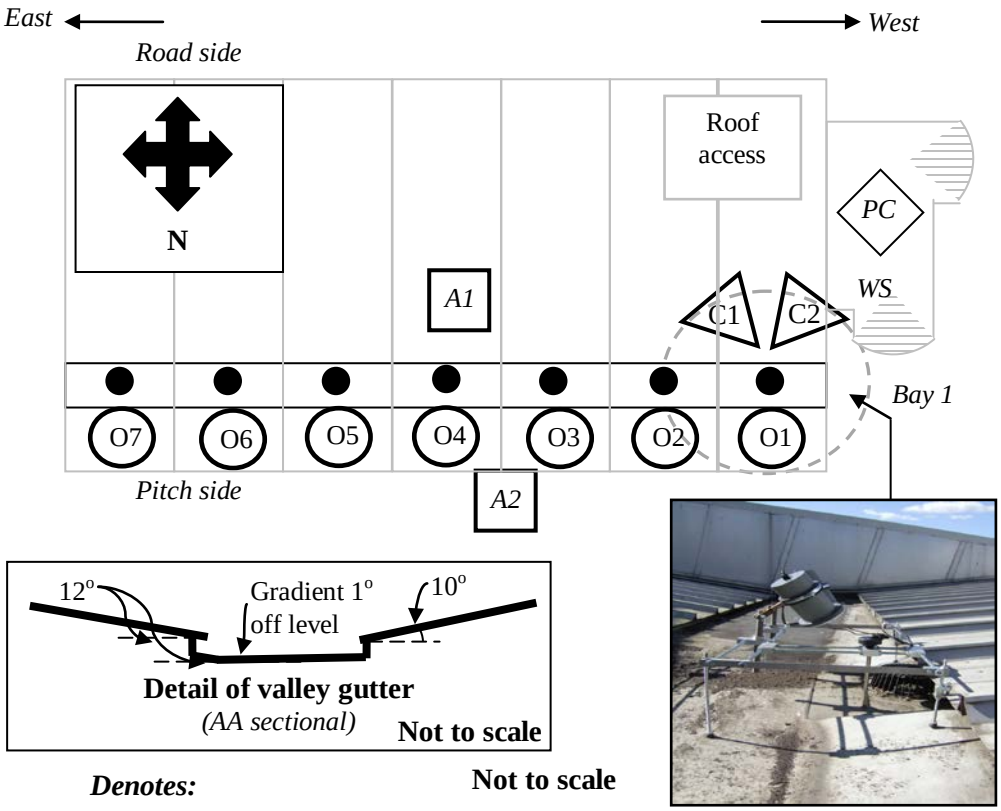

Figure 4.4(a) Ibrox stadium, layout of monitored area.

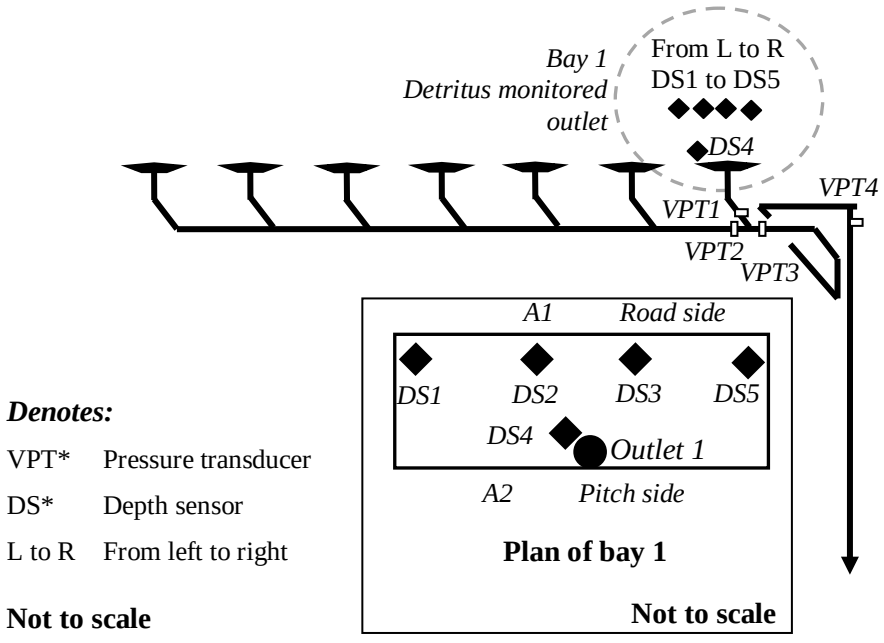

Figure 4.4(b) Ibrox stadium, instrumentation.

Date	Total *'days of rain'*	Rainfall (mm/hr)							
		1<5	6<10	11<20	21<30	31<40	41<50	51<100	101<
2010									
March	18	41	6	3	1	0	0	0	0
April	19	36	2	3	0	0	0	0	0
May	27	42	7	1	3	1	0	0	0
June	9	60	5	3	0	0	0	0	0
July	18	59	13	4	0	0	0	0	0
August	16	52	6	5	1	1	0	0	0
Sept	15	49	7	2	3	1	0	0	0
Oct	11	53	4	0	0	0	0	0	0
Nov	18	51	5	1	2	0	0	0	0
Dec	5	4	0	0	0	0	0	0	0
2011									
Jan	8	9	1	0	0	0	0	0	0
Feb	26	51	8	5	3	5	2	0	0
March	11	34	6	13	4	3	3	0	0
April	16	43	3	5	2	2	0	0	0
May	23	37	3	10	8	7	3	4	0
June	20	57	2	0	3	1	0	0	0
July	13	51	1	0	0	2	0	0	0
August	13	48	3	4	5	3	0	0	0
Sept	14	44	2	8	1	6	0	0	0

Table 4.1 NRS, storms recorded.

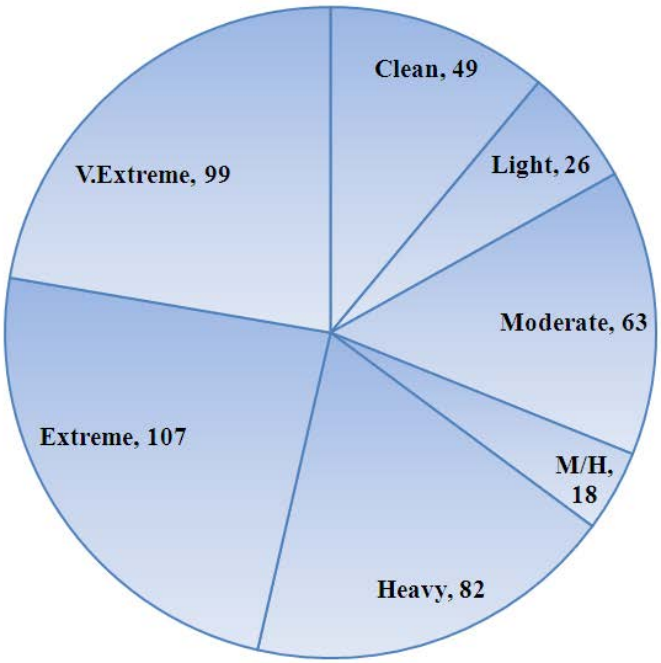

Note* *444 days recorded.*

Figure 4.5(a) NRS, Outlet 1-West: Measured detritus conditions.

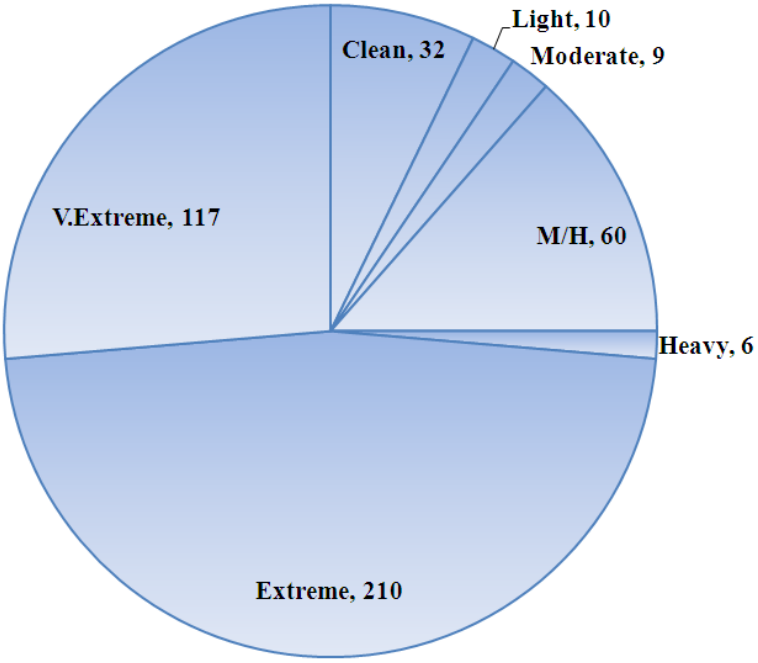

Note* *444 days recorded.*

Figure 4.5(b) NRS, Outlet 2-East: Measured detritus conditions.

Image	Plate reference	Scale value	Approximate coverage (%)	Comments
	a	0	0	*Clean*
	b	1	≤ 8	*Light scattering of detritus*
	c	2	≤ 20	*Moderate, side covered with detritus*
	d	3	≤ 32	*Moderate/Heavy, 0.5 side covered with detritus*
	e	4	≤ 64	*Heavy detritus levels, roof guard clear*
	f	5	≤ 85	*Extreme detritus levels, little open area to outlet*
	g	6	≤ 100	*V. Extreme detritus levels, no open area to outlet*

Figure 4.6 (a to g) NRS, image categorisation.

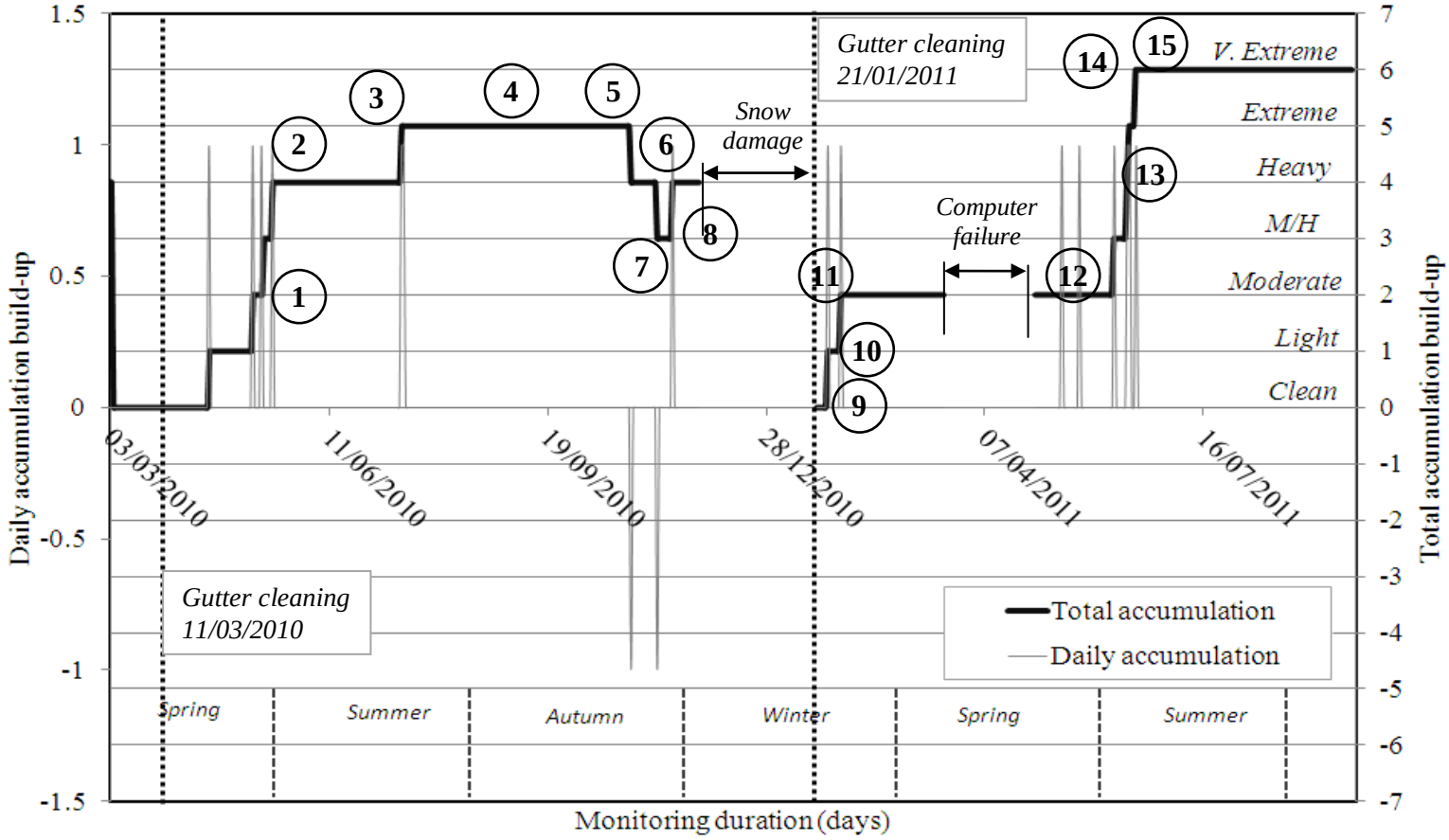

Figure 4.7(a) NRS, Outlet 1-West: Change in detritus level mapped against weather effects.
(refer to Table 3.2 for case details).

Case point	Date	To date	Total (days)	Dry period (days)	Dry period with light rainfall that had no affect (days)	Wet days that affected system (days)	Number of rainfall events
1	11th March 2010	30th May 2010	80	69	5	6	18
2	31st May 2010	20th July 2010	51	43	6	2	39
3	21st July 2010	0	1	0	0	1	10
4	22nd July 2010	31st Oct 2010	122	103	20	1	48
5	1st Nov 2010	0	1	0	0	1	3
6	2nd Nov 2010	15th Nov 2010	14	9	3	2	9
7	16th Nov 2010	20th Nov 2010	5	5	0	0	0
8	21st Nov 2010	29th Nov 2010	9	6	2	1	8
9	27th Jan 2010	6th Feb 2011	11	7	2	2	42
10	7th Feb 2011	0	1	0	0	1	5
11	8th Feb 2011	14th March 2011	34	31	6	0	33
12	7th May 2011	10th June 2011	34	22	9	3	62
13	11th June 2011	0	1	7	1	3	16
14	22nd July 2011	0	1	0	0	1	4
15	23rd July 2011	30th Oct 2011	100	81	17	2	33

Table 4.2 NRS, Outlet 1-West: Categorization changes in detritus accumulations.

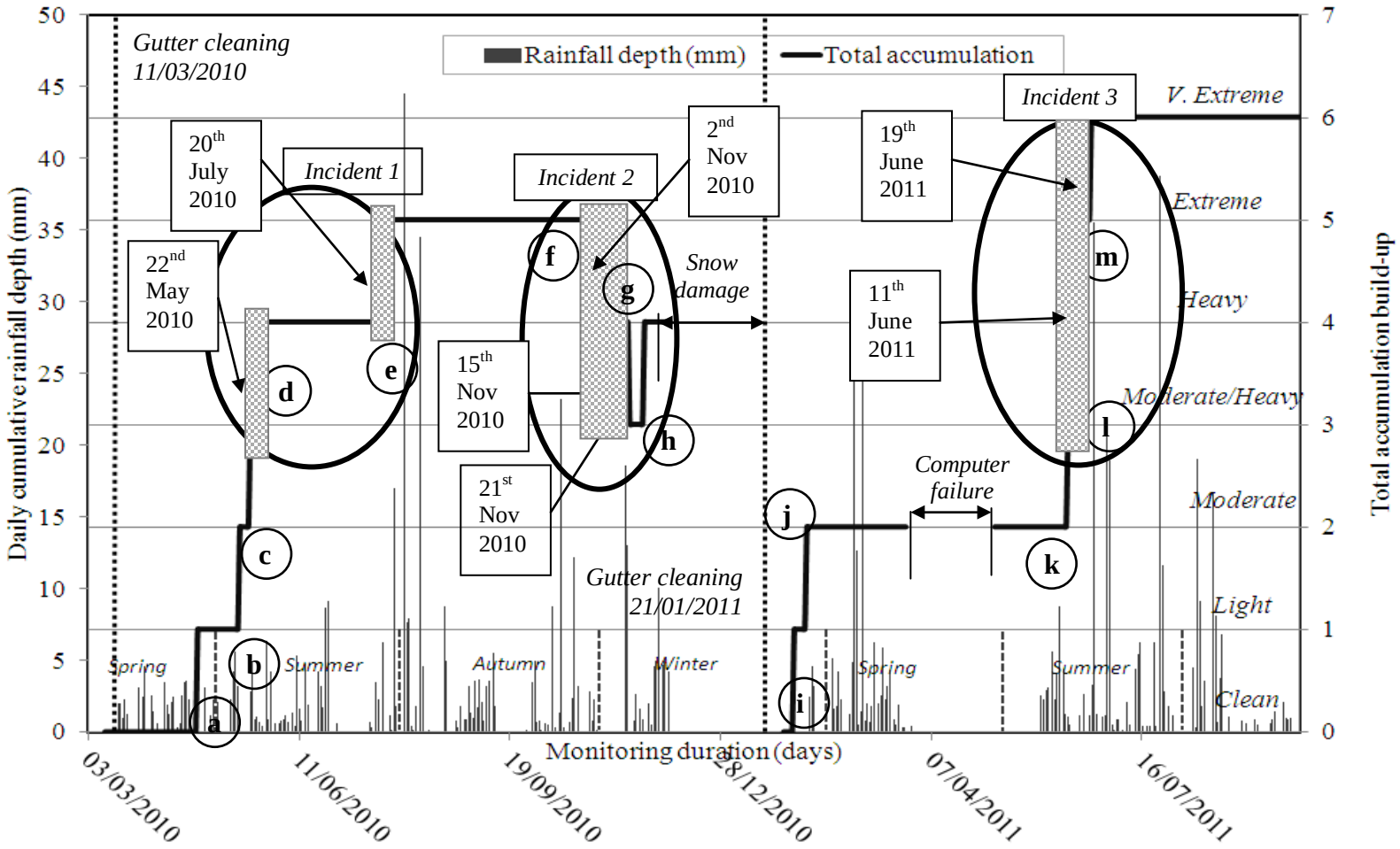

Figure 4.7(b) NRS, Outlet 1-West: Change in detritus level mapped against total daily rainfall accumulation.

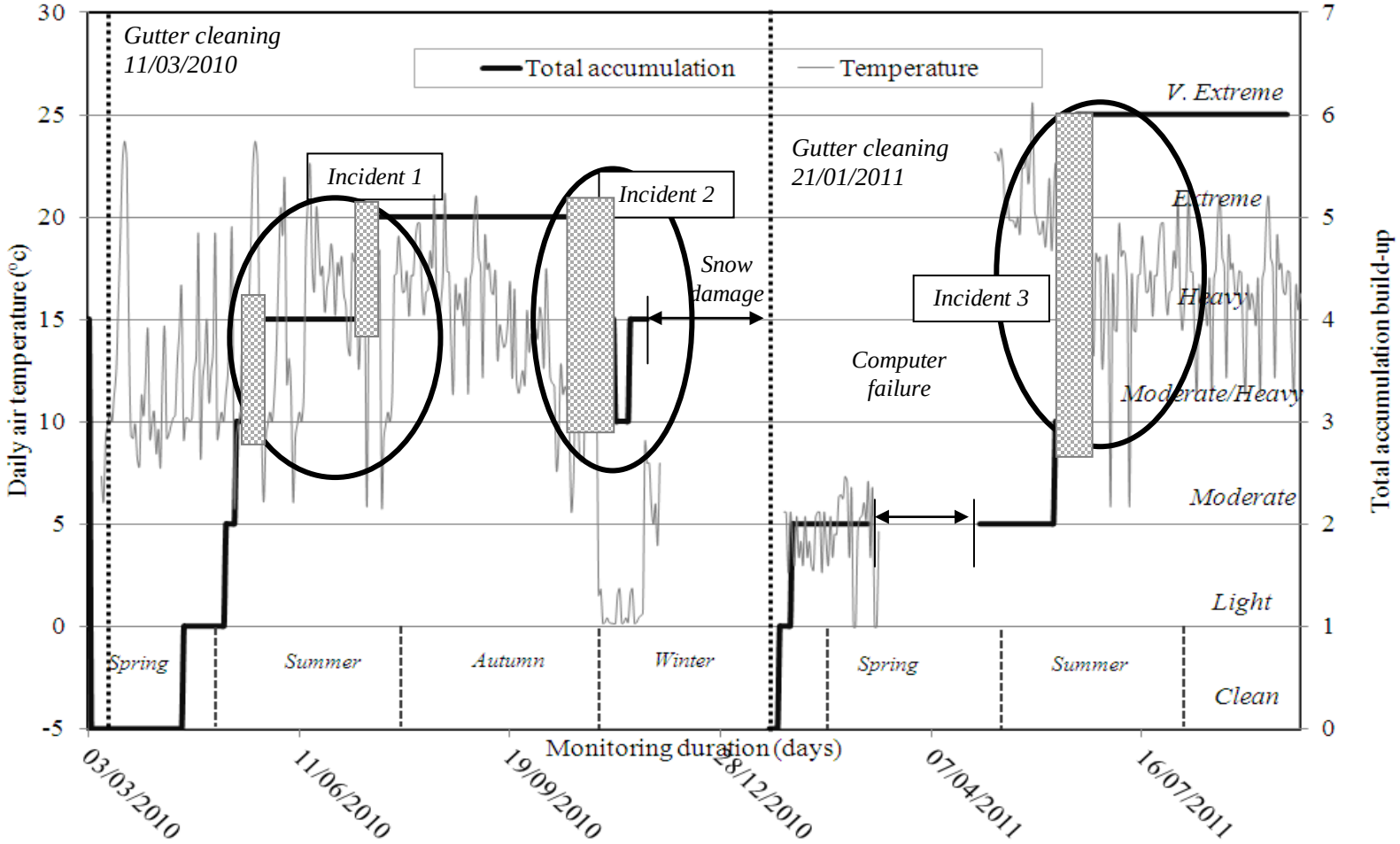

Figure 4.7(c) NRS, Outlet 1-West: Change in detritus level mapped against average daytime air temperature.

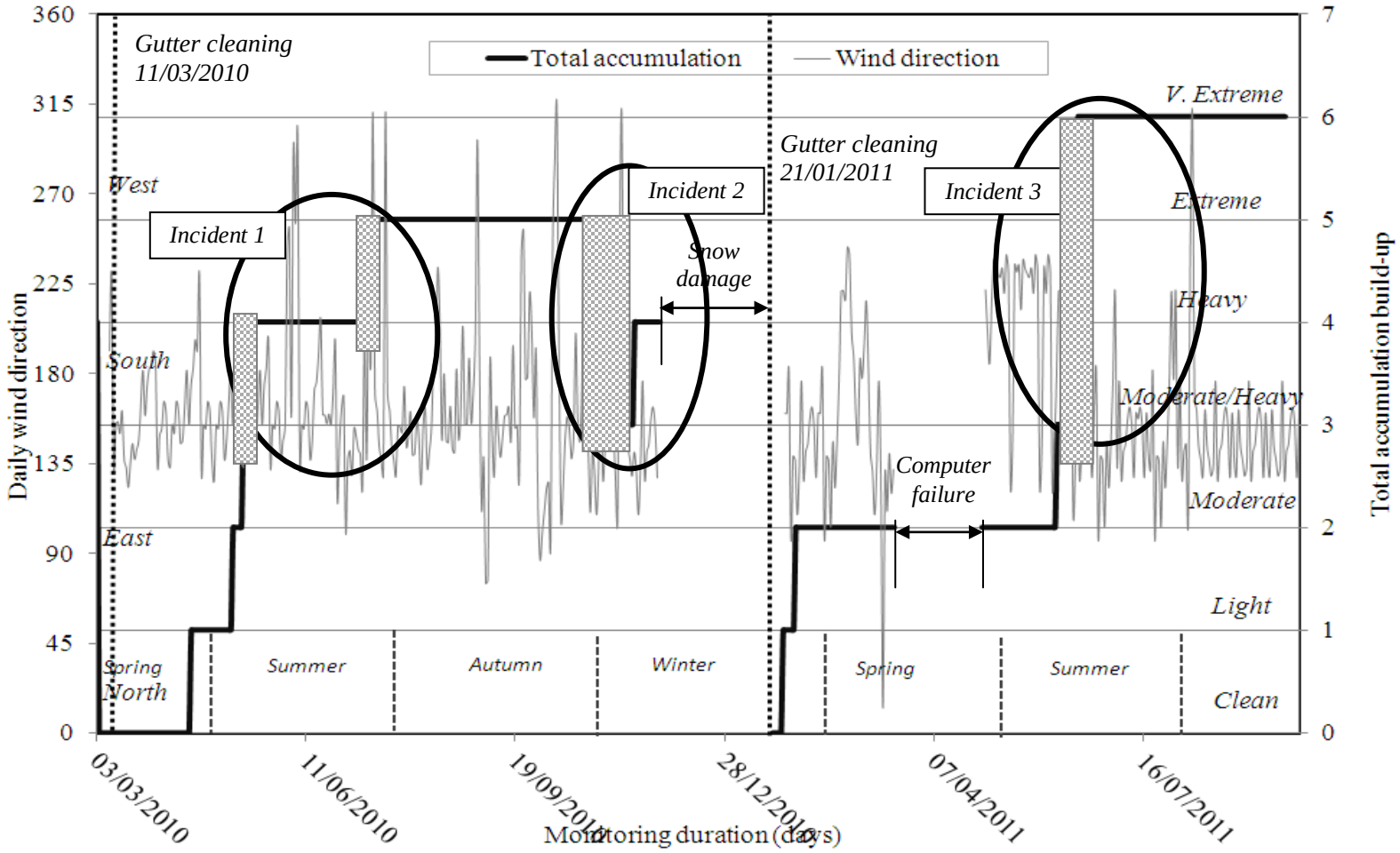

Figure 4.7(d) NRS, Outlet 1-West: Change in detritus level mapped against average daily wind direction.

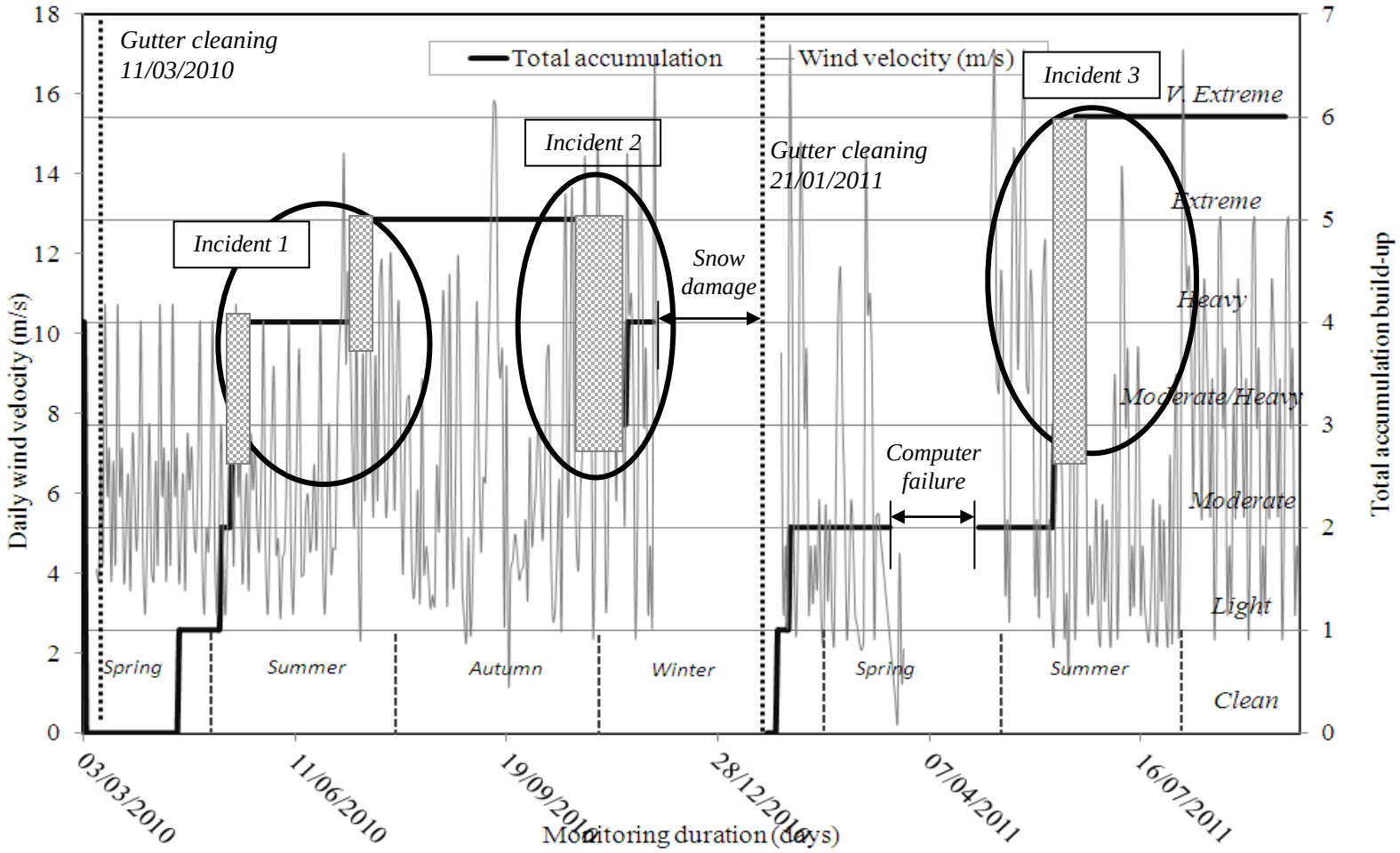

Figure 4.7(e) NRS, Outlet 1-West: Change in detritus level mapped against average daily wind velocity.

Case point	Storm (date)	Storm (time)	Average intensity (mm/hr)	Max intensity (mm/hr)	Duration (min)	Pre-storm detritus (1,2,3,4,5,6)	Pre-storm gutter depth (mm)	Gutter depth during storm (mm)	Post-storm detritus (1,2,3,4,5,6)	Post-storm gutter depth (mm)
A	24th April 2010	00.39.01	5.08	5.007	5.58	0	0	30.11	1	26.39
B	14th May 2010	17:13:32	5.58	6.175	7.31	1	27.21	35.61	2	33.72
C	18th May 2010	06:44:47	5.77	6.935	4.59	2	38.98	41.23	3	39.86
D	22nd May 2010	19:14:54	5.92	7.8405	5.46	3	25.9	27.8	4	27.15
E	20th July 2010	15:52:16	6.65	12.1	82.32	4	72.30	76.66	5	70.80
F	2nd Nov 2010	18:19:50	5.97	17.396	11.48	5	71.42	78.27	4	77.69
G	15th Nov 2010	05:09:03	5.51	7.4773	9.59	4	44.72	63.38	3	71.74
H	21st Nov 2010	05:08:34	5.76	22.43	9.53	3	75.01	79.69	4	79.68
I	1st Feb 2011	15:56:11	6.48	6.374	4.59	0	59.56	59.8	1	57.49
J	6th Feb 2011	04:21:45	5.36	6.514	20.08	1	62.11	65.58	2	64.66
K	10th June 2011	14:44:06	8.06	19.955	8.52	2	60.05	70.19	3	71.14
L	11th June 2011	16:00:11	5.19	12	8.11	3	56.05	67.07	5	74
M	19th June 2011	16:47:13	5.51	9.021	5.04	5	58.02	57.07	6	58.59

Table 4.3 NRS, Outlet 1-West: Case details of detritus accumulations.

Case point	Temperature (°c)	Relative humidity (%)	Wind velocity (m/s)	Wind direction (N,E, etc)
A	6.8	63.8	3.6	SW
B	17.7	42.2	5.5	S
C	18.5	39.7	6.2	S
D	21.9	54.3	9.2	SE
E	23.5	52.8	3.0	S
F	0.8	0.2	13.3	SE
G	1.3	0.2	1.2	SE
H	25.5	0.2	2.8	SE
I	30.4	29.5	0.8	SW
J	31.8	30.1	12.0	SW
K	21.4	21.6	2.8	SE
L	33.0	33.3	7.4	SW
M	33.5	33.8	5.2	SW

Table 4.4 NRS, Outlet 1-West: Weather conditions.

Case point	Pipe work pressure (mH20)			Case point	Pipe work pressure (mH20)
	VPT1	VPT2	VPT3		VPT4
A	-0.339	-0.092	-0.198	**A**	-0.024
B	-0.309	-0.091	-0.213	**B**	-0.018
C	-0.421	-0.113	-0.226	**C**	-0.0533
D	-0.007	-0.055	-0.221	**D**	-0.0313
E	-0.324	-0.063	-0.071	**E**	-0.2193
F	-0.429	-0.079	-0.057	**F**	-0.0103
G	-0.286	-0.025	-0.023	**G**	-0.0979
H	-0.463	-0.025	-0.029	**H**	-0.1093
I	-0.092	-0.197	-0.129	**I**	-0.0803
J	-0.457	-0.239	-0.100	**J**	-0.0821
K	-0.471	-0.14	-0.113	**K**	-0.0785
L	-0.375	-0.098	-0.212		
M	-0.080	-0.110	-0.158		

Table 4.5 NRS, Outlet 1 & 2 respectively: Peak pipework pressure conditions

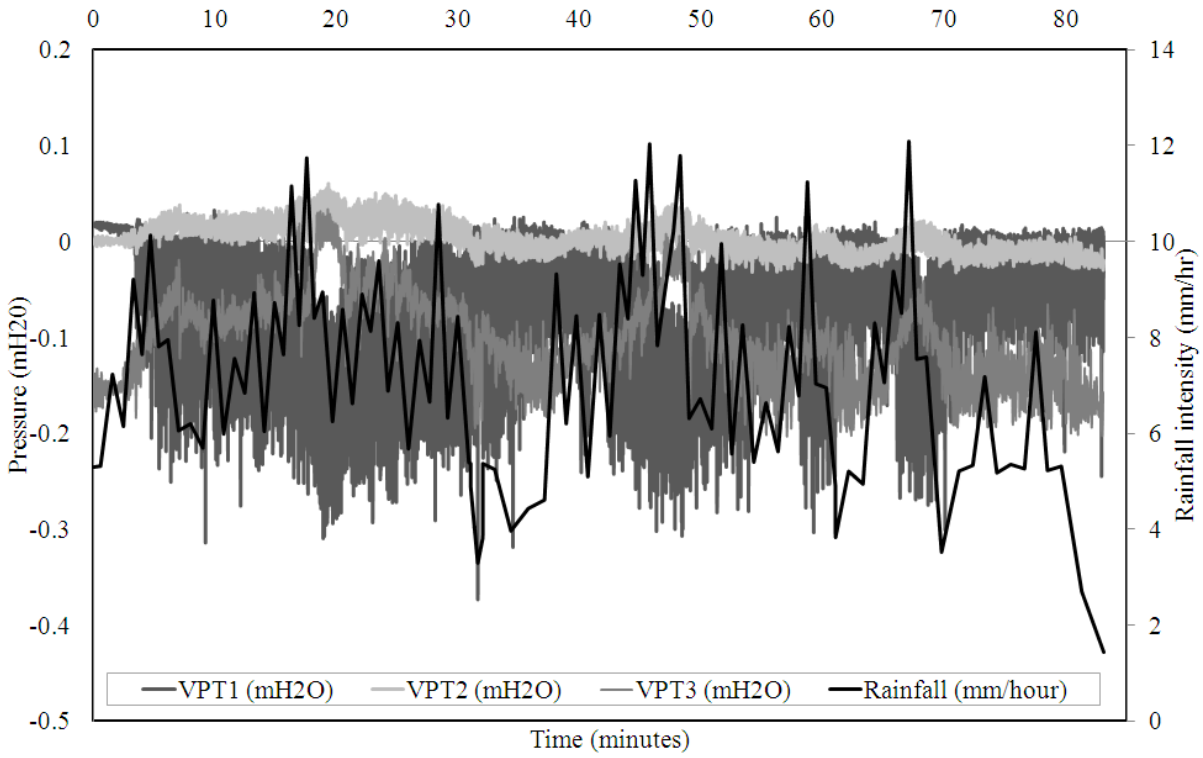

Figure 4.8(a) NRS, Outlet 1-West: Measured pipework pressure data on 20th July 15:52:16 2010 (refer to Fig. 4.3 for system layout).

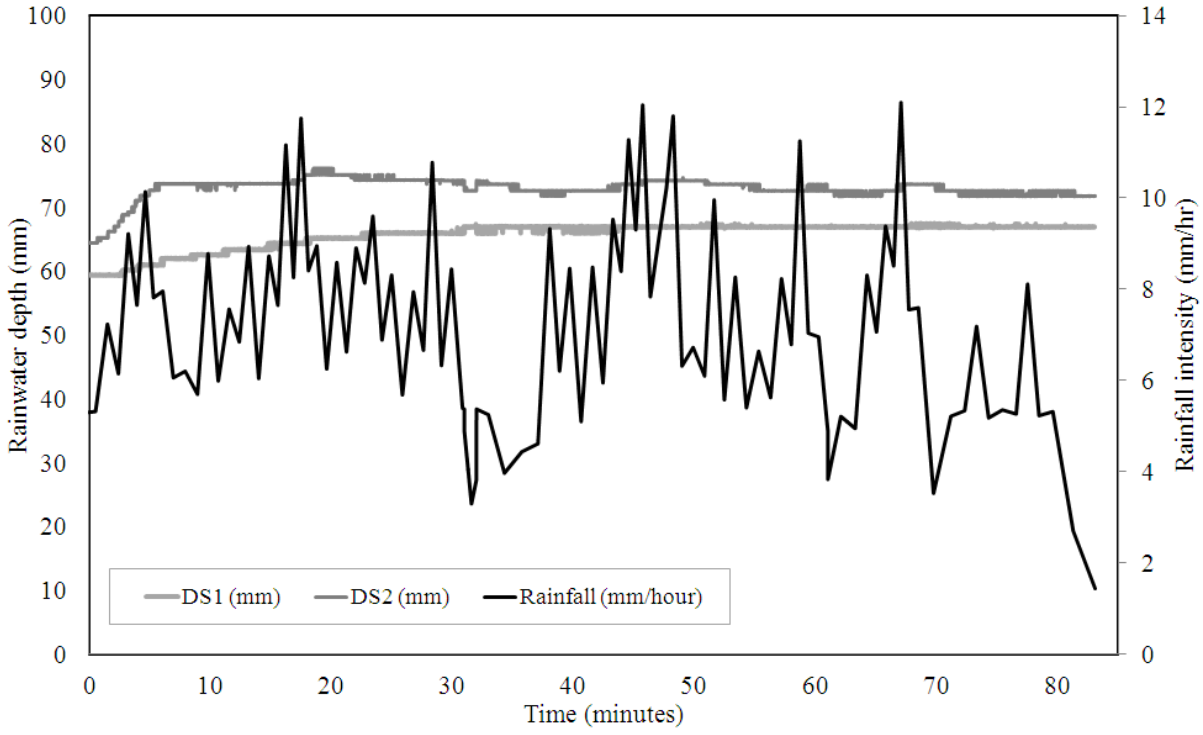

Figure 4.8(b) NRS, Outlet 1-West: Measured gutter depth data on 20th July 15:52:16 2010 (refer to Fig. 4.3 for system layout).

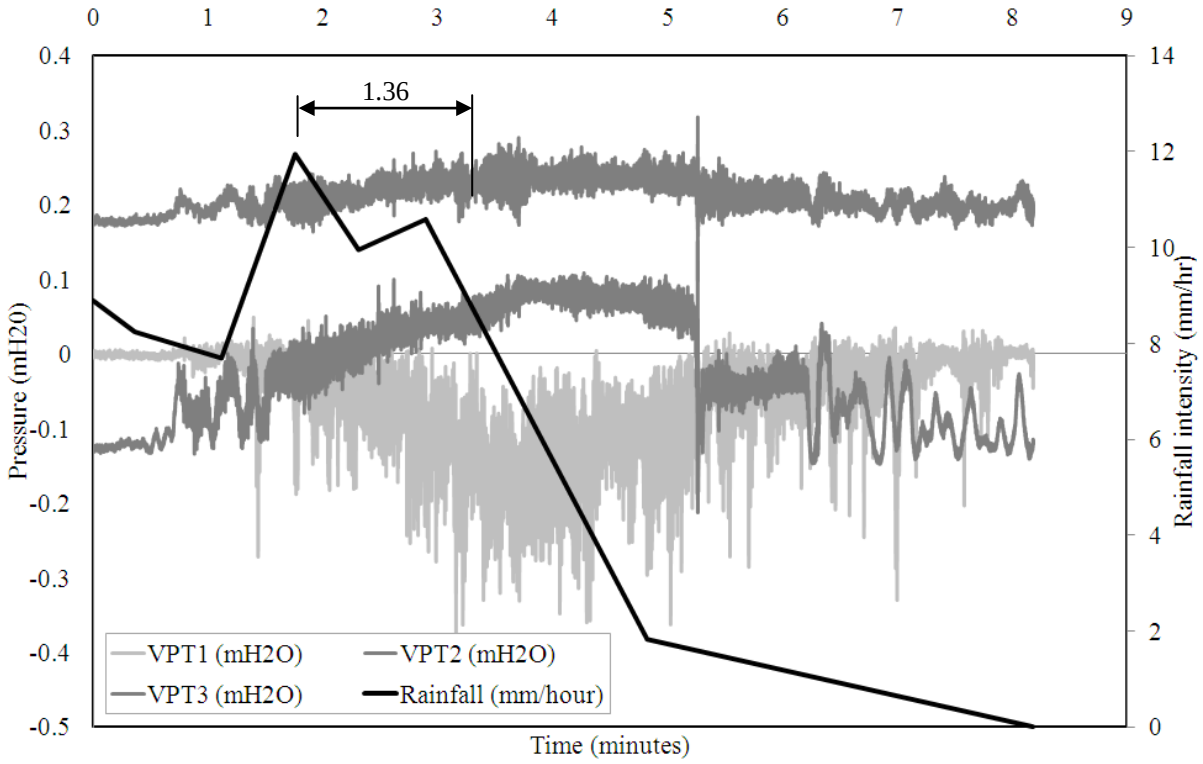

Figure 4.9(a) NRS, Outlet 1-West: Measured pipework pressure data on 11th June 16:00:11 2011 (refer to Fig. 4.3 for system layout).

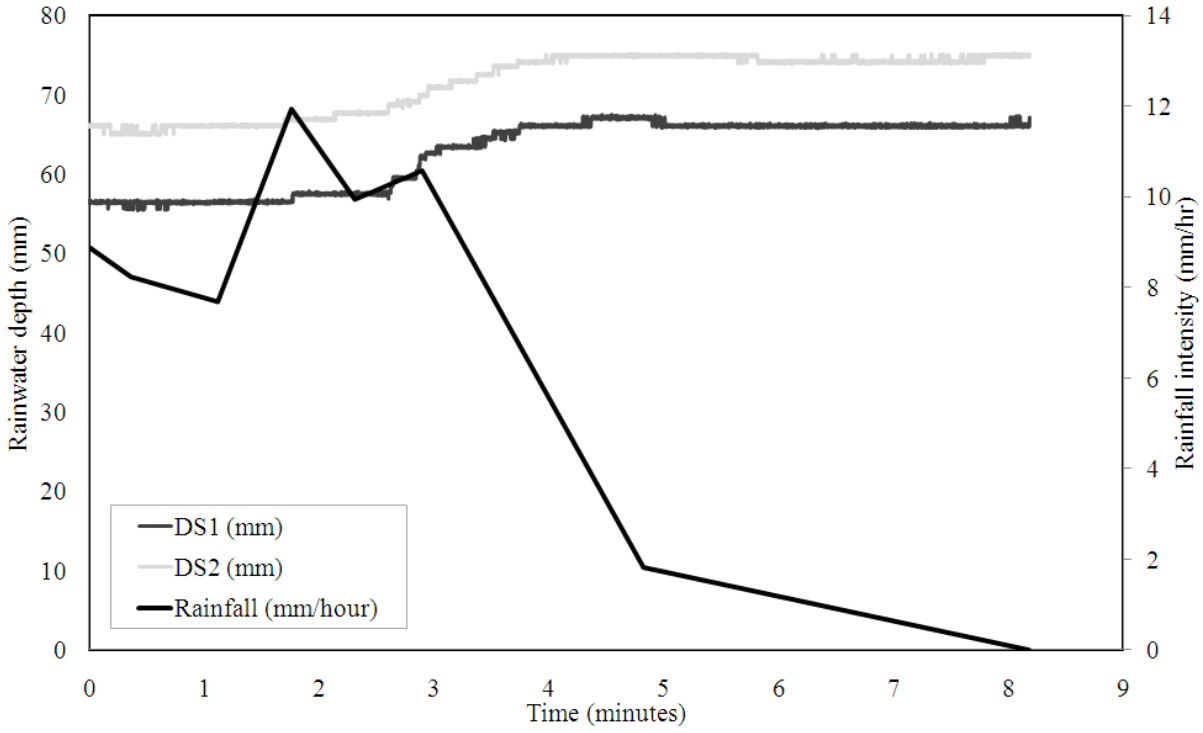

Figure 4.9(b) NRS, Outlet 1-West: Measured gutter depth data on 11th June 16:00:11 2011 (refer to Fig. 4.3 for system layout).

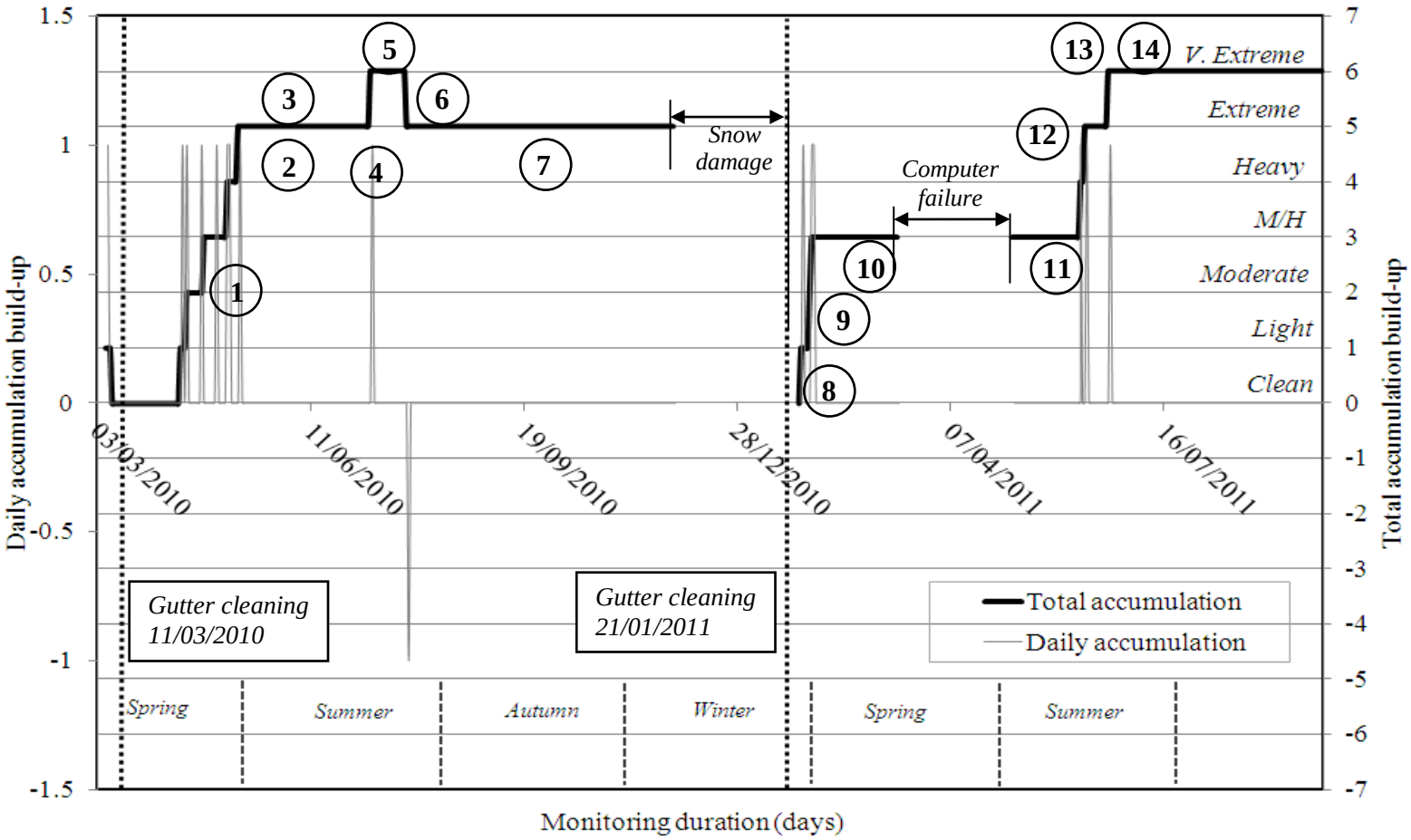

Figure 4.10(a) NRS, Outlet 2-East: Change in detritus level mapped against weather effects.

(refer to Table 4.6 for case details).

Case point	Date	To date	Total (days)	Dry period (days)	Dry period with light rainfall that had no affect (days)	Wet days that affected system (days)	Number of rainfall events
1	11th March 2010	8th May 2010	58	56	2	4	11
2	9th May 2010	0	1	0	0	1	1
3	8th May 2010	9th July 2010	64	53	9	2	21
4	10th July 2010	0	1	0	0	1	2
5	12th July 2010	26th July 2010	15	10	5	0	30
6	27th July 2010	0	1	0	0	1	1
7	28th July 2010	29th Nov 2010	124	95	29	0	69
8	27th Jan 2011	2nd Feb 2011	7	4	0	3	4
9	3rd Feb 2011	0	1	0	0	1	24
10	4th Feb 2011	14th March 2011	37	30	7	0	29
11	7th May 2011	7th June 2011	31	22	9	0	57
12	8th June 2011	21st June 2011	13	10	1	1	15
13	22nd June 2011	0	1	0	0	1	4
14	23rd July 2011	30th Oct 2011	100	81	17	2	33

Table 4.6 NRS, Outlet 2-East: Categorization changes in detritus accumulations.

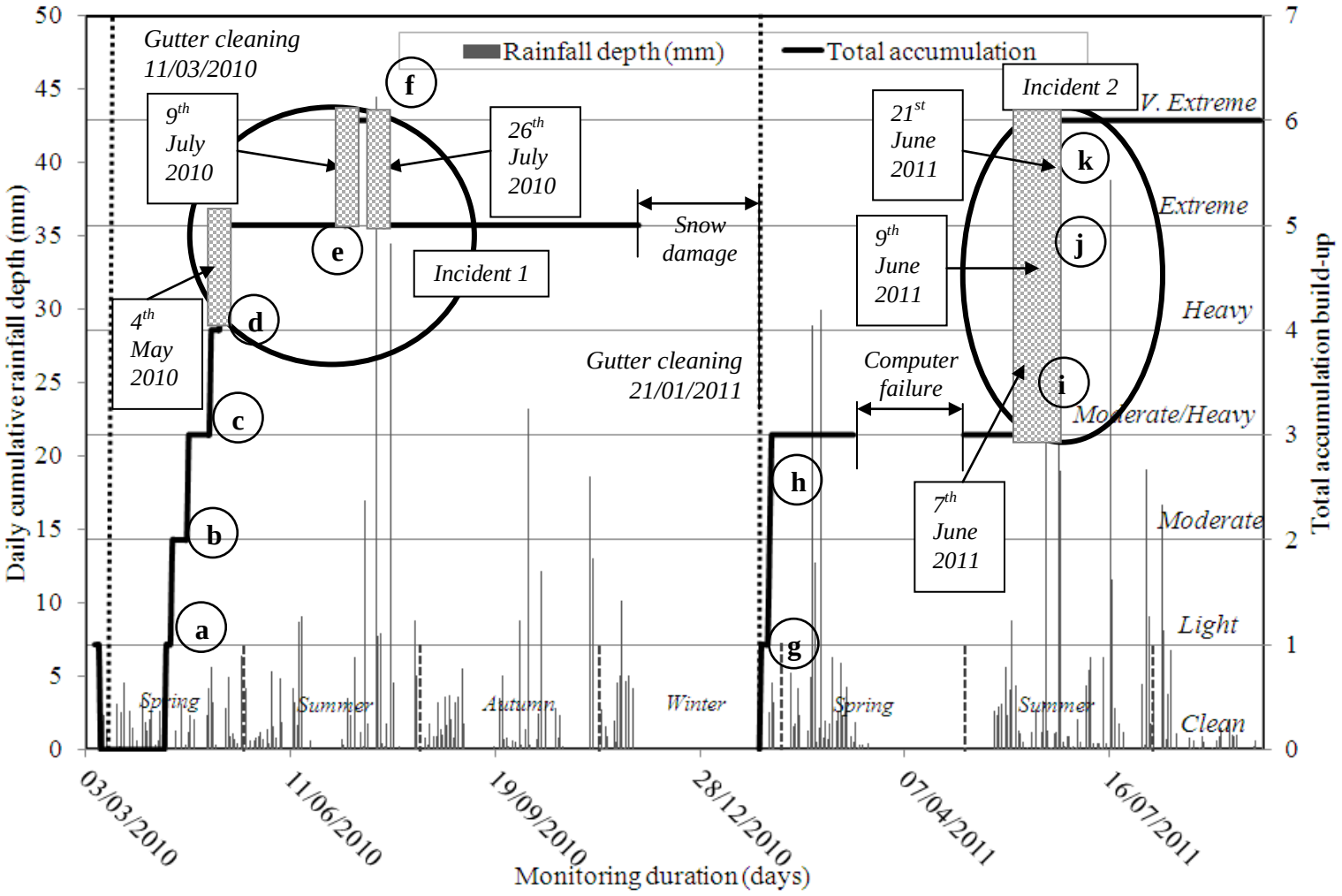

Figure 4.10(b) NRS, Outlet 2-East: Change in detritus level mapped against total daily rainfall accumulation.

Case point	Storm (date)	Storm (time)	Average intensity (mm/hr)	Max intensity (mm/hr)	Duration (min)	Pre-storm detritus (1,2,3,4,5,6)	Pre-storm gutter depth (mm)	Gutter depth during storm (mm)	Post-storm detritus (1,2,3,4,5,6)	Post-storm gutter depth (mm)
A	12th April 2010	00:10:58	5.88	7.759	4.58	0	57.34	58.91	1	57.46
B	15th April 2010	03:47:00	5.34	6.689	6.51	1	54.6	55.53	3	55.34
C	23rd April 2010	07:58:03	5.52	6.255	12.28	3	61.23	61.81	4	61.85
D	4th May 2010	00:02:17	5.88	6.77	4.59	4	54.106	54.23	5	55.32
E	9th July 2010	15:08:40	13.6	20.1	8.51	5	53.2	68	6	78.3
F	26th July 2010	14:01:03	5.094	11.52	21.33	6	120.301	143.7	5	151.75
G	28th Jan 2011	22:01:03	5.05	8.119	4.59	0	67.28	67.31	1	64.68
H	1st Feb 2011	16:11:40	5.87	10.83	10.15	1	70.68	74.67	3	74.15
I	7th June 2011	16:07:26	5.66	6.27	4.57	3	65.08	69.67	4	68.29
J	9th June 2011	07:34:49	6.78	22.31	9.44	4	69.07	69.89	5	71.54
K	21st June 2011	15:51:33	17.16	35.20	5.41	5	70.67	70.91	6	66.72

Table 4.7 NRS, Outlet 2-East: Case details of detritus accumulations.

Case point	Temperature (°c)	Relative humidity (%)	Wind speed (m/s)	Wind direction (N,E, etc)
A	7.3	65.1	6.1	S
B	15.1	40.6	8.3	S
C	10.4	38.2	5.4	SE
D	9.6	62.8	2.9	S
E	12.6	72.5	15.2	W
F	17.4	82.9	9.1	SE
G	33.8	33.7	31.6	SW
H	33.1	31.9	26.5	SW
I	26.0	26.1	2.6	S
J	23.0	22.9	3.5	S
K	28.0	27.9	11.1	S

Table 4.8 NRS, Outlet 2-East: Weather conditions.

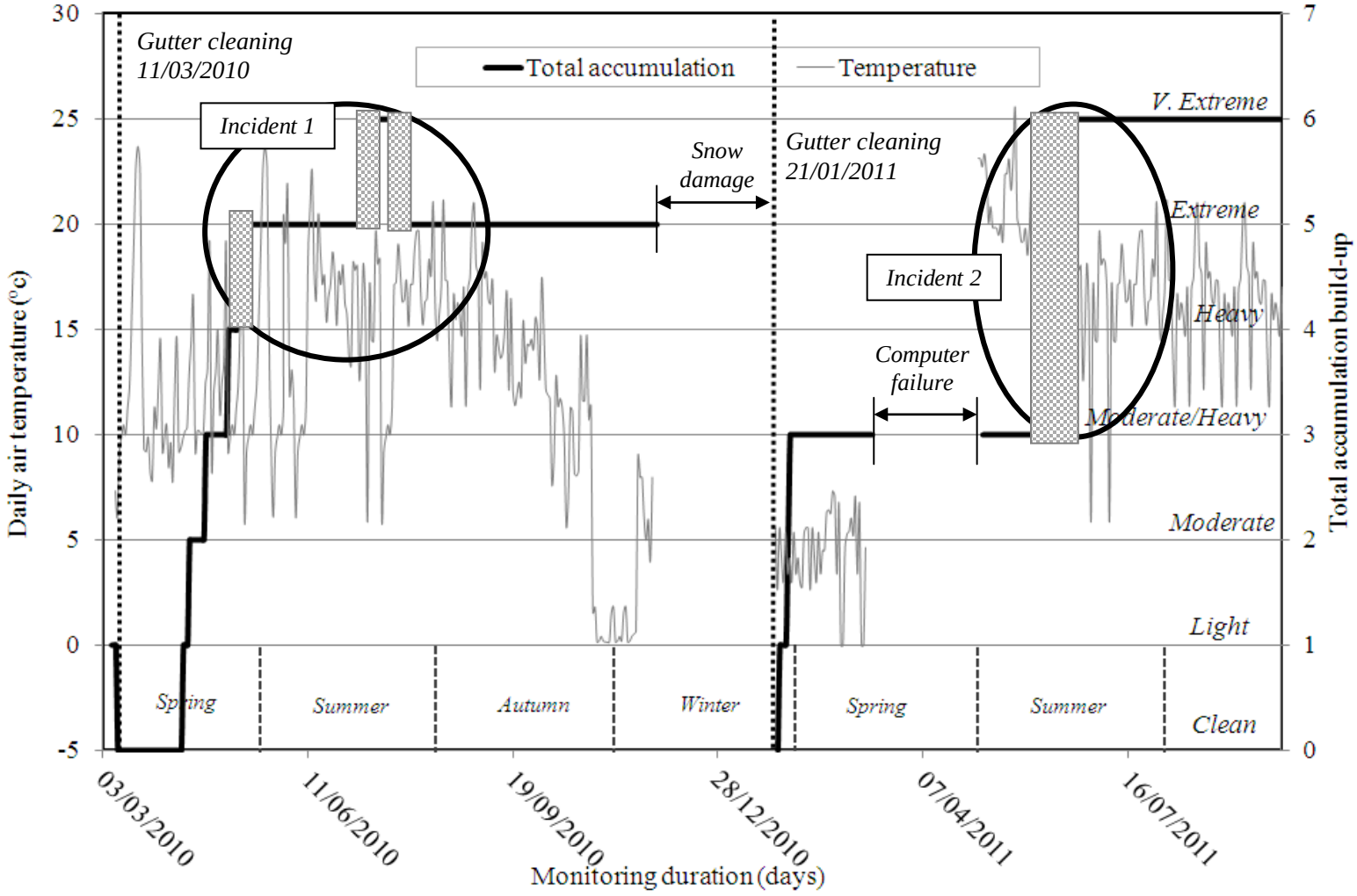

Figure 4.10(c) NRS, Outlet 2-East: Change in detritus level mapped against average daytime air temperature.

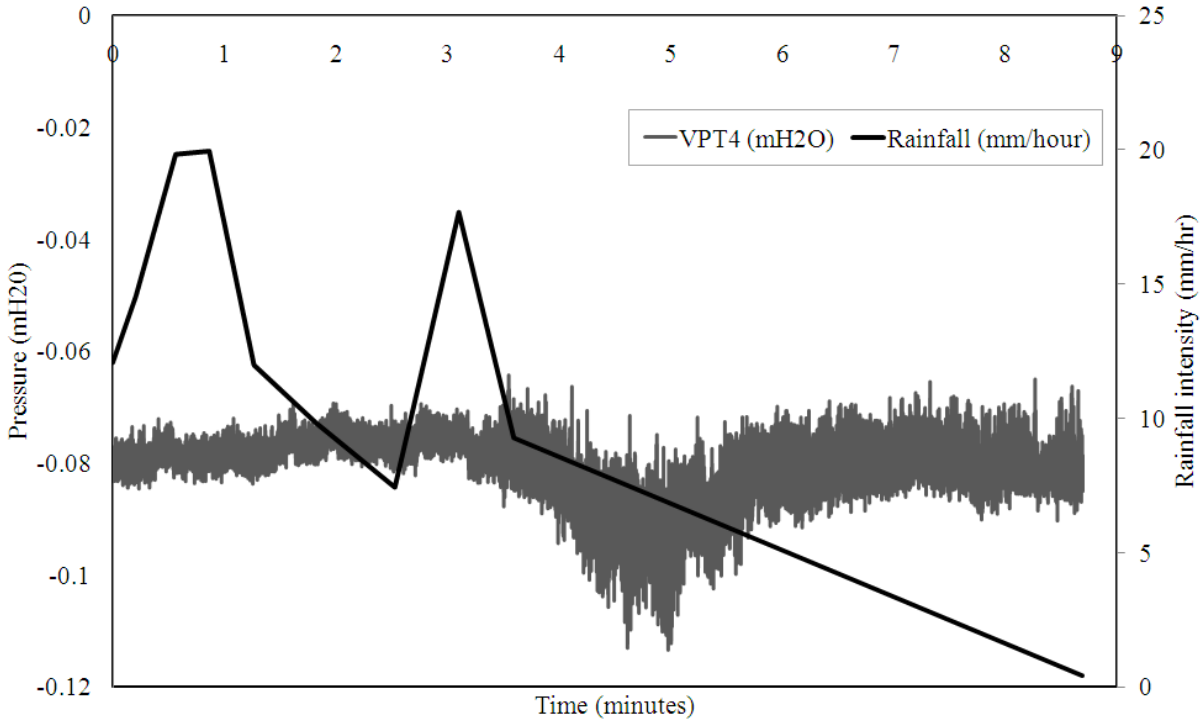

Figure 4.11(a) NRS, Outlet 2-East: Measured pipework pressure data on 9th July 15:08:40 2010 (refer to Fig 4.3 for system layout).

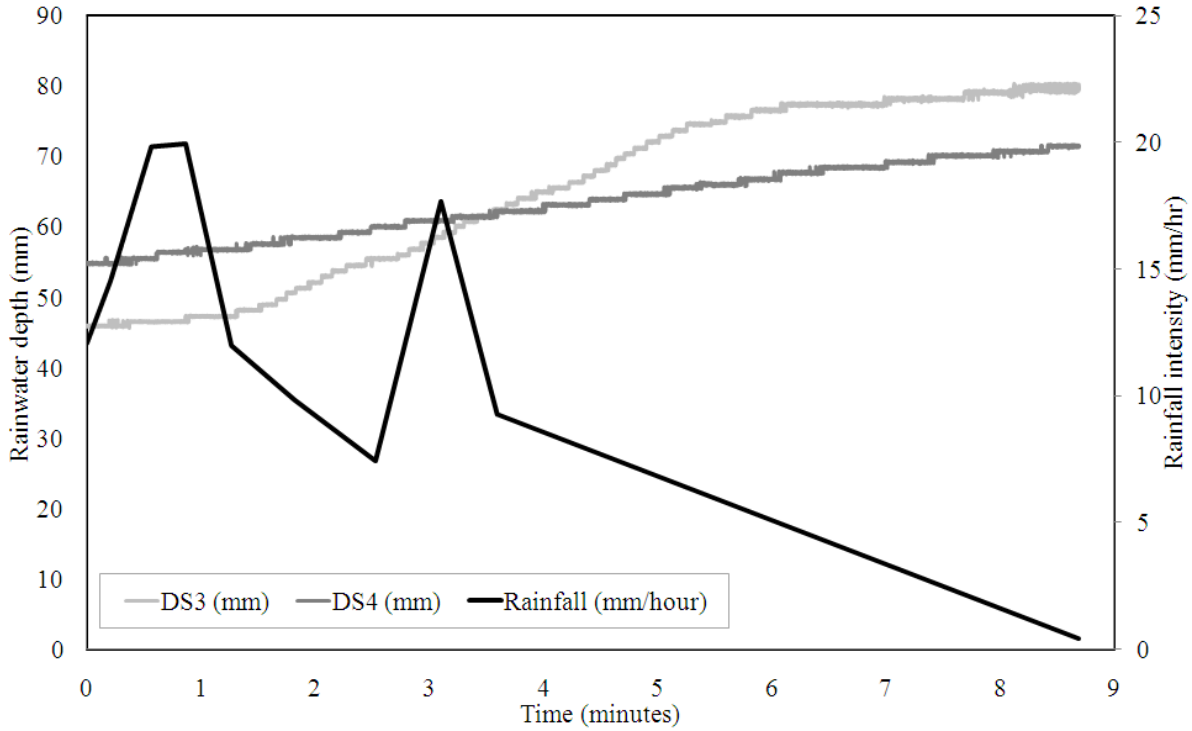

Figure 4.11(b) NRS, Outlet 2-East: Measured pipework pressure data on 9th July 15:08:40 2010 (refer to Fig 4.3 for system layout).

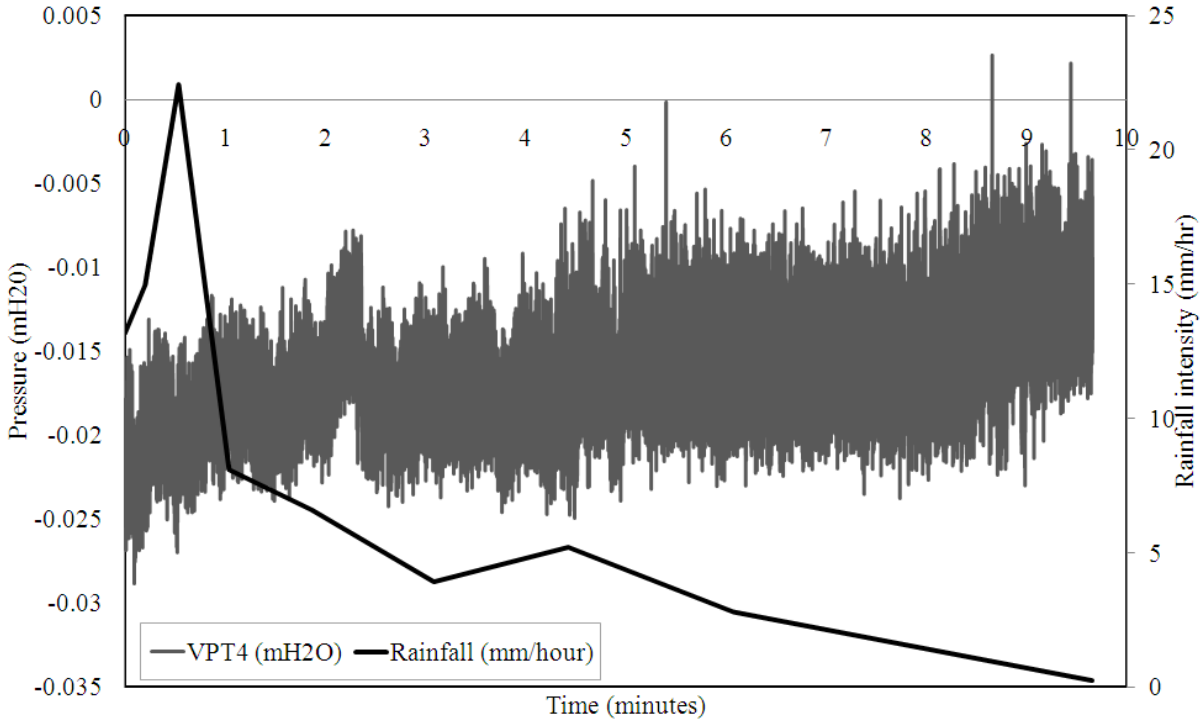

Figure 4.12(a) NRS, Outlet 2-East: Measured pipework pressure data on 9th June 07:34:49 2011 (refer to Fig 4.3 for system layout).

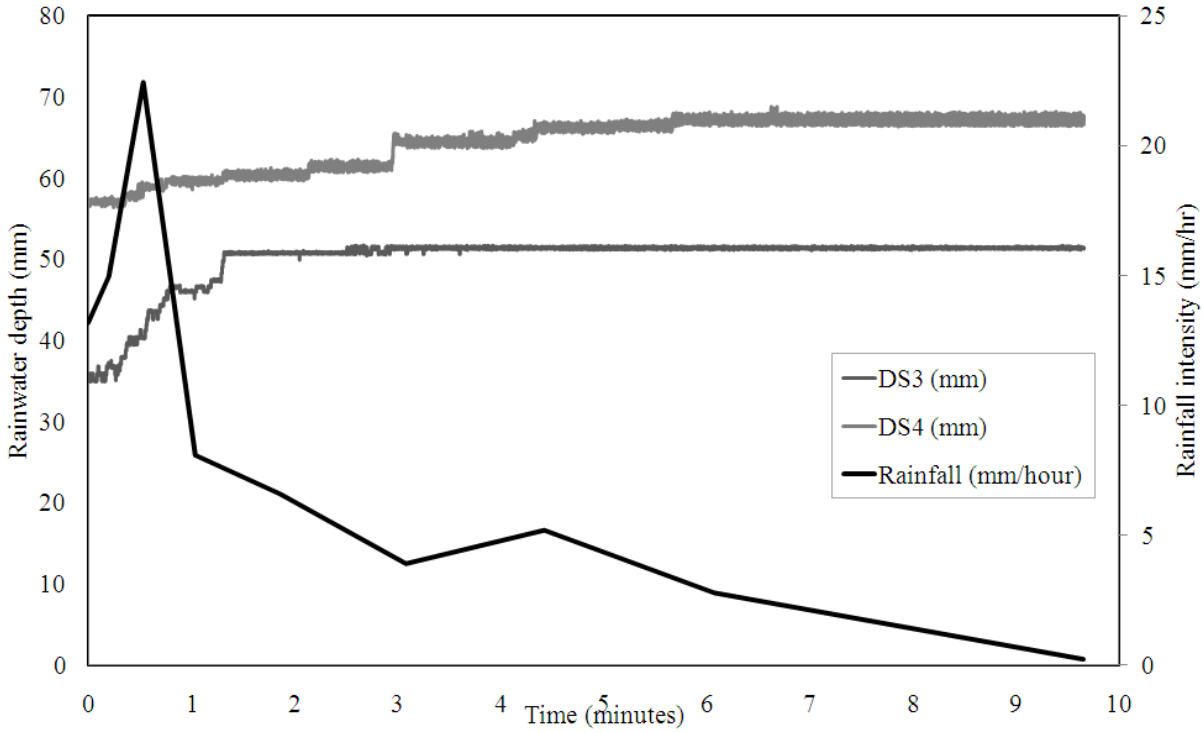

Figure 4.12(b) NRS, Outlet 2-East: Measured gutter depth data on 9th June 07:34:49 2011 (refer to Fig 4.3 for system layout).

Date	Total *'days of rain'*	Rainfall (mm/hr)							
		1 <5	**6<10**	**11<20**	**21<30**	**31<40**	**41<50**	**51<100**	**101<**
2010									
Sept	15	62	5	1	1	1	0	0	0
Oct	20	59	9	2	0	0	0	0	0
Nov	19	58	7	3	0	2	2	0	0
Dec	6	4	1	0	0	0	0	0	0
2011									
Jan	6	10	2	0	0	0	0	0	0
Feb	21	59	10	8	1	0	0	0	0
March	20	51	9	7	2	1	0	0	0
April	18	48	12	5	0	0	0	0	0
May	21	46	0	2	7	7	4	4	0
June	18	46	7	3	1	1	0	0	0
July	19	40	8	6	3	0	1	0	0
August	23	43	9	4	2	3	0	0	0
Sept	19	58	11	6	6	4	2	0	0

Table 4.9 Ibrox stadium: Storms recorded.

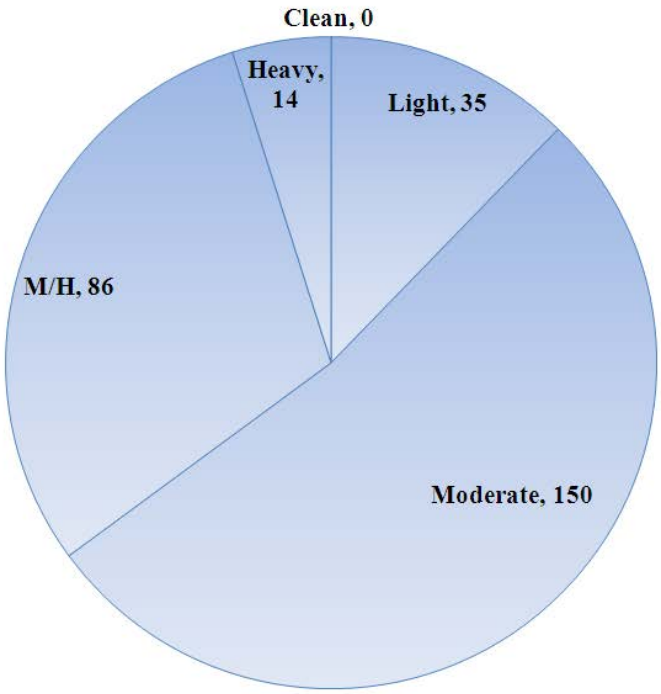

Note* *285 days recorded.*

Figure 4.13 Ibrox stadium: Detritus conditions.

Image	Plate reference	Scale value	Approximate coverage (%)	Comments
	a	0	0	*Clean*
	b	1	≤ 2	*Light scattering of detritus*
	c	2	≤ 6	*Moderate detritus levels*
	d	3	≤ 8	*Moderate/Heavy detritus levels*
	e	4	≤ 10	*Heavy detritus levels*

Figure 4.14(a to e) Ibrox stadium: Image categorisation.

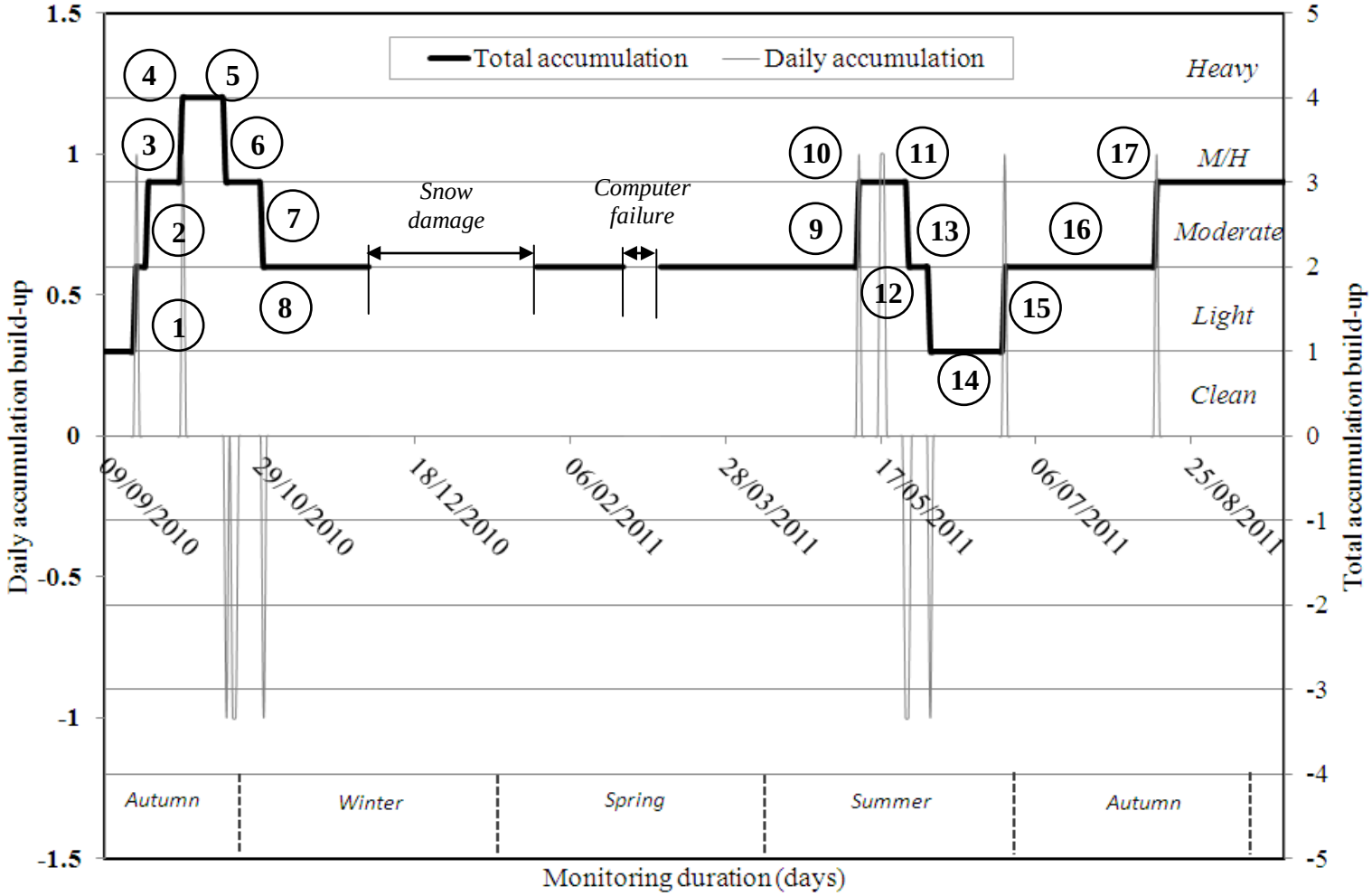

Figure 4.15(a) Ibrox stadium: Change in detritus level mapped against weather effects.

(refer to Table 4.10 for case details).

Case point	Date	To date	Total (days)	Dry period (days)	Dry period with light rainfall that had no affect (days)	Wet days that affected system (days)	Number of rainfall events
1	19th Sept 2010	0	1	0	0	1	6
2	23rd Sept 2010	0	1	0	0	2	4
3	24th Sept 2010	3rd Oct 2010	11	8	2	1	5
4	4th Oct 2010	17th Oct 2010	13	10	3	1	8
5	18th Oct 2010	0	1	0	0	1	2
6	19th Oct 2010	28th Oct 2010	12	6	5	1	14
7	29th Oct 2010	0	1	18	13	4	36
8	30th Oct 2010	3rd Dec 2010	35	0	0	1	6
9	7th March 2011	10th May 2011	63	46	15	2	56
10	11th May 2011	25th May 2011	16	14	2	0	3
11	26th May 2011	0	1	0	0	1	3
12	27th May 2011	1st June 2011	7	4	3	0	6
13	2nd June 2011	0	1	0	0	1	4
14	3rd June 2011	24th June 2011	28	28	0	0	14
15	25th June 2011	0	1	0	0	1	2
16	26th June 2011	14th Aug 2011	48	30	18	0	61
17	15th Aug 2011	30th Sept 2011	47	26	21	0	55

Table 4.10 Ibrox stadium: Categorization changes in detritus accumulations.

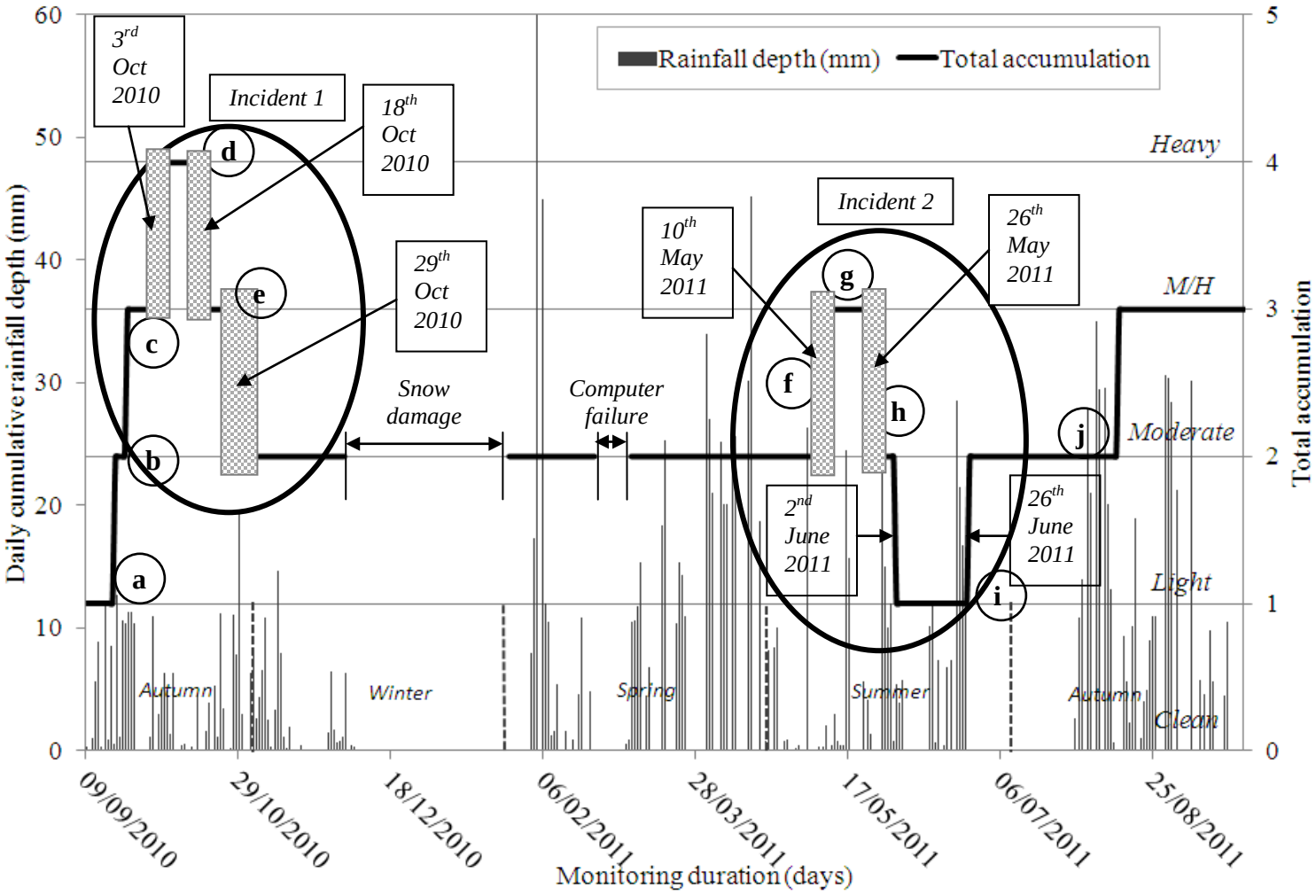

Figure 4.15(b) Ibrox stadium: Change in detritus level mapped against daily rainfall accumulation.

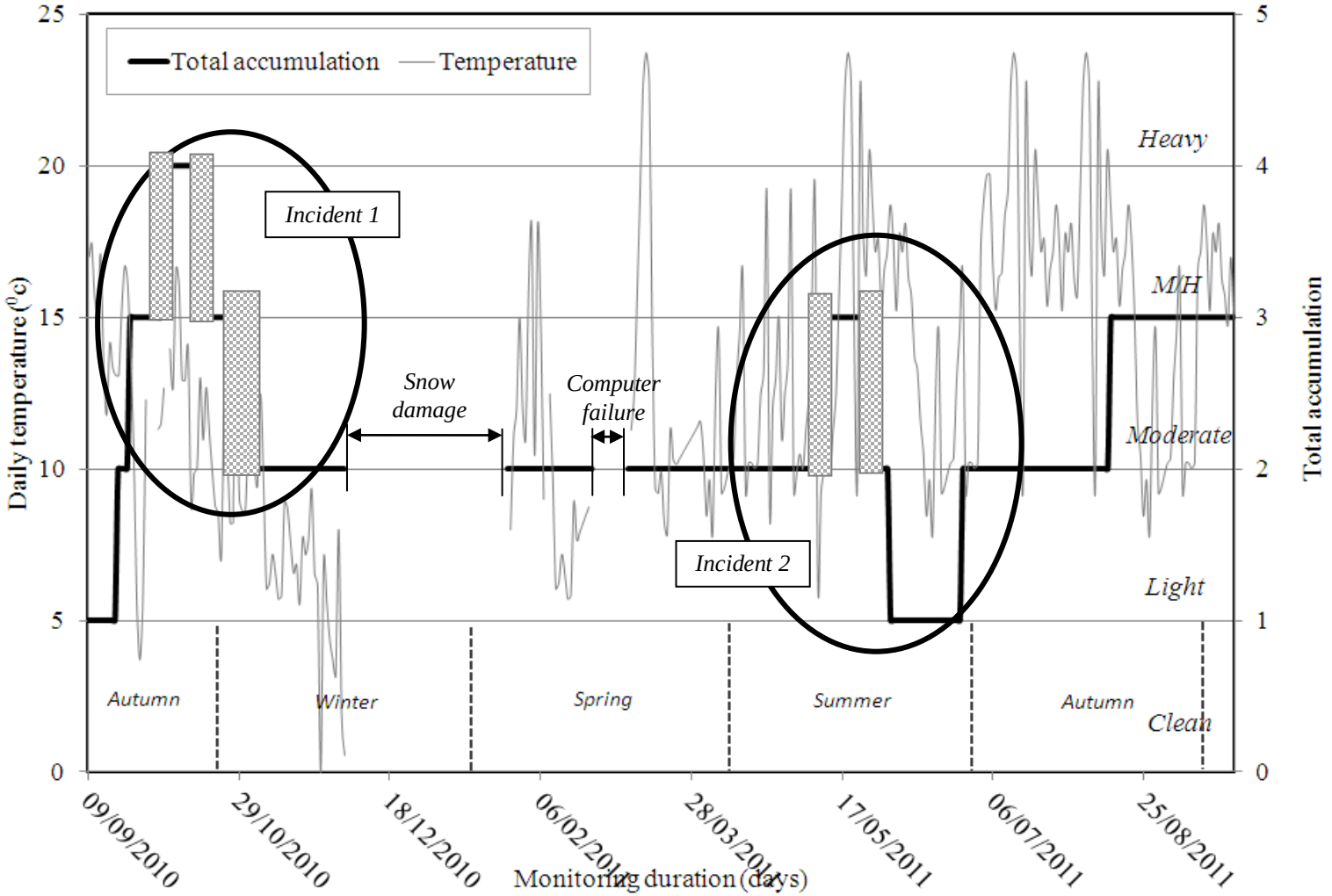

Figure 4.15(c) Ibrox stadium: Change in detritus level mapped against average daytime air temperature.

Case point	Storm (date)	Storm (time)	Average intensity (mm/hr)	Max intensity (mm/hr)	Duration (min)	Pre-storm detritus (1,2,3,4,5,6)	Pre-storm gutter depth (mm)	Gutter depth during storm (mm)	Post-storm detritus (1,2,3,4,5,6)	Post-storm gutter depth (mm)
A	19th Sept 2010	04:21:05	8.477	19.736	23.54	1	38	49	2	40
B	23rd Sept 2010	02:05:29	13.406	45.497	18.16	2	41	53	3	45
C	3rd Oct 2010	18:42:33	5.363	6.004	13.58	3	41	43	4	35
D	18th Oct 2010	11:37:51	9.925	24.074	12.48	4	36	38	3	38
E	29th Oct 2010	18:36:24	10.34	19.89	24.26	3	26	32	2	28
F	10th May 2011	10:53:02	71.74	35.52	105.31	2	302	50	3	30
G	26th May 2011	13:24:48	42.67	42.14	350.57	3	28	57	2	36
H	2nd June 2011	00:45:49	6.94	98.7	72.39	2	30	31	1	28
I	26th June 2011	03:50:28	38.03	74.6	125.30	1	31	34	2	29
J	14th Aug 2011	07:51:25	43.58	105.7	37.14	2	29	38	3	35

Table 4.11 Ibrox stadium: Case details of detritus accumulations.

Case point	Temperature (°c)	Relative humidity (%)	Wind speed (m/s)	Wind direction (N,E, etc)
A	11.3	87.1	0.9	S
B	13.4	89.7	1.2	SW
C	12.3	86.4	2.2	W
D	10.6	87.1	7.2	W
E	10.3	86.8	7.0	SW
F	11.1	59.1	0.6	N
G	10.4	67.1	0.6	N
H	9.6	61.8	0.8	N
I	11.0	65.2	0.7	N
J	12.1	62.9	0.8	N

Table 4.12 Ibrox stadium: Weather conditions.

Case point	Pipework pressure (mH20)			
	VPT1	**VPT2**	**VPT3**	**VPT4**
A	-0.1758	-0.1765	-0.2634	-1.3017
B	-1.4713	-1.6138	-1.9876	-4.4823
C	-0.1641	-0.1754	-0.267	-1.3513
D	-0.8189	-0.925	-1.0466	-1.7748
E	-0.0245	-0.0188	-0.0918	-0.1015
F	-0.065	-0.1987	-0.269	-0.0186
G	-0.0613	-0.1074	-0.2247	-0.0237
H	-0.0677	-0.9088	-0.9943	-0.0077
I	-0.0659	-0.4454	-0.5184	-0.0178
J	-0.0618	-0.216	-0.2923	-0.0196

Table 4.13 Ibrox stadium: Peak pipework pressure.

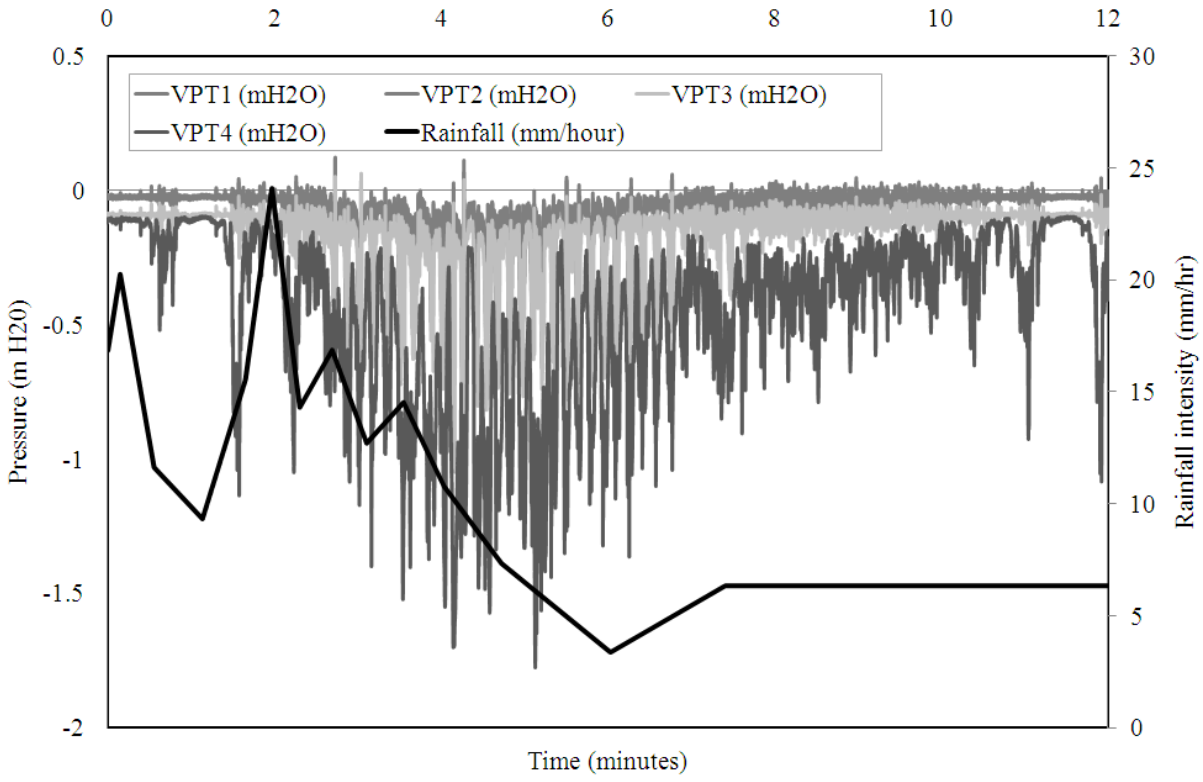

Figure 4.16(a) Ibrox stadium: Measured pipework pressure data on 18th October 11:37:51 2010 (refer to Fig. 4.4 for system layout).

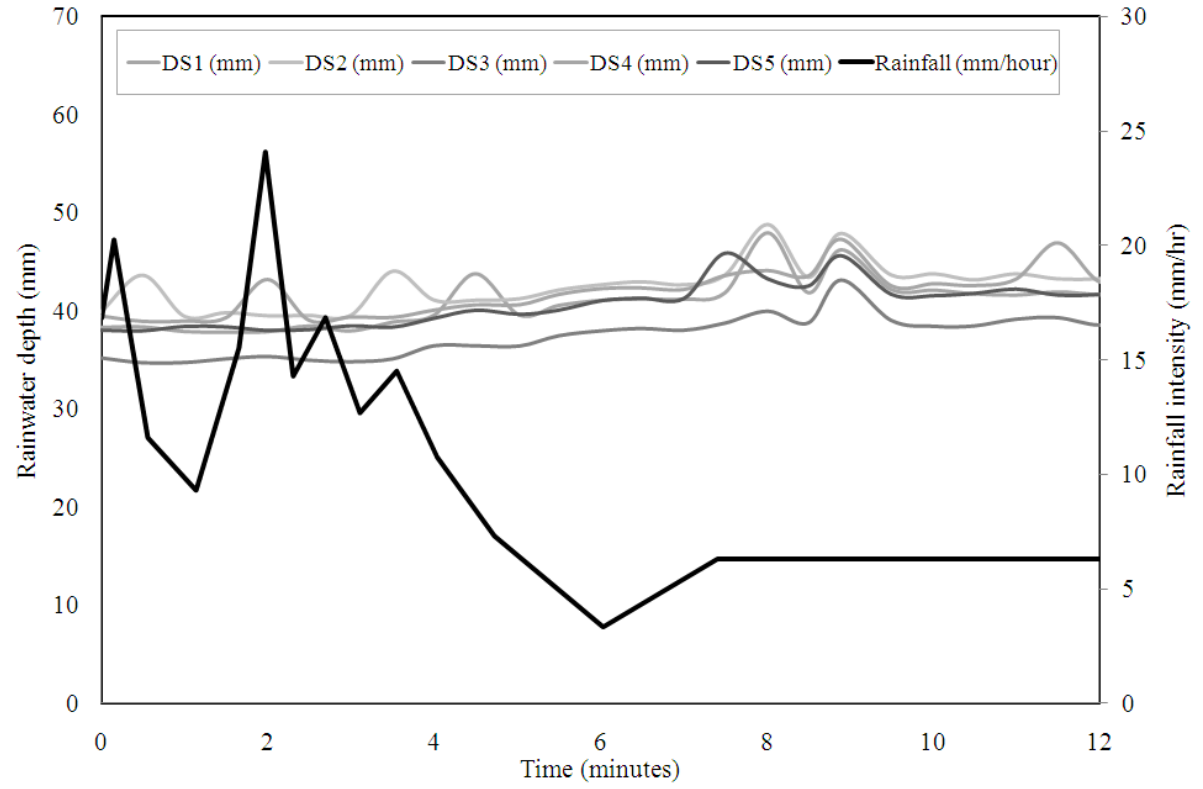

Figure 4.16(b) Ibrox stadium: Measured gutter depth data on 18th October 11:37:51 2010 (refer to Fig. 4.4 for system layout).

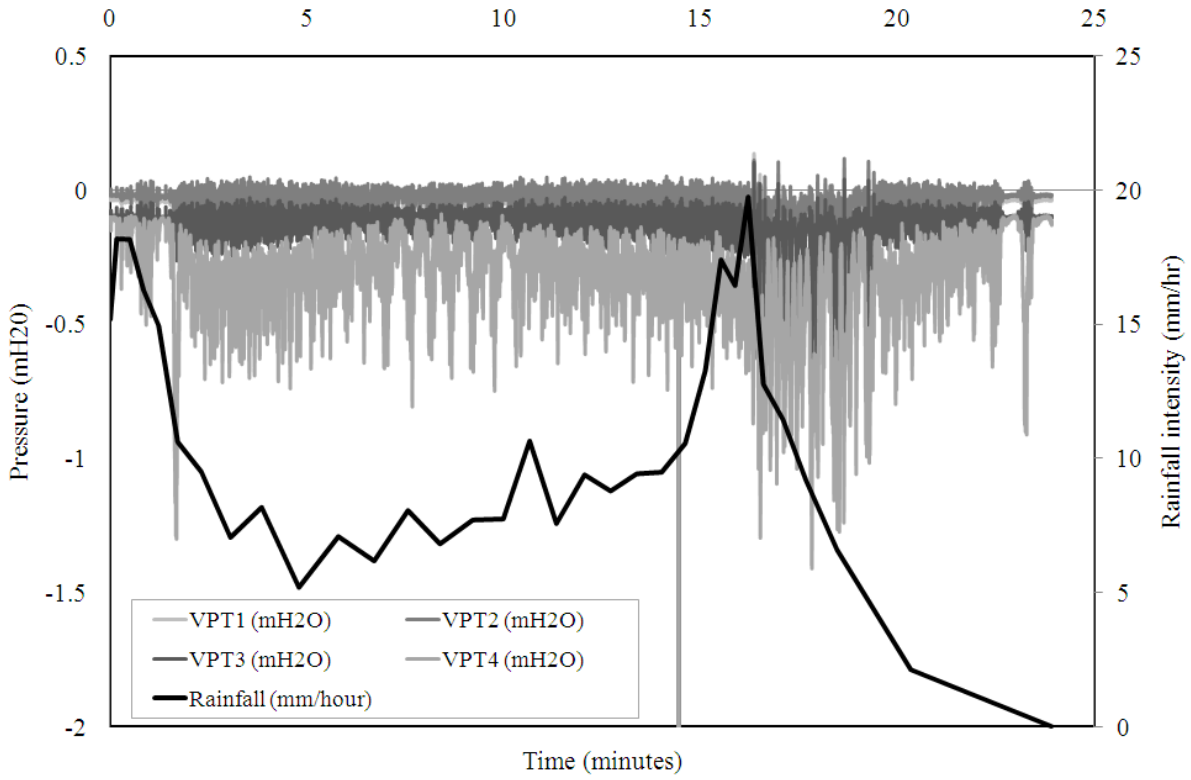

Figure 4.17(a) Ibrox stadium: Measured pipework pressure data on 29th October 18:36:24 2010 (refer to Fig. 4.4 for system layout).

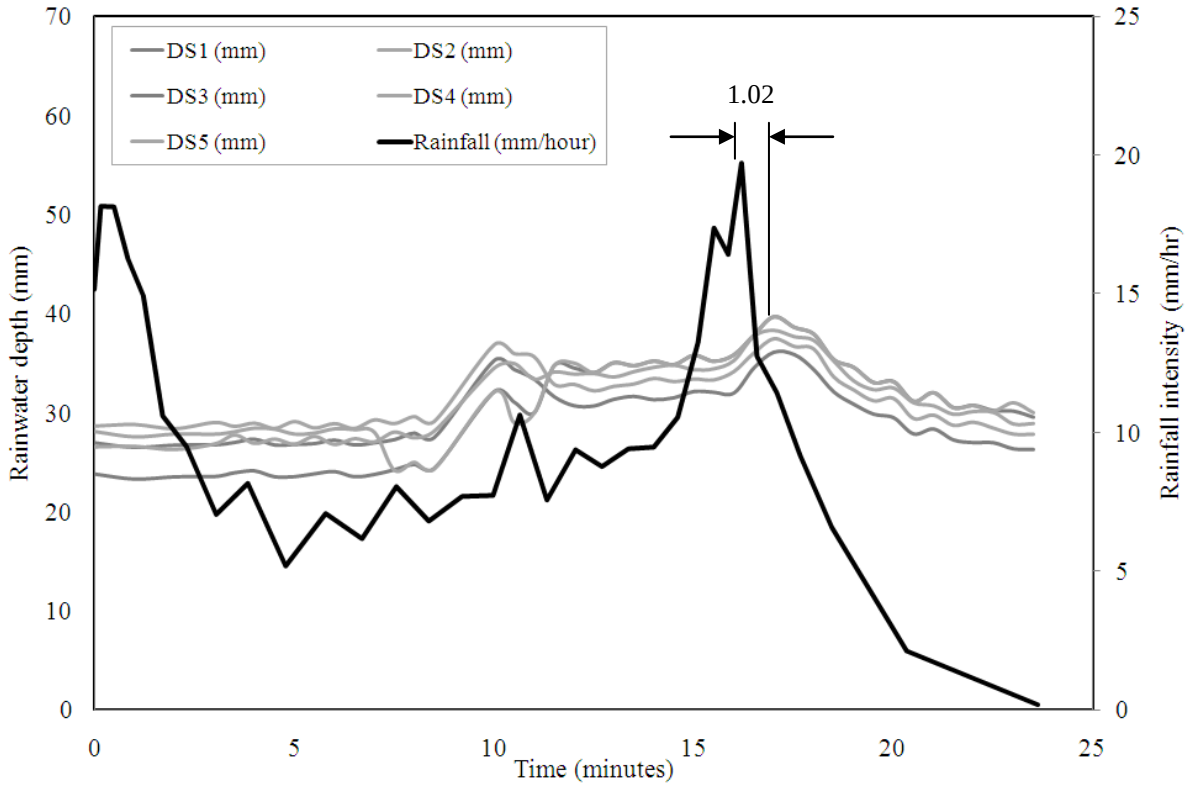

Figure 4.17(b) Ibrox stadium: Measured gutter depth data on 29th October 18:36:24 2010 (refer to Fig. 4.4 for system layout).

Illustrations for Chapter 5.

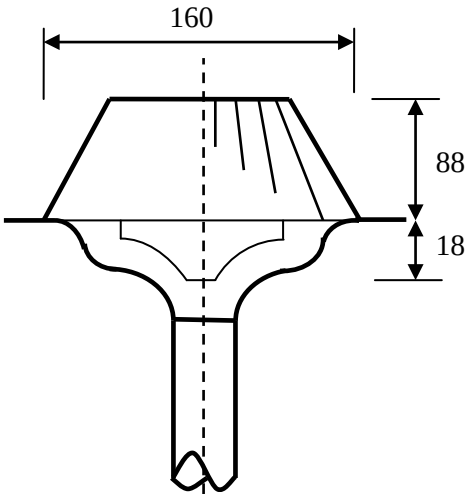

(a)

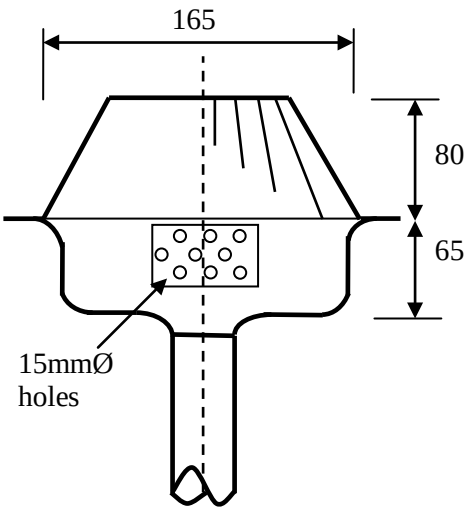

(b)

***Dimensions in mm** **Not to scale**

Figure 5.1(a&b) Outlet A and B respectively.

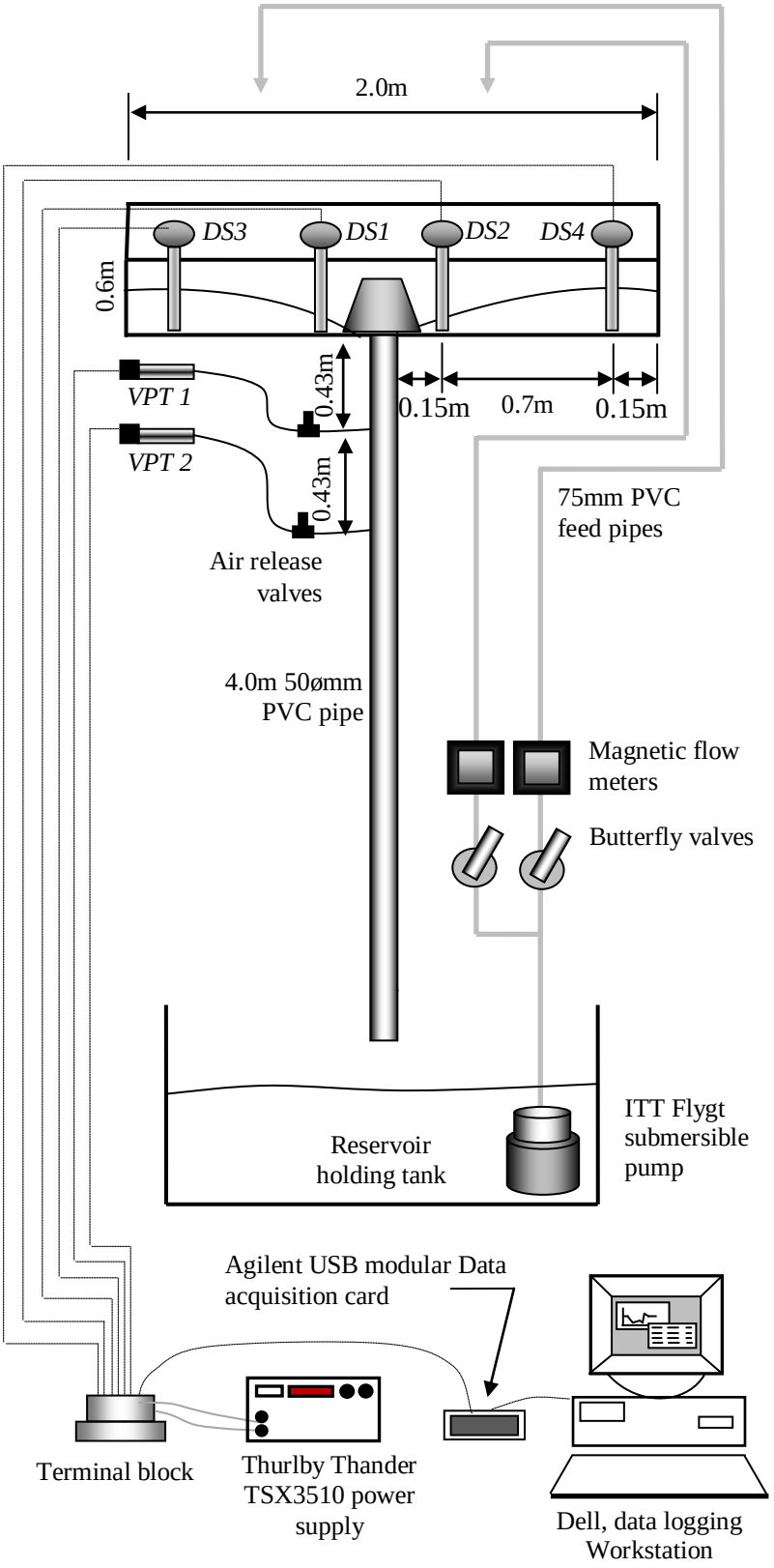

Denotes: VPT* Pressure transducer DS* Depth sensor

Figure 5.2(a) Laboratory test apparatus.

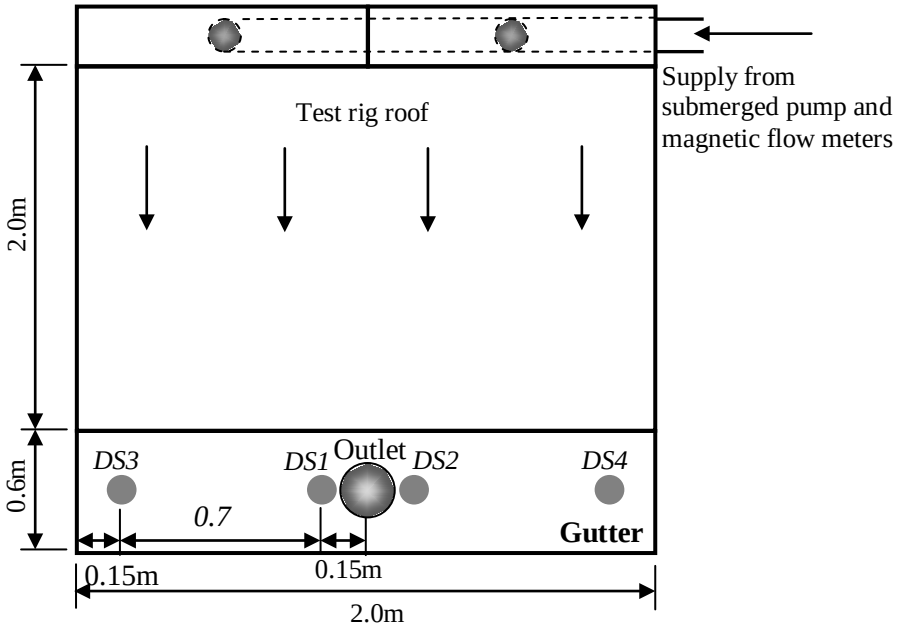

Not to scale

Denotes: DS* Depth sensor

Figure 5.2(b) Plan of laboratory test apparatus.

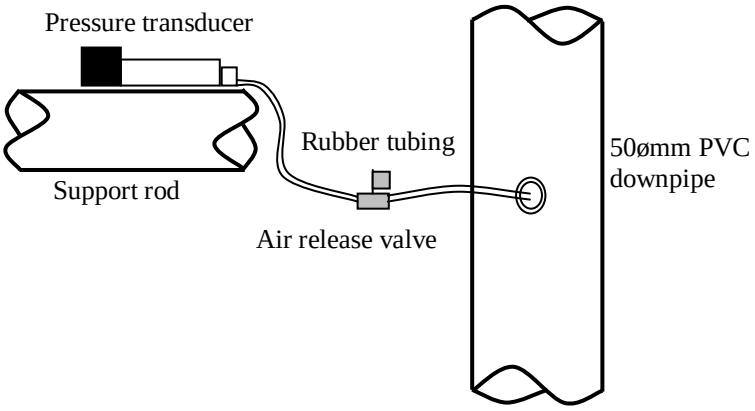

Figure 5.2(c) Pressure transducer connection to discharge pipe.

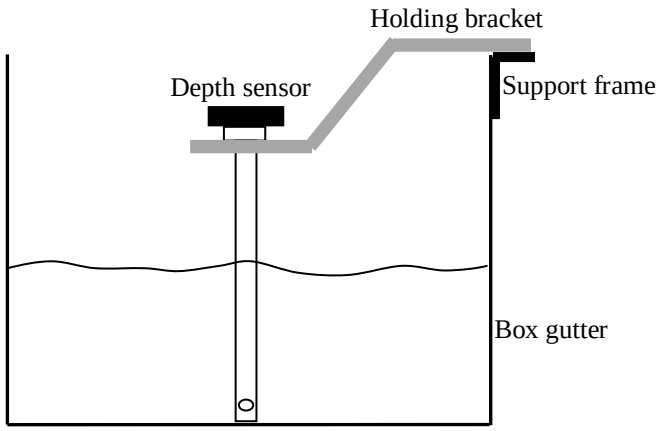

Figure 5.2(d) Depth sensor attachment to galvanised box gutter.

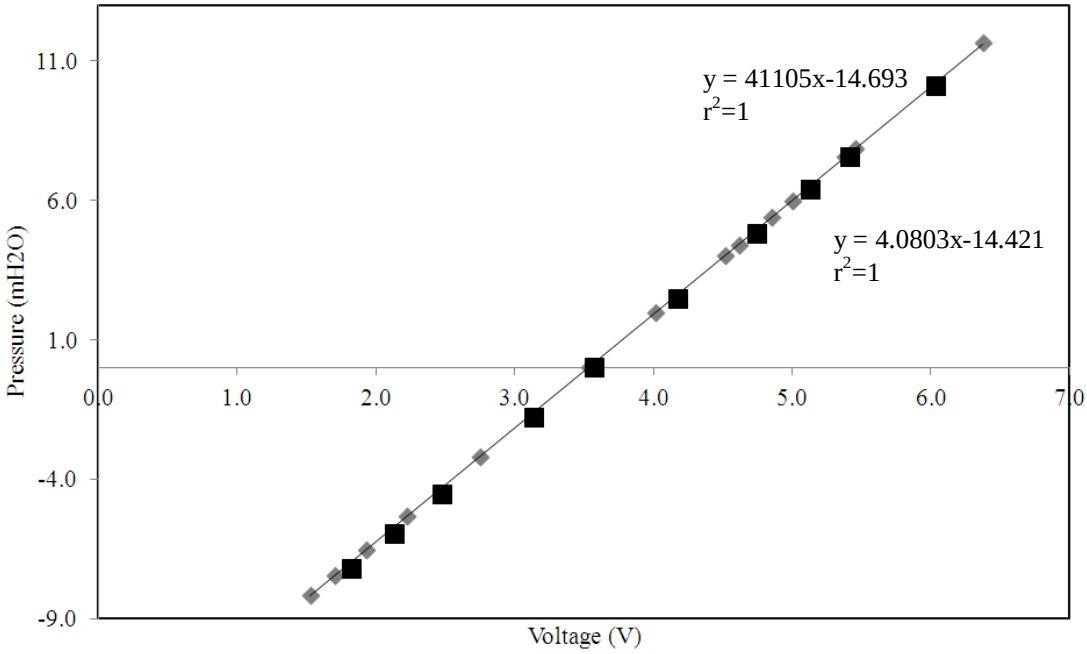

Figure 5.3(a) Pressure transducer calibrations for VPT1 and VPT2.

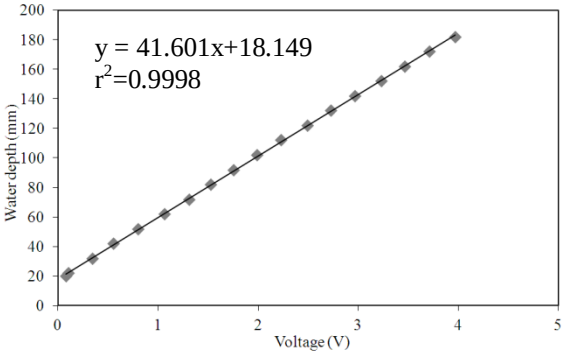

(b) DS1

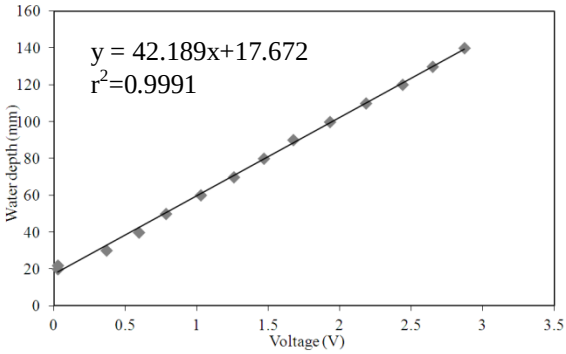

(c) DS2

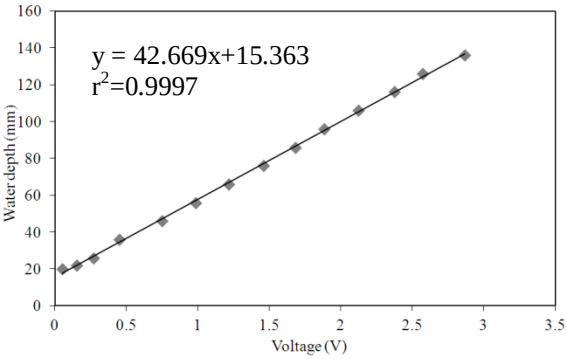

(d) DS3

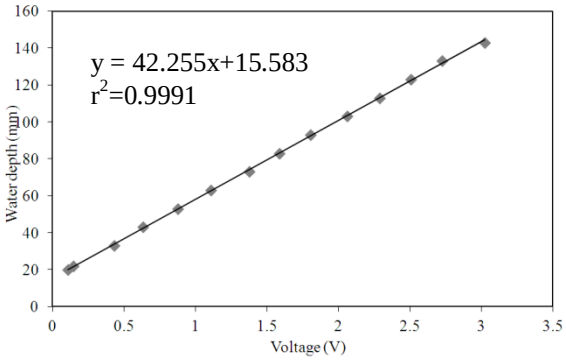

(e) DS4

Figure 5.3 (b to e) Depth sensor calibrations.

Figure 5.4(a) Outlet B, before loose detritus test.

Figure 5.4(b) Outlet B, after loose detritus test.

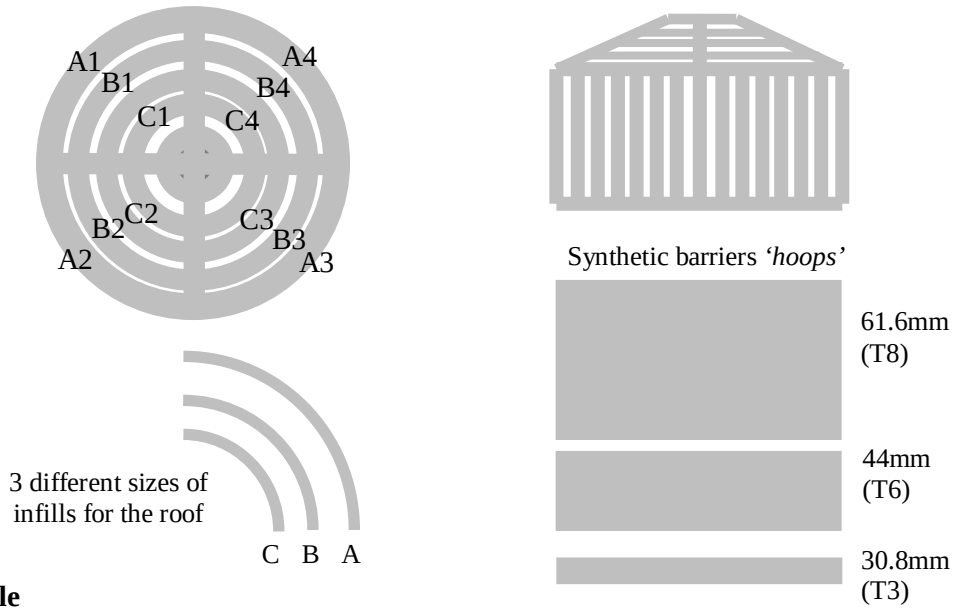

Not to scale

Figure 5.5 Outlet A, leaf-guard: Plan and elevation.

Leaf guard test (T)	Barrier height (mm)	Roof infill reference	Plate-baffle leaf-guard blockage (%)
1	22.0	-	25
2	26.4	-	30
3	30.8	-	35
4	35.2	-	40
5	39.6	-	45
6	44.0	-	50
7	52.8	-	60
8	61.6	-	70
9	61.6 A	A2	73.5
10	61.6 B	A2+B2	77
11	61.6 C	A's	84
12	61.6 D	A's+B2+B4	88.48
13	61.6 E	A's+B's	92.96
14	61.6 F	A's+B's+C2+C4	95.56

Table 5.1 Outlet A, leaf-guard: Conversion of hoop heights to percentage blockage.

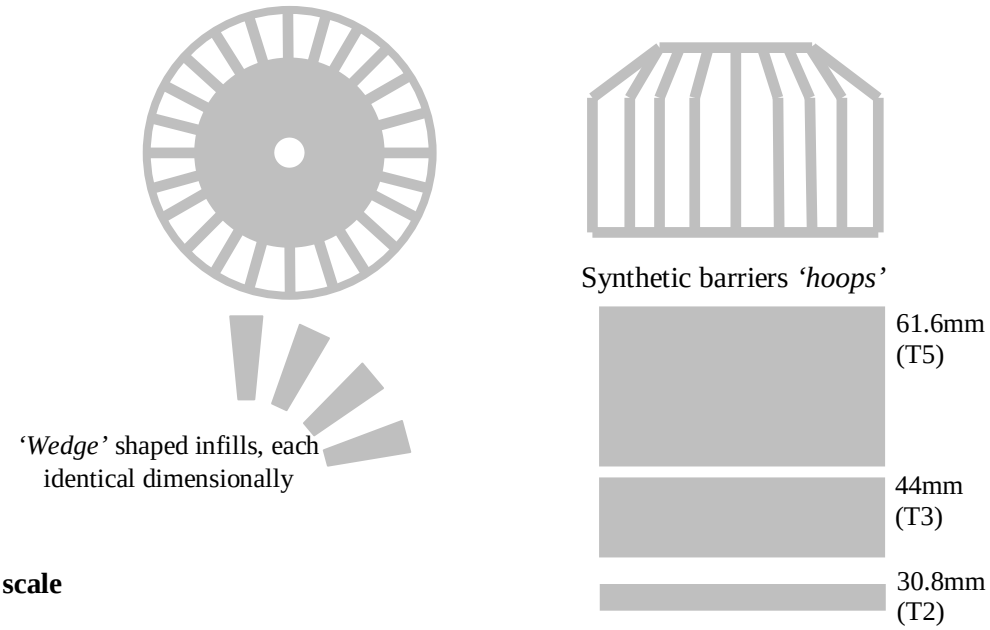

Not to scale

Figure 5.6 Outlet B, leaf-guard: Plan and elevation.

Leaf guard test (T)	Barrier height (mm)	No. of roof infills	Cup-baffle leaf-guard blockage (%)
1	22	-	30
2	30	-	48
3	44	-	60
4	52	-	68
5	61	-	74
6	61 A	4	76
7	61 B	8	79
8	61 C	12	81
9	61 D	16	84
10	61 E	20	86

Table 5.2 Outlet B, leaf-guard: Conversion of hoop heights to percentage blockage.

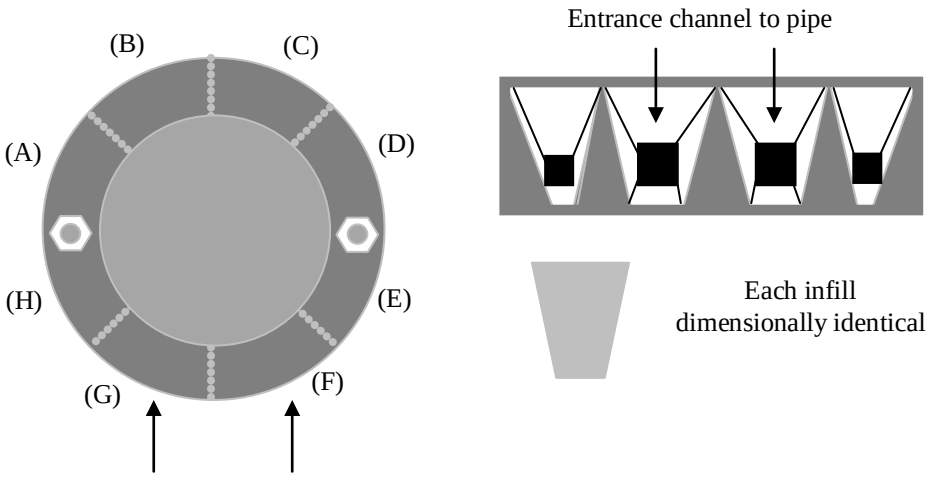

Figure 5.7 Outlet A, baffle: Plan and elevation.

Baffle test (T)	No. of synthetic infills	Infill reference	Plate-baffle percentage blockage (%)
A	1	A	12.5
B	2	A+C	25
C	3	A+C+G	37.5
D	4	A+C+E+G	50
E	6	A+B+C+E+F+G	75
F	7	A+B+C+E+F+G+0.5H+0.5D	87.5

Table 5.3 Outlet A, baffle: Conversion of infills to percentage blockage.

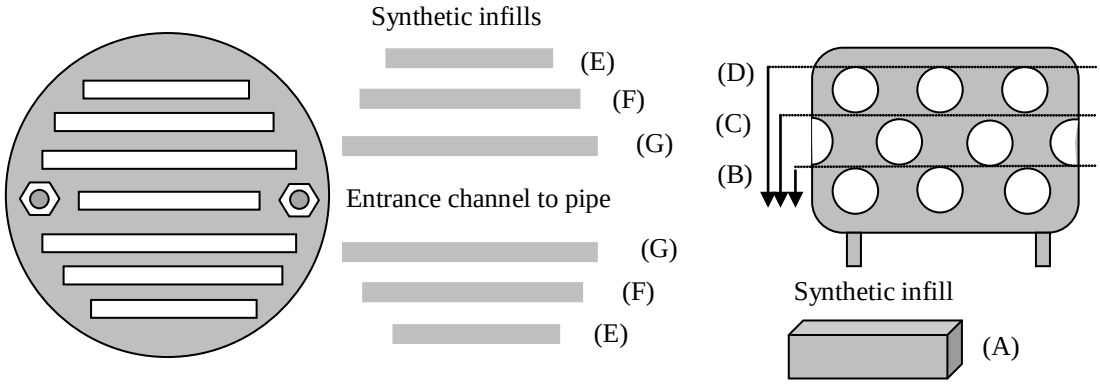

Not to scale

Figure 5.8 Outlet B, baffle: Plan and elevation.

Baffle test (T)	No. of synthetic infills	Infill reference	Cup-baffle percentage blockage (%)
A	1	A	75
B	2	A+B	80
C	3	A+B+C	84
D	4	A+B+C+D	87
E	5	A+B+C+D+E	88
F	7	A+B+C+D+E+F	91
G	9	A+B+C+D+E+F+G	93

Table 5.4 Outlet B, baffle: Conversion of infills to percentage blockage.

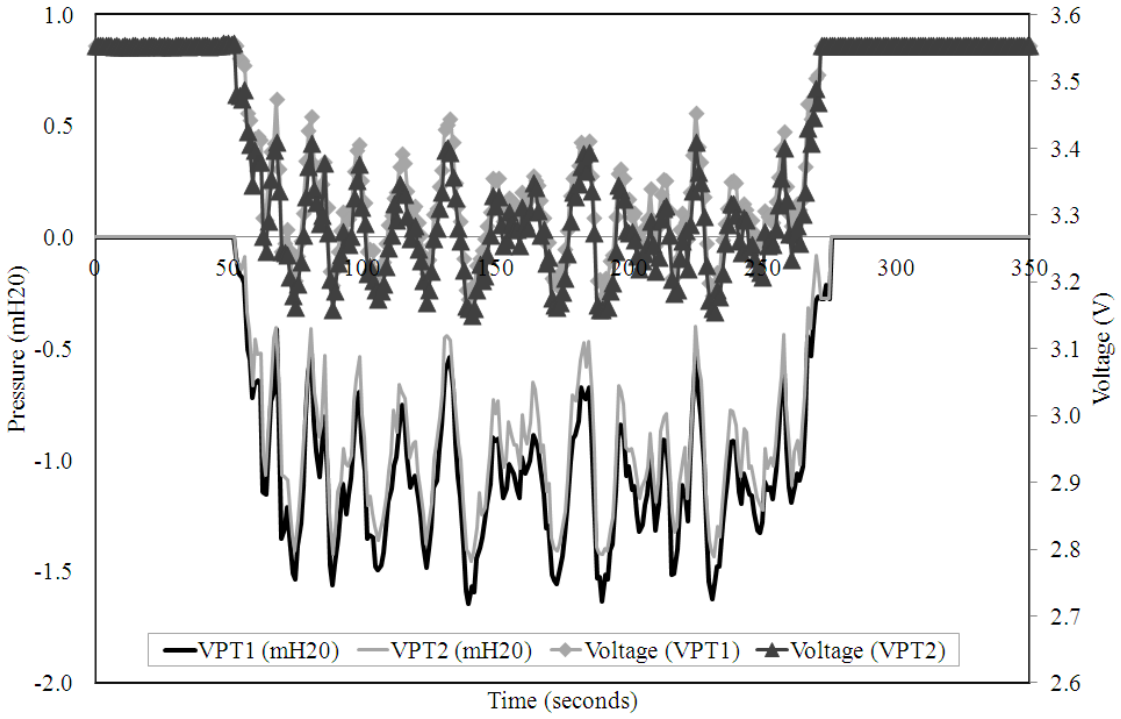

Figure 5.9(a) Outlet A, voltage signal at 5l/s with corresponding pressure.

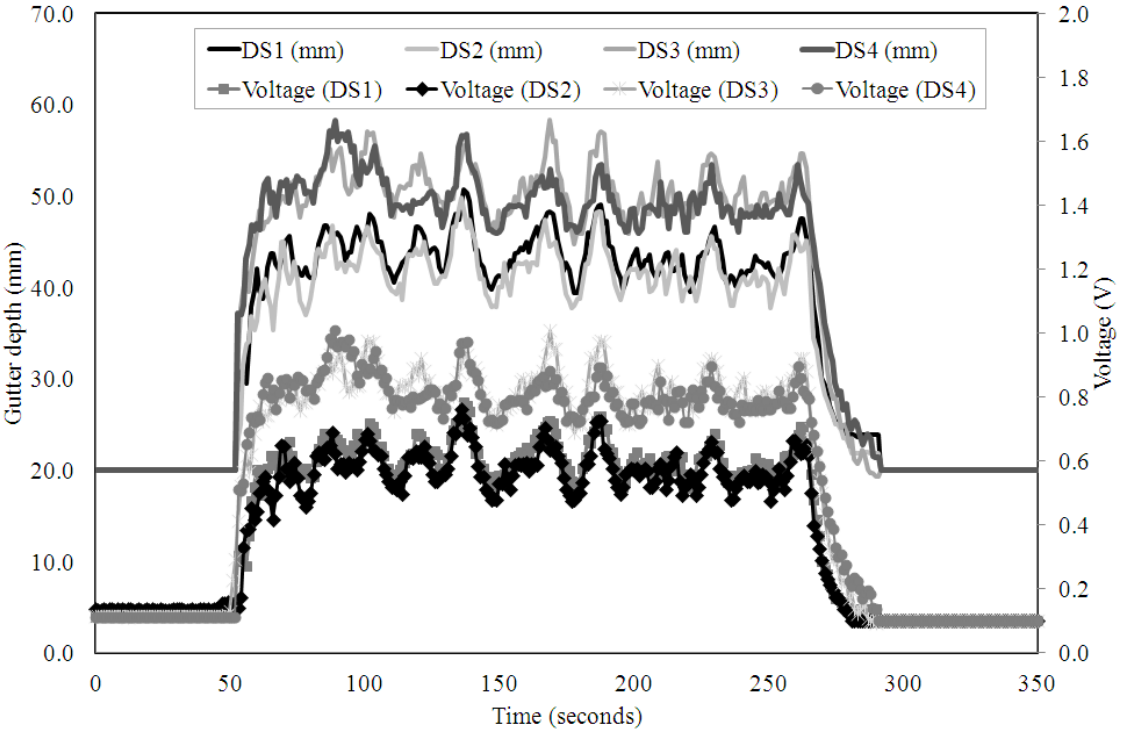

Figure 5.9(b) Outlet A, voltage signal at 5l/s with corresponding depths.

Flow rate (l/s)	Water depth in gutter (mm)				VPT1 Pressure (mH20)	VPT2 Pressure (mH20)	General observations
	DS1	DS2	DS3	DS4			
1	23.478	21.868	19.936	17.639	-0.095	-0.077	0
2	22.712	21.845	17.822	17.638	-0.112	-0.073	0
3	32.225	23.212	36.923	40.203	-0.459	-0.368	0
4	34.273	32.772	37.349	39.093	-0.648	-0.560	0
5	37.186	34.755	41.305	43.093	-0.648	-0.560	Phasing, commencement of noise
6	36.918	34.768	43.709	45.784	-1.354	-1.162	0
7	37.596	36.315	39.155	42.307	-1.637	-1.431	High pitch noise commences
8	39.238	38.541	41.469	44.469	-1.926	-1.563	0
9	63.824	65.733	67.01	69.145	-2.088	-1.752	Full-bore flow

Table 5.5(a) Outlet A, tabulated data.

Flow rate (l/s)	Water depth in gutter (mm)				VPT1 Pressure (mH20)	VPT2 Pressure (mH20)	General observations
	DS1	DS2	DS3	DS4			
1	22.817	21.678	21.952	19.644	-0.167	-0.070	0
2	25.808	23.485	23.510	25.816	-0.255	-0.202	0
3	25.864	23.8	23.758	31.63	-0.411	-0.334	0
4	30.740	29.090	35.867	40.469	-0.560	-0.455	0
5	27.371	26.134	36.171	41.506	-1.005	-0.874	Phasing
6	29.581	30.022	39.726	43.519	-1.202	-1.087	0
7	30.121	29.397	44.259	39.583	-1.436	-1.231	0
8	34.513	34.901	45.893	44.297	-1.819	-1.472	0
9	40.101	38.265	50.755	44.516	-1.999	-1.640	Full-bore flow

Table 5.5(b) Outlet B, tabulated data.

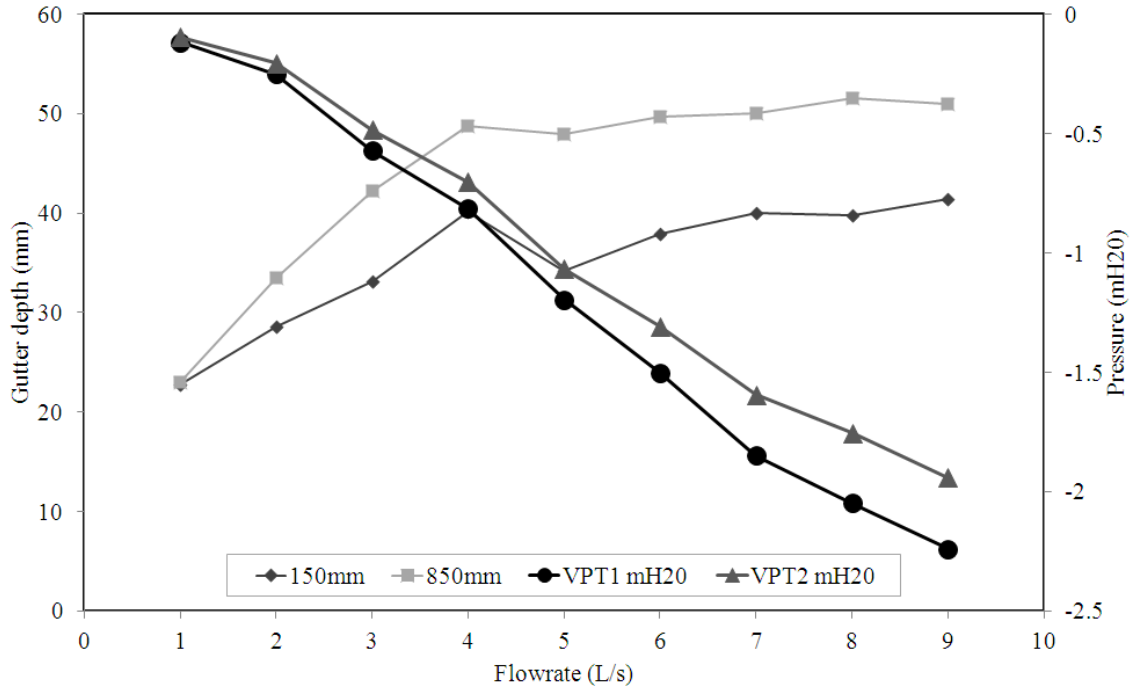

Denotes: 150mm and 850mm refers to distance from outlet.

Figure 5.10(a) Outlet A, gutter depths and system pressures.

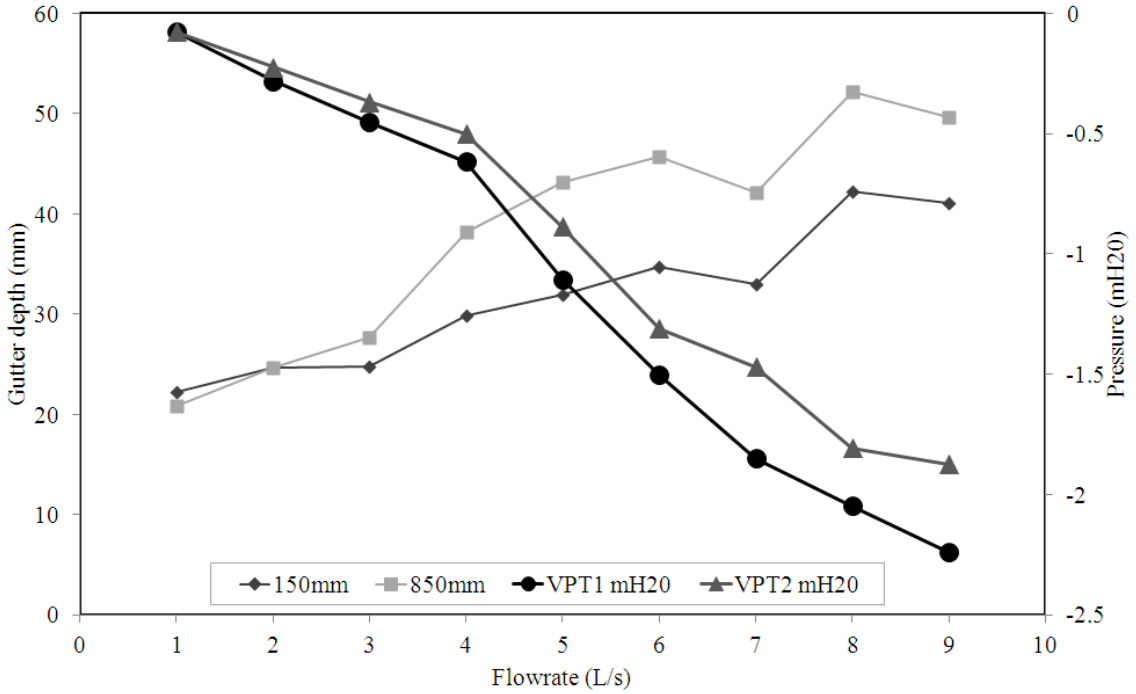

Denotes: 150mm and 850mm refers to distance from outlet.

Figure 5.10(b) Outlet B, gutter depths and system pressures.

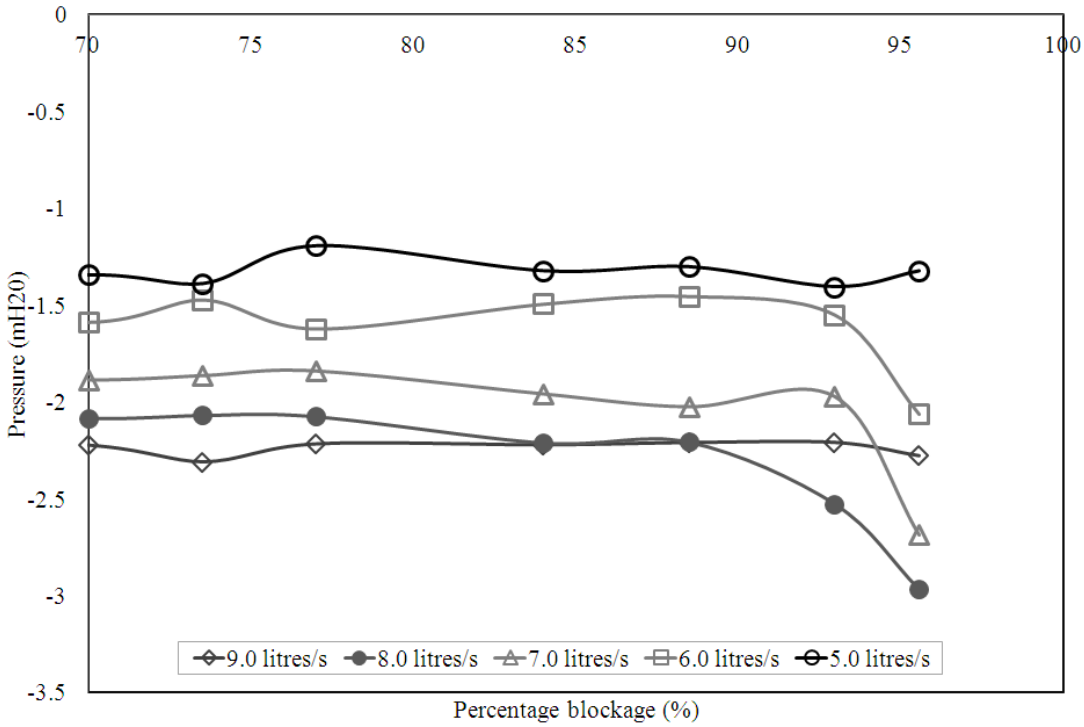

Figure 5.11(a) Outlet A, leaf-guard hoops (pressures at top of discharge pipe).

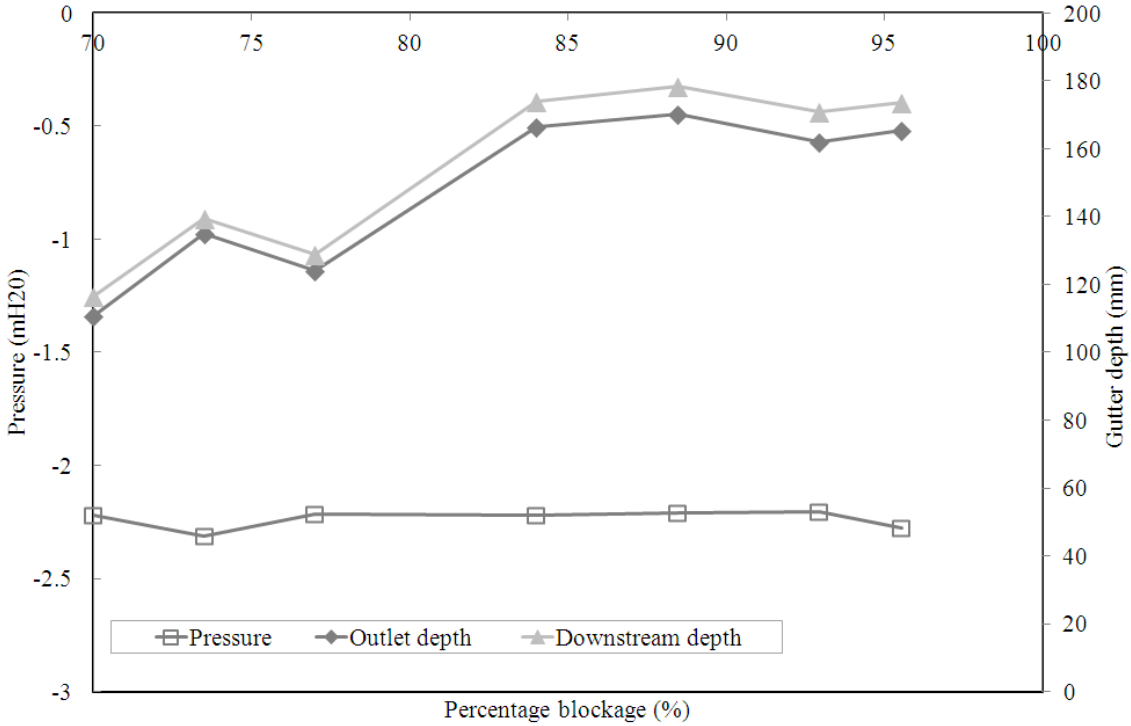

Figure 5.11(b) Outlet A, leaf-guard: hoops at maximum design capacity (pressures at top of discharge pipe).

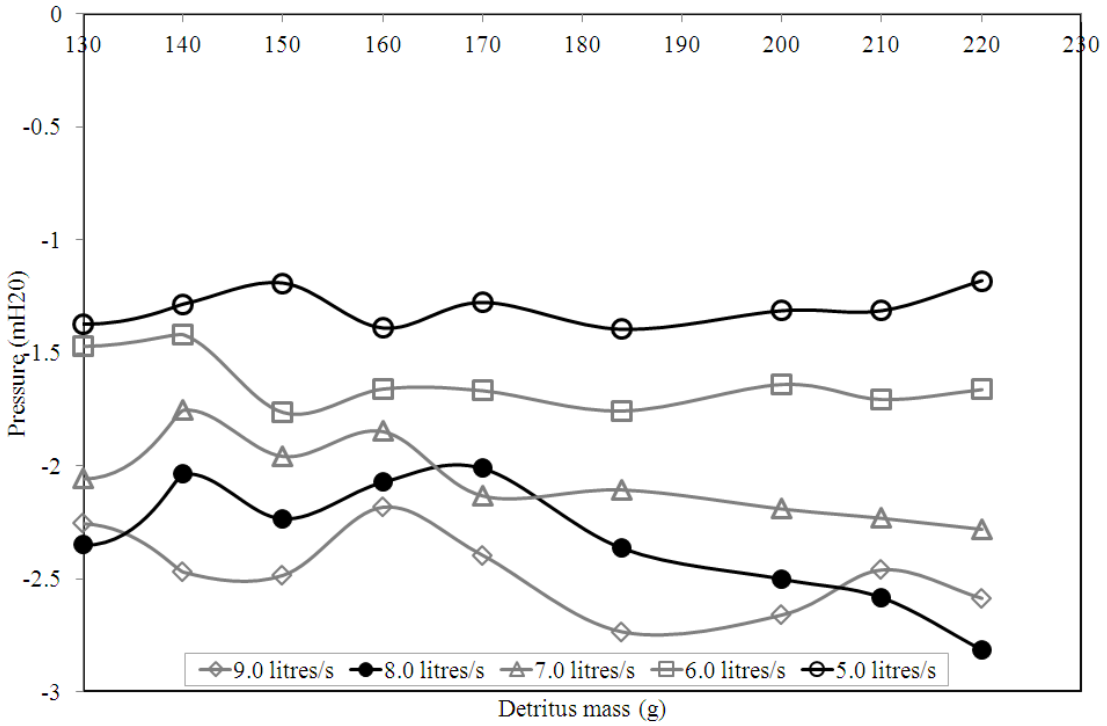

Figure 5.11(c) Outlet A, leaf-guard detritus (pressures at top of discharge pipe).

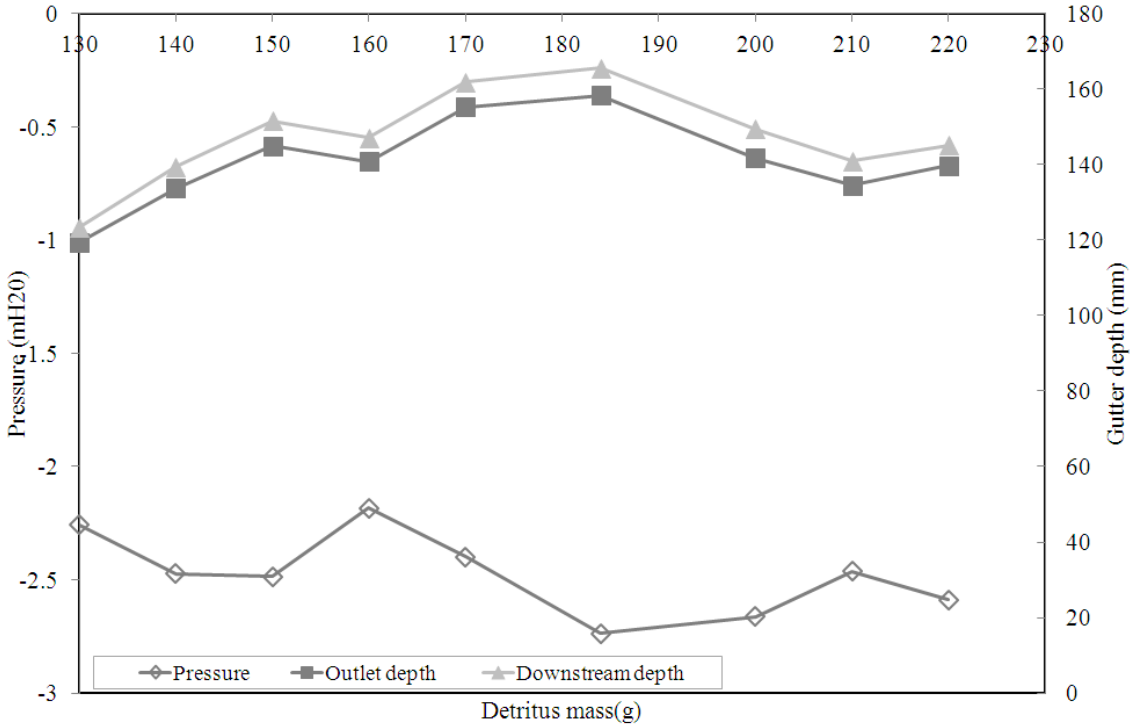

Figure 5.11(d) Outlet A, leaf-guard: Detritus at maximum design capacity (pressure at top of discharge pipe).

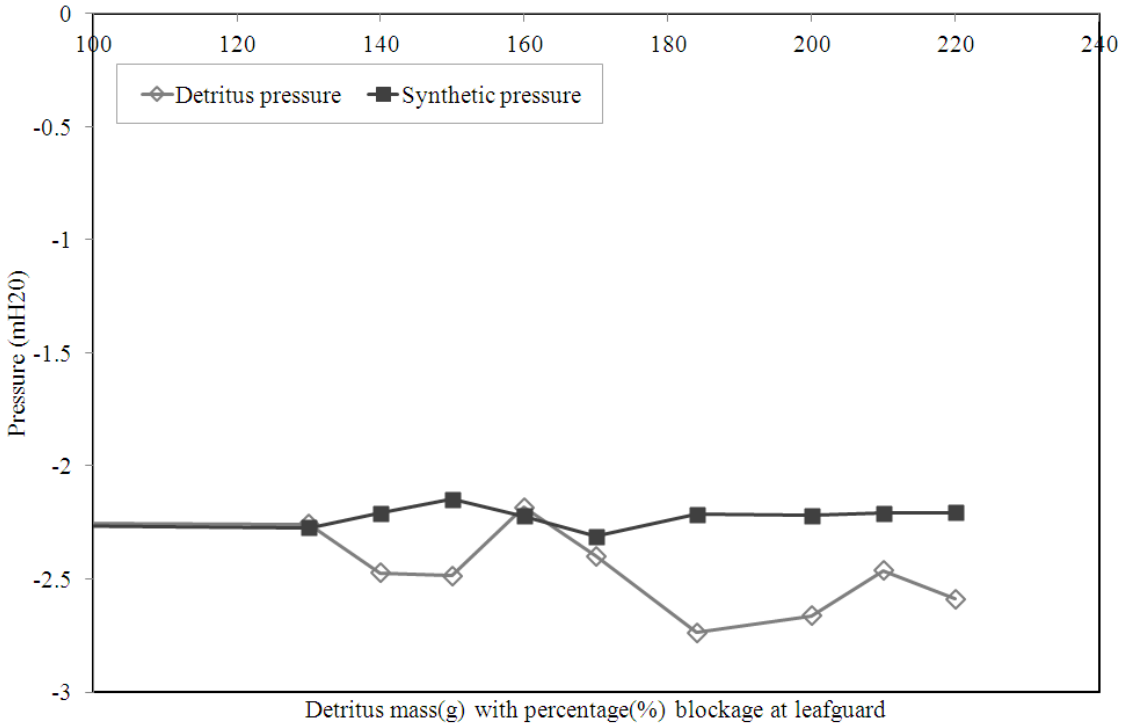

Figure 5.11(e) Outlet A, leaf-guard blockages at maximum system capacity.

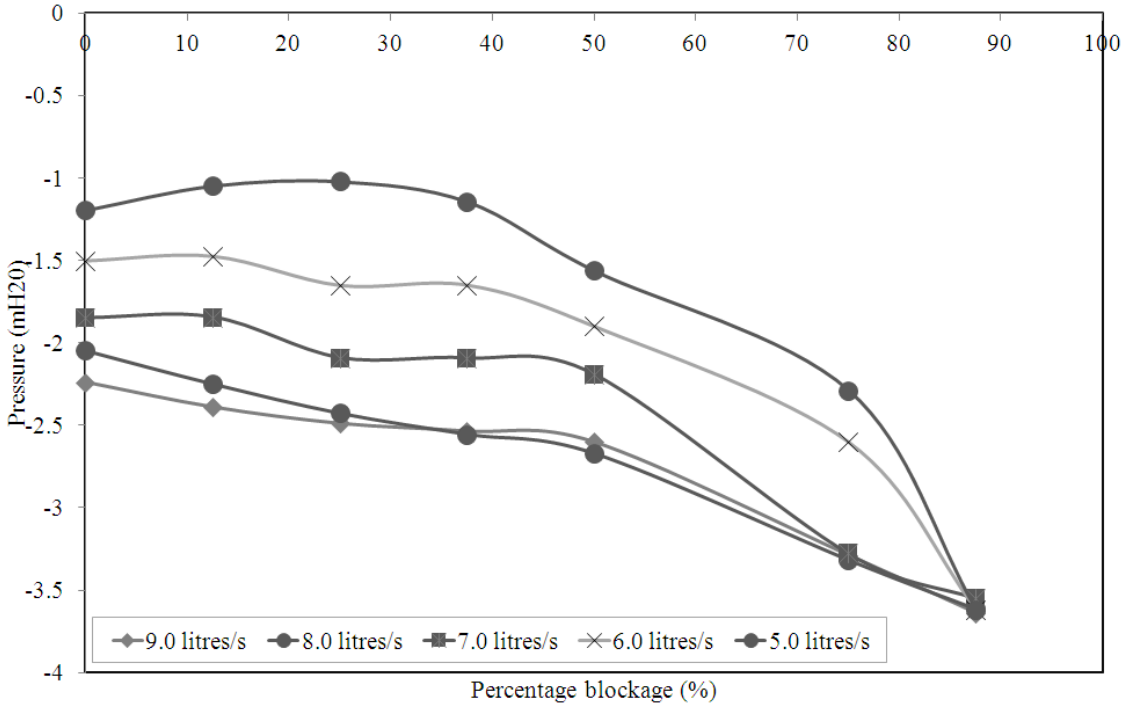

Figure 5.12(a) Outlet A, baffle infills (pressures at top of discharge pipe).

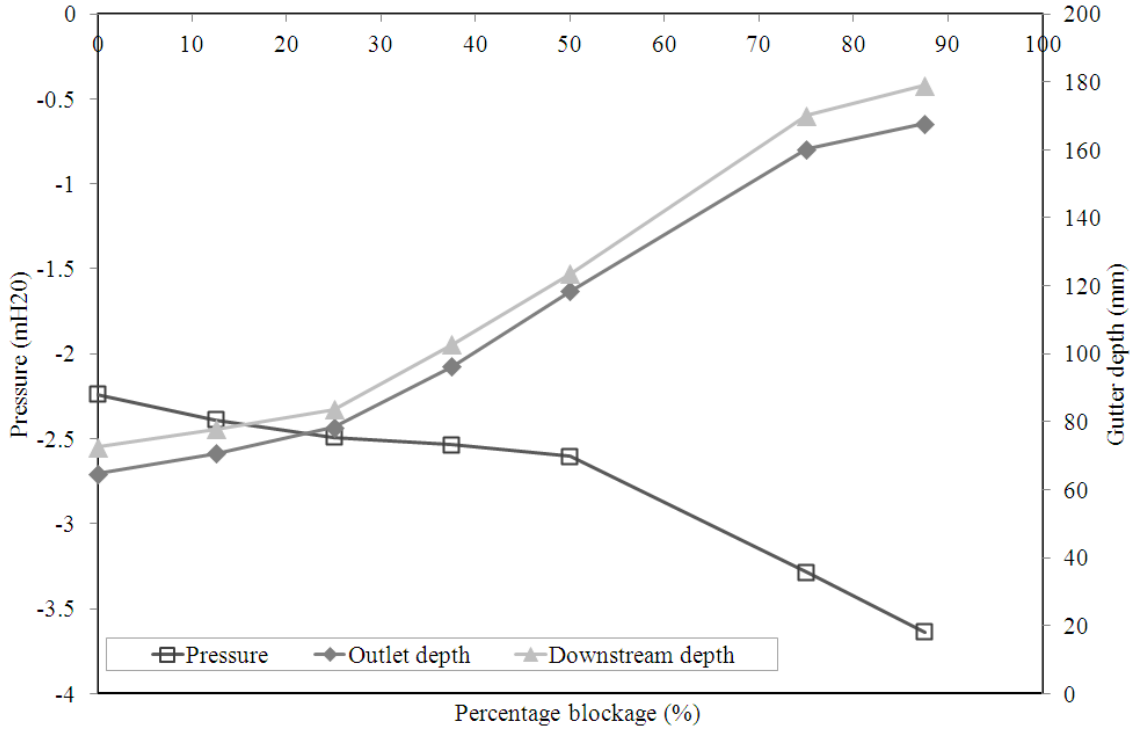

Figure 5.12(b) Outlet A, baffle: Infills at maximum design capacity (pressures at top of discharge pipe).

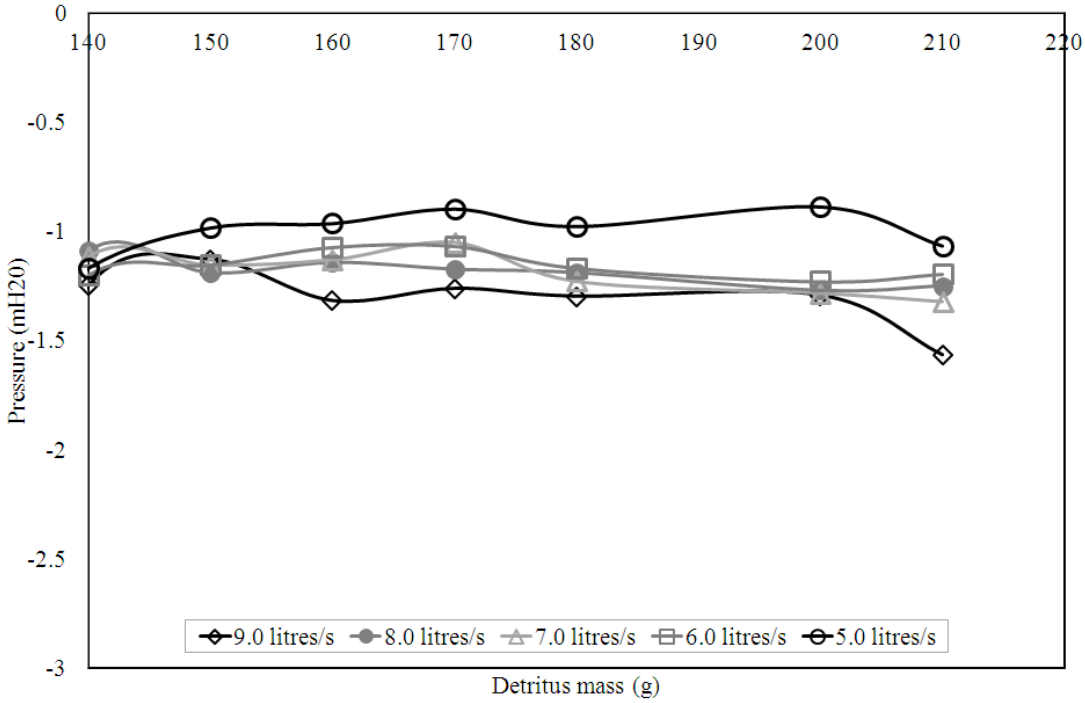

Figure 5.12(c) Outlet A, baffle detritus (pressures at top of discharge pipe).

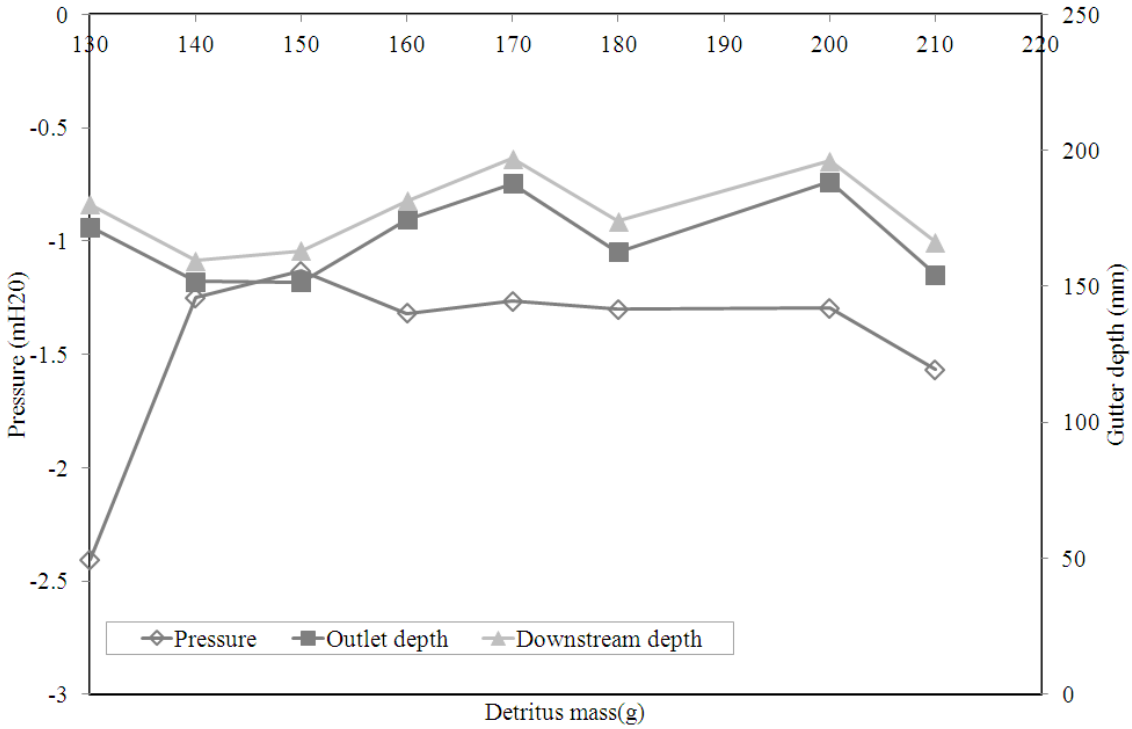

Figure 5.12(d) Outlet A, baffle: Detritus at maximum design capacity (pressure at top of discharge pipe).

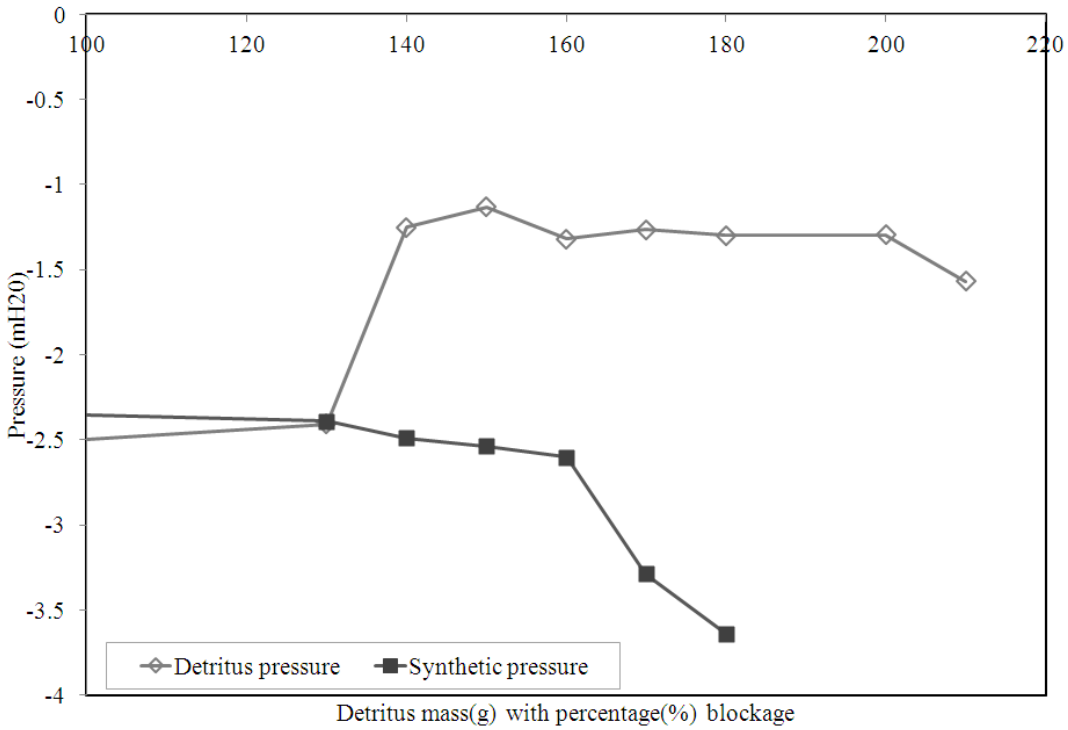

Figure 5.12(e) Outlet A, baffle blockages at maximum system capacity.

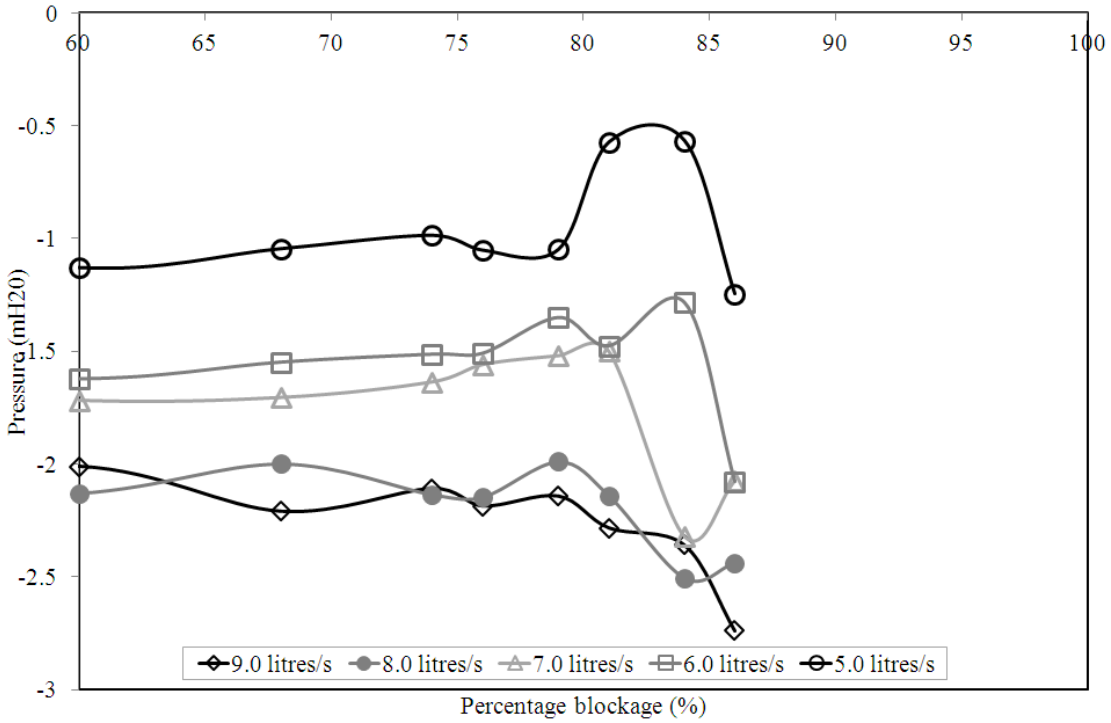

Figure 5.13(a) Outlet B, leaf-guard hoops (pressures at top of discharge pipe).

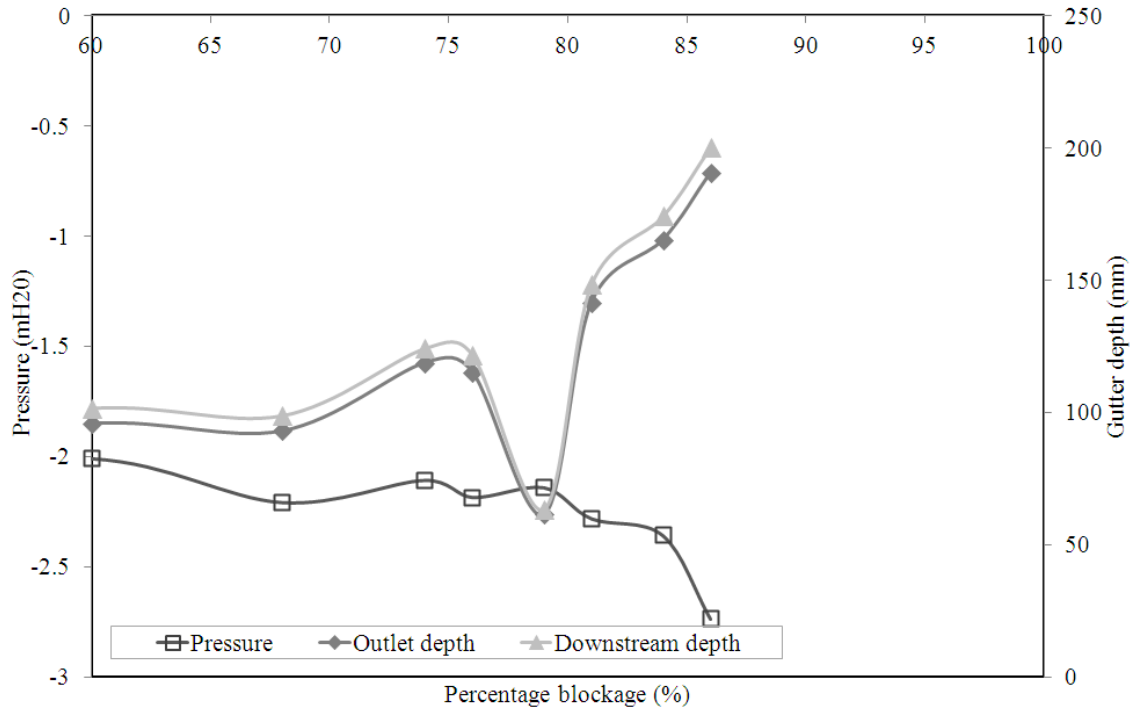

Figure 5.13(b) Outlet B, leaf-guard: Hoops at maximum design capacity (pressure at top of discharge pipe)

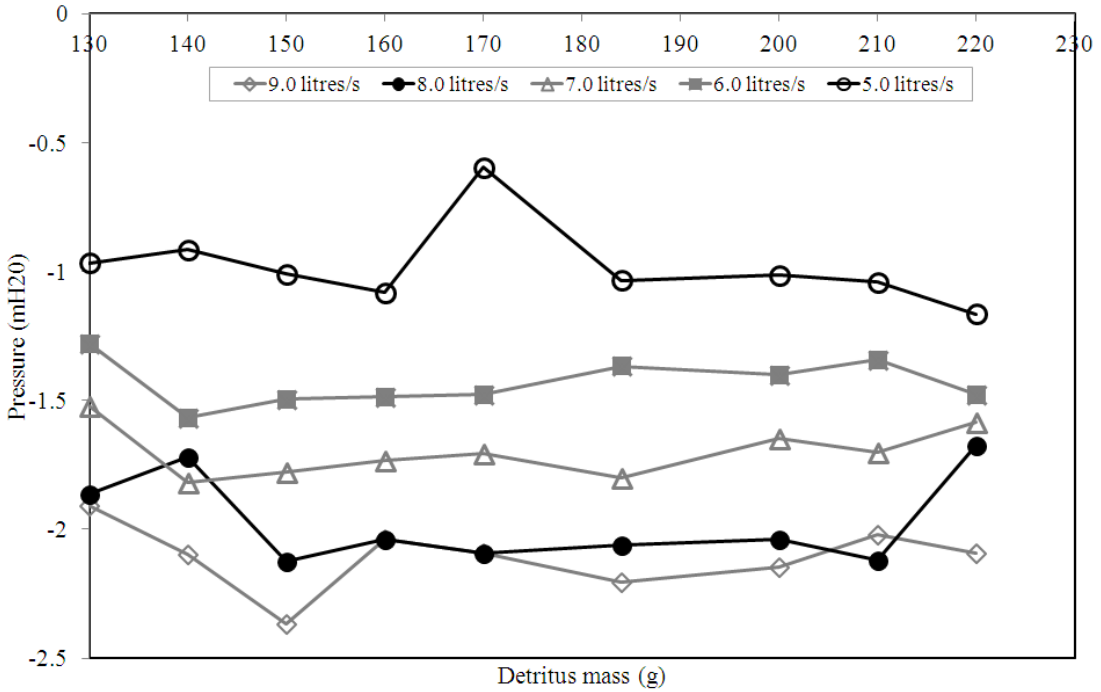

Figure 5.13(c) Outlet B, leaf-guard detritus (pressures at top of discharge pipe).

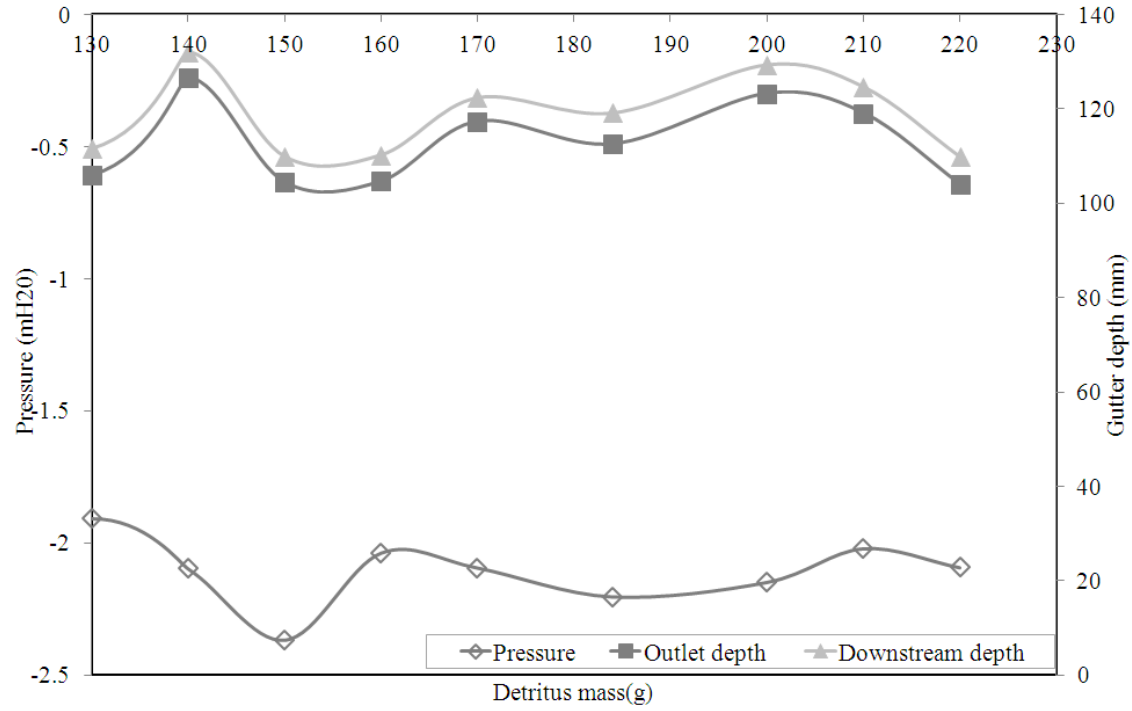

Figure 5.13(d) Outlet B, leaf-guard: Detritus at maximum design capacity (pressures at top of discharge pipe).

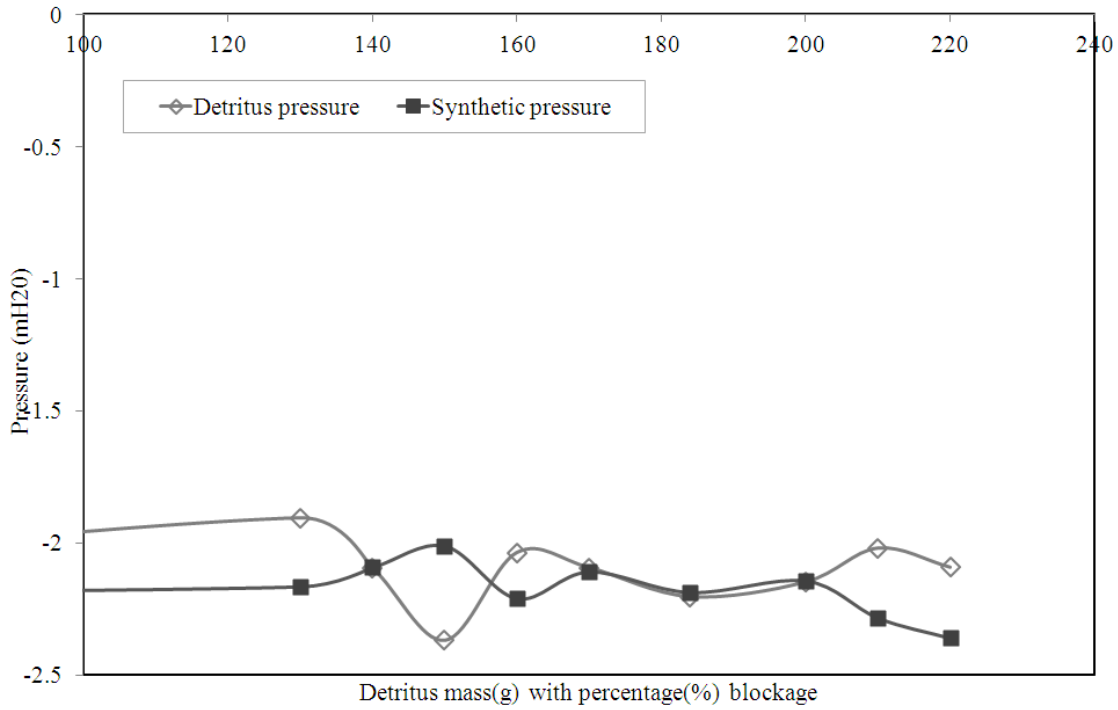

Figure 5.13(e) Outlet B, leaf-guard blockages at maximum system capacity.

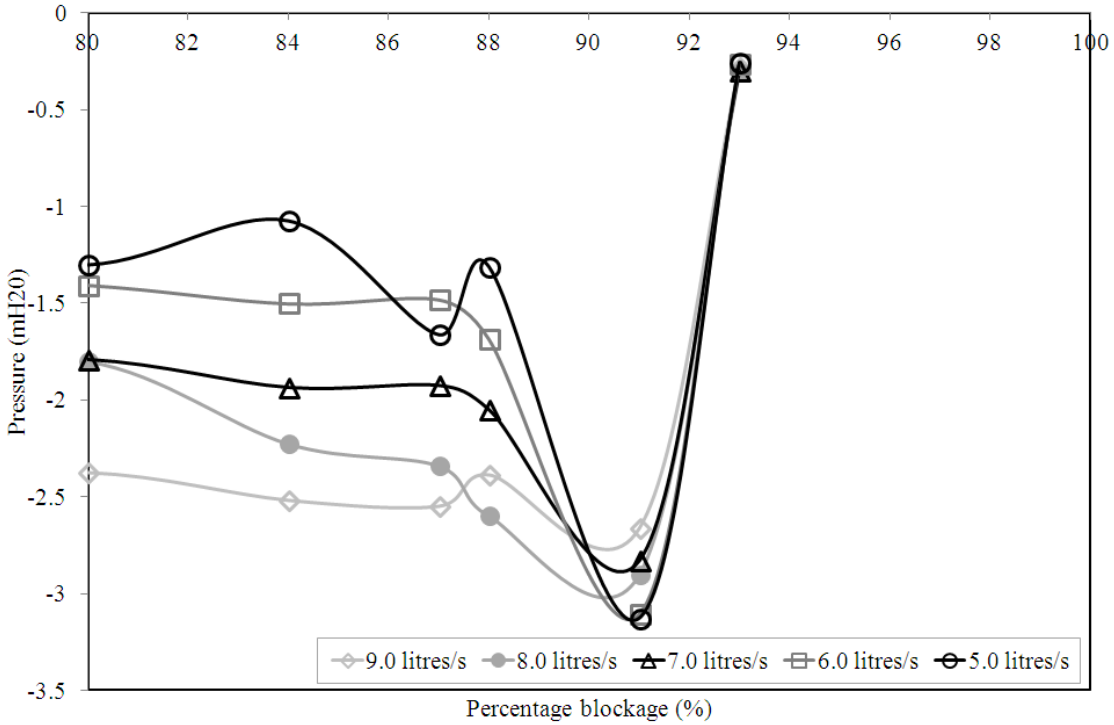

Figure 5.14(a) Outlet B, baffle infills (pressures at top of discharge pipe).

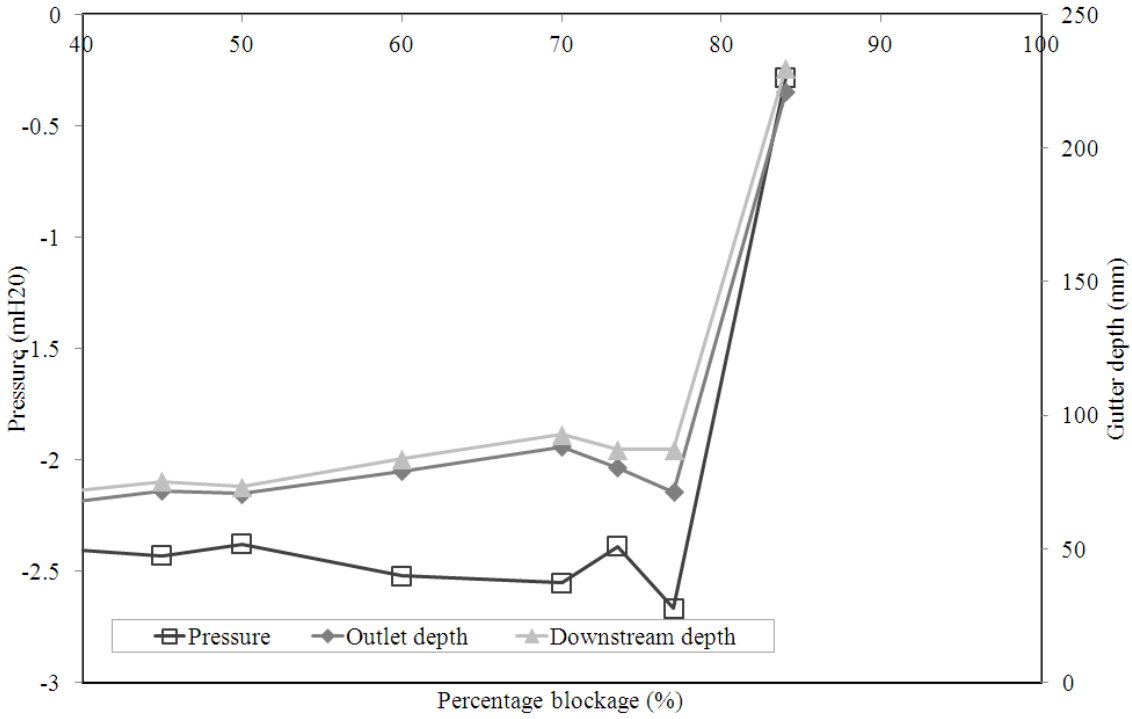

Figure 5.14(b) Outlet B, baffle: Infills at maximum design capacity (pressures at top of discharge pipe).

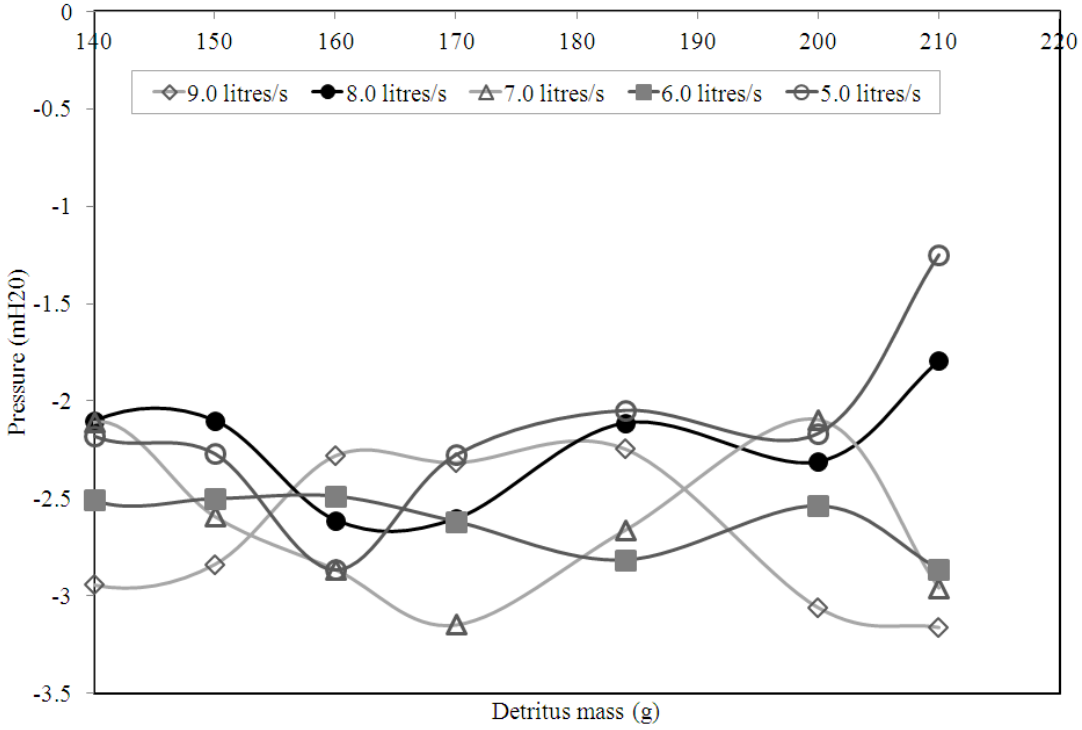

Figure 5.14(c) Outlet B, baffle detritus (pressures at top of discharge pipe**).**

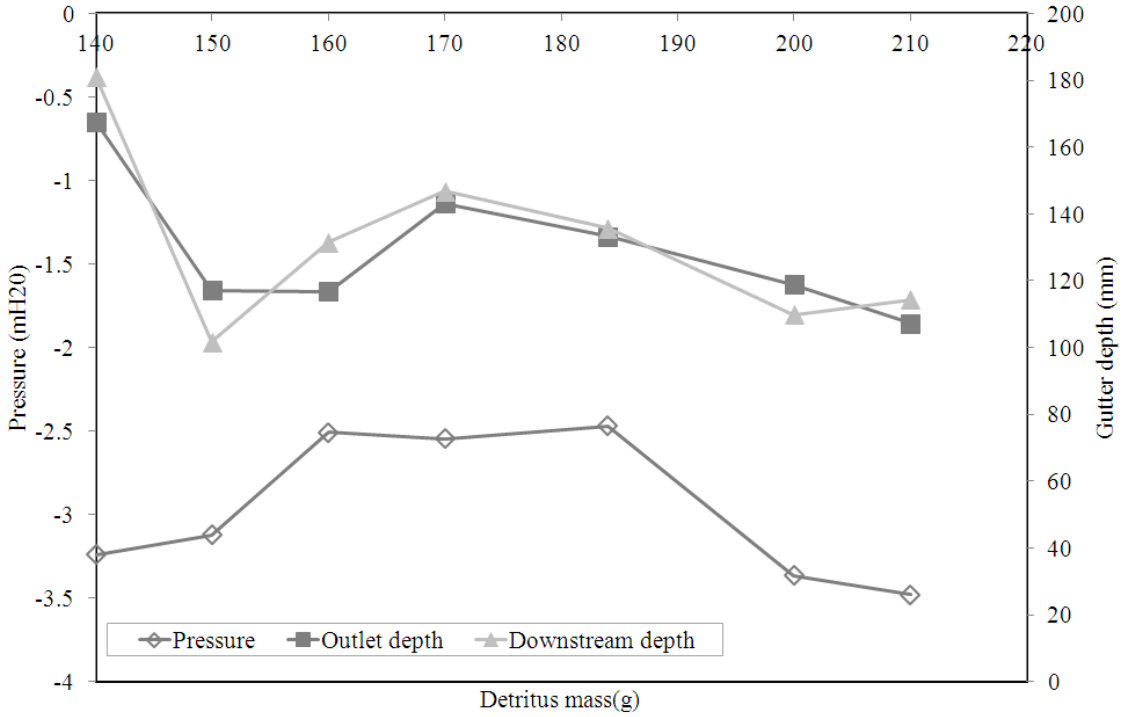

Figure 5.14(d) Outlet B, baffle: Detritus at maximum design capacity (pressures at top of discharge pipe).

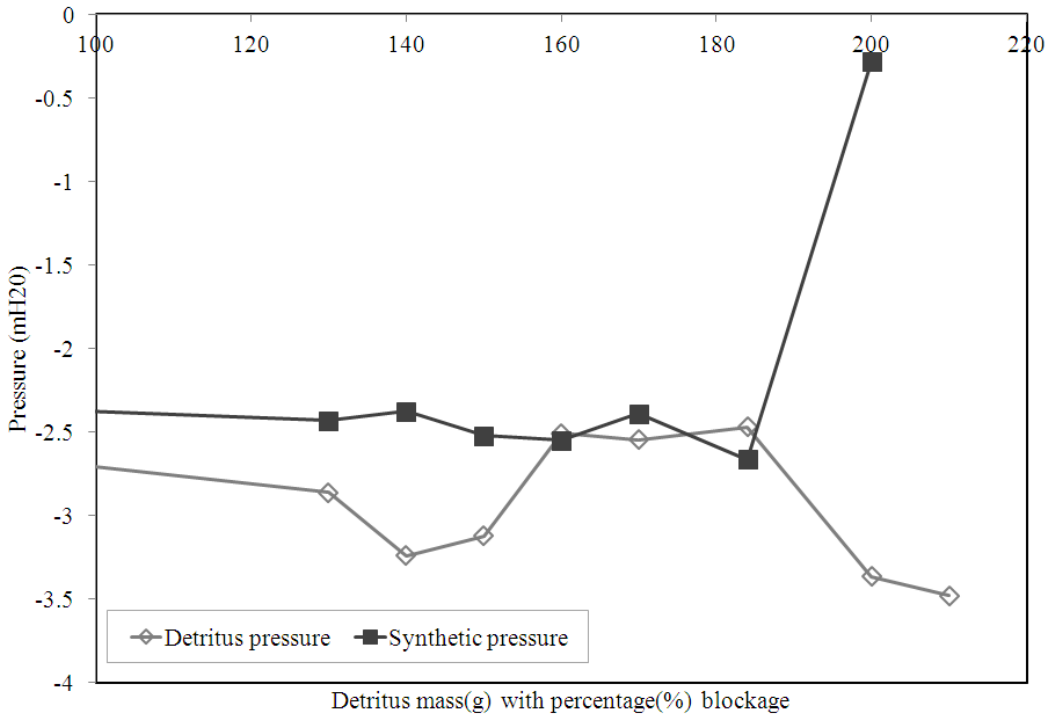

Figure 5.14(e) Outlet A, baffle blockages at maximum system capacity.

Illustrations for Chapter 6.

	Flow rates (l/s)				
%	**9**	**8**	**7**	**6**	**5**
0	1.4	1.6	1.7	2.0	2.1
40	1.4	2.6	4.4	11.2	32.9
45	1.5	2.1	4.3	11.1	31.0
50	1.5	2.5	4.1	11.0	22.1
60	1.5	2.4	4.1	10.7	20.9
70	1.5	2.4	4.2	9.9	21.0
73.5	1.6	2.4	4.3	11.7	21.4
77	1.5	2.0	3.7	9.4	29.5
84	1.5	2.0	3.4	11.3	23.8
88.48	1.5	1.3	3.6	12.0	24.6
92.96	1.4	0.6	1.5	10.4	20.9
95.56	1.4	0.5	1.4	5.4	23.7

Table 6.1 Outlet A, synthetic hoops at leaf-guard: loss coefficients.

	Flow rates (l/s)				
g	**9**	**8**	**7**	**6**	**5**
0	1.4	1.6	1.7	2.0	2.1
130	1.4	1.2	1.9	4.7	5.5
140	1.0	1.9	3.0	5.1	6.5
150	0.9	1.4	2.2	2.9	7.7
160	1.5	1.8	2.6	3.4	5.4
170	1.1	2.0	1.7	3.4	6.5
184	0.6	1.2	1.7	3.0	5.3
200	0.7	0.9	1.5	3.6	6.1
210	0.8	0.8	1.4	3.2	6.1
220	0.8	0.5	1.3	3.4	7.8

Table 6.2 Outlet A, detritus at leaf-guard: loss coefficients.

	Flow rates (l/s)				
%	**9**	**8**	**7**	**6**	**5**
0	1.4	1.6	1.7	2.0	2.1
12.5	1.1	1.9	4.3	11.5	38.3
25	0.9	1.5	3.1	9.0	40.3
37.5	0.9	1.2	3.1	9.0	32.0
50	0.8	1.0	2.7	6.5	16.6
75	0.1	0.3	0.6	3.0	7.2
87.5	0.1	0.1	0.4	1.0	2.3

Table 6.3 Outlet A, synthetic infills at baffle: loss coefficients.

	Flow rates (l/s)				
g	**9**	**8**	**7**	**6**	**5**
0	1.4	1.6	1.7	2.0	2.1
130	2.2	13.2	14.8	22.5	64.0
140	11.2	35.4	43.9	55.2	125.9
150	13.9	37.9	41.0	59.8	177.5
160	10.9	41.2	42.8	69.4	184.9
170	10.9	39.0	49.7	70.0	213.4
184	10.2	37.9	36.0	58.3	179.8
200	2.2	2.3	2.3	2.4	2.4
210	6.7	34.3	31.0	55.6	151.0

Table 6.4 Outlet A, detritus at baffle: loss coefficients.

	Flow rates (l/s)				
%	**9**	**8**	**7**	**6**	**5**
0	1.4	1.6	1.9	2.0	2.2
30	1.5	2.0	4.9	12.4	40.7
48	1.7	2.0	5.4	9.8	47.0
60	1.9	2.1	4.9	9.0	31.8
68	1.6	2.1	5.0	10.0	37.2
74	1.6	2.0	5.5	10.5	42.0
76	1.5	2.0	6.1	10.6	36.8
79	1.5	2.5	6.5	13.5	37.0
81	1.2	2.1	6.7	11.1	125.9
84	1.1	1.2	2.2	15.0	129.2
86	0.5	1.3	3.0	5.1	26.0

Table 6.5 Outlet B, synthetic hoops at leaf-guard: loss coefficients.

	Flow rates (l/s)				
g	**9**	**8**	**7**	**6**	**5**
0	1.4	1.6	1.9	2.0	2.2
130	2.2	2.3	2.8	4.8	10.3
140	1.7	2.9	1.7	2.9	11.6
150	1.1	2.9	1.8	3.2	9.3
160	1.8	1.8	2.1	3.3	8.0
170	1.7	1.6	2.0	3.4	7.9
184	1.4	1.9	1.7	4.1	8.8
200	1.5	1.8	2.3	3.8	9.2
210	1.9	1.6	2.1	3.6	8.7
220	1.7	3.2	2.5	3.4	6.8

Table 6.6 Outlet B, detritus at leaf-guard: loss coefficients.

	Flow rates (l/s)				
%	**9**	**8**	**7**	**6**	**5**
0	1.4	1.6	1.9	2.0	2.2
45	1.0	3.1	4.3	13.3	27.9
50	1.0	3.3	4.4	12.3	23.4
60	0.8	1.8	3.6	10.6	34.9
70	0.8	1.5	3.6	11.0	14.0
73.5	1.0	1.1	3.1	8.2	23.1
77	0.6	0.6	1.1	1.7	3.2
84	180.7	181.5	234.2	463.2	764.7

Table 6.7 Outlet B, synthetic infills at baffle: loss coefficients.

	Flow rates (l/s)				
g	**9**	**8**	**7**	**6**	**5**
0	1.4	1.6	1.9	2.0	2.2
130	0.4	3.1	2.5	8.7	28.0
140	0.3	5.4	5.5	5.6	17.7
150	0.2	5.4	3.3	5.6	16.3
160	0.8	3.1	2.5	5.5	9.8
170	0.8	3.1	1.9	5.0	16.2
184	0.9	5.3	3.0	4.2	20.2
200	0.1	1.9	2.0	2.0	2.3
210	0.1	7.8	2.3	4.0	55.8

Table 6.8 Outlet B, detritus at baffle: loss coefficients.

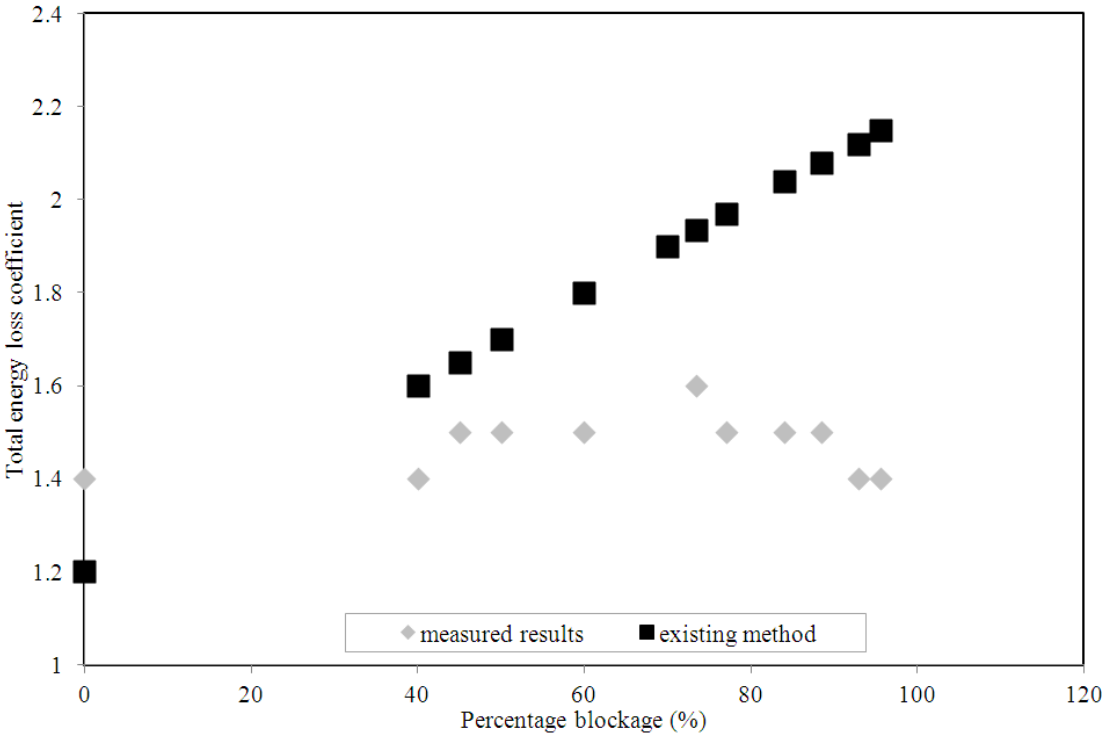

Figure 6.1 Outlet A, synthetic hoops at leaf-guard.

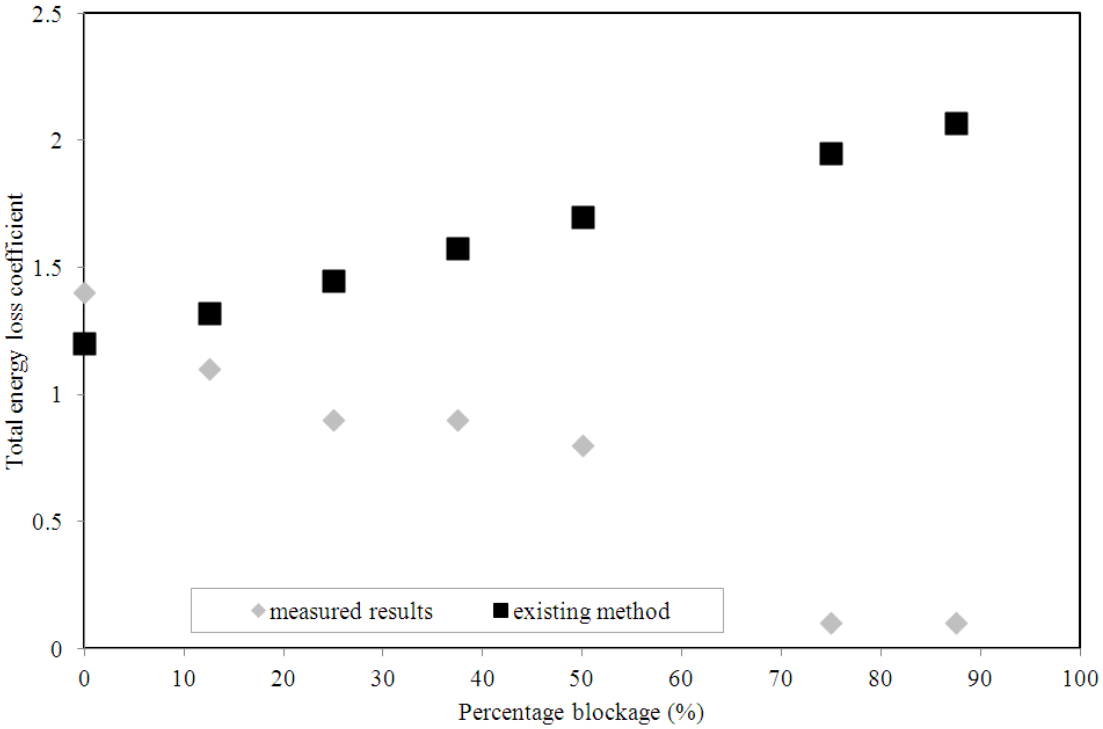

Figure 6.2 Outlet A, synthetic infills at baffle.

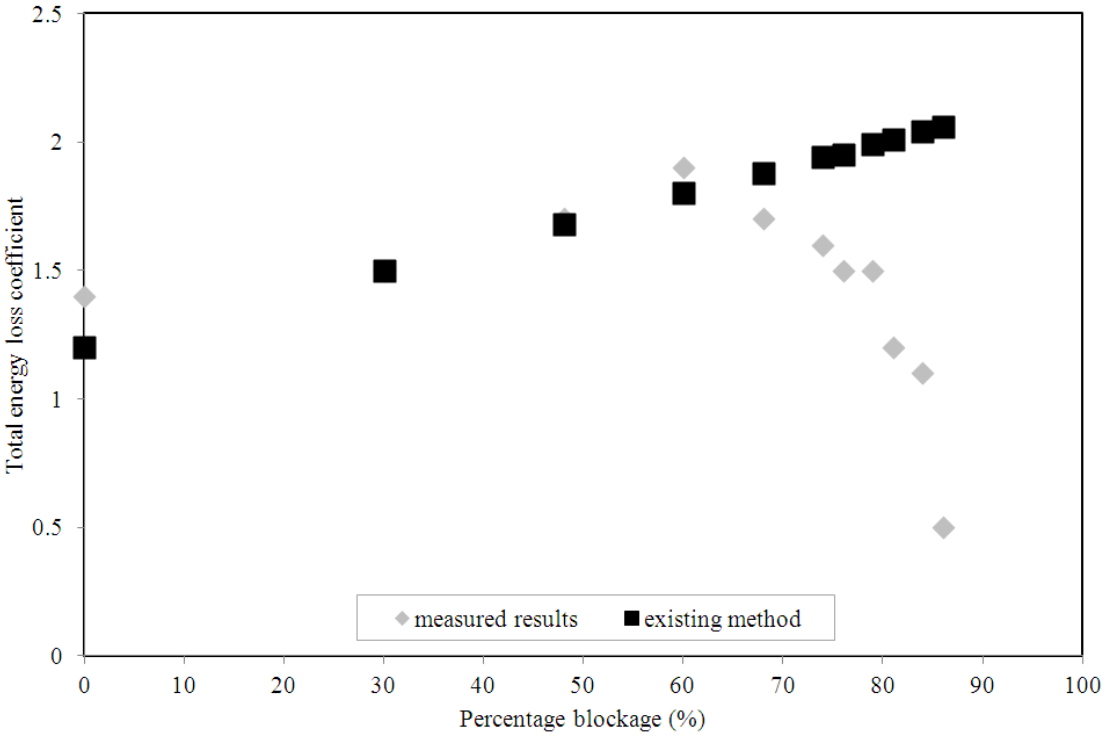

Figure 6.3 Outlet B, synthetic hoops at leaf-guard.

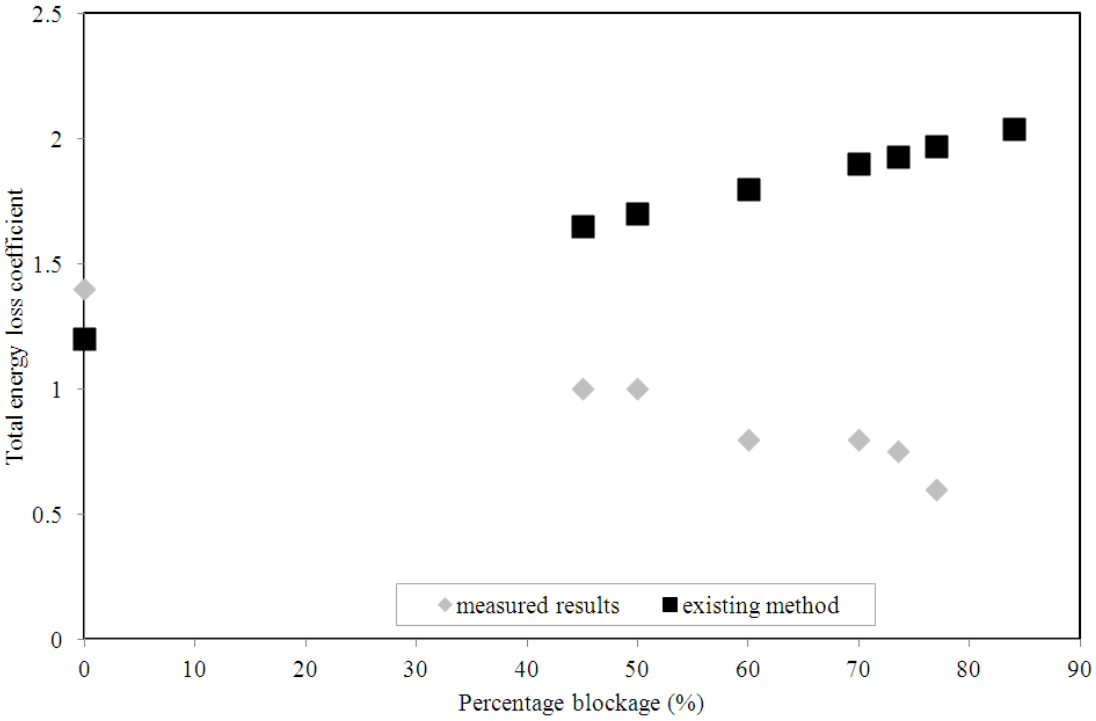

Figure 6.4 Outlet B, synthetic infills at baffle.

Illustrations for Chapter 7.

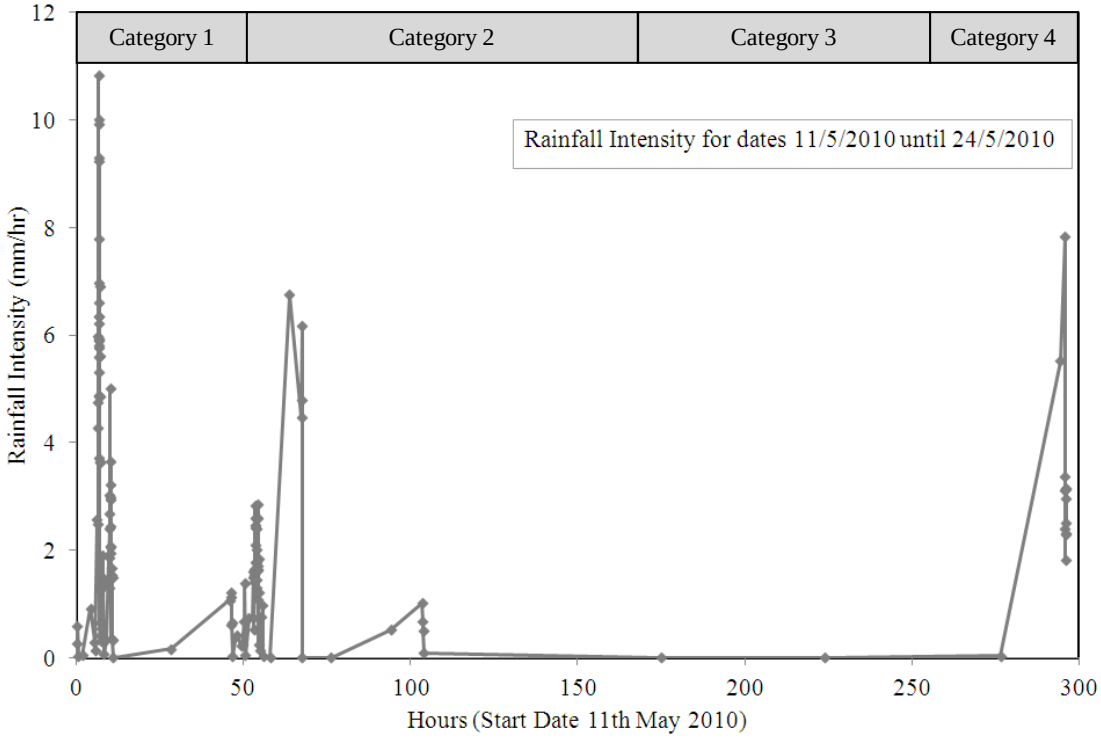

Figures 7.1(a) NRS, System 1-West: Start date 11th May, detritus change.

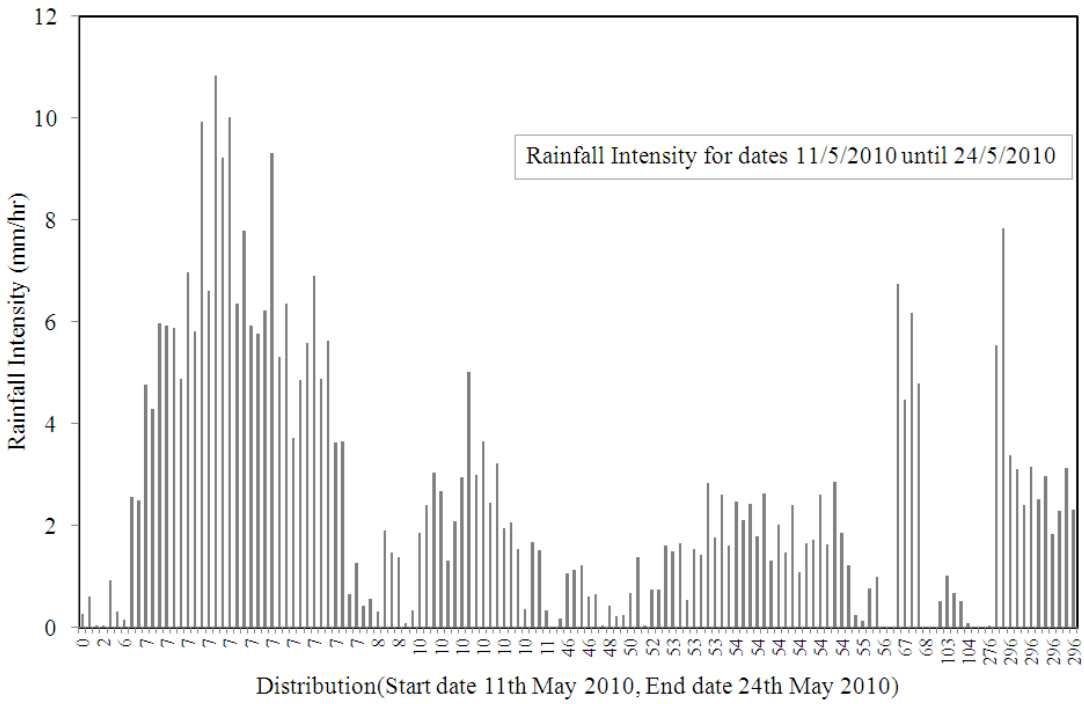

Figures 7.1(b) NRS, System 1-West: Start date 11th May, rainfall distribution.

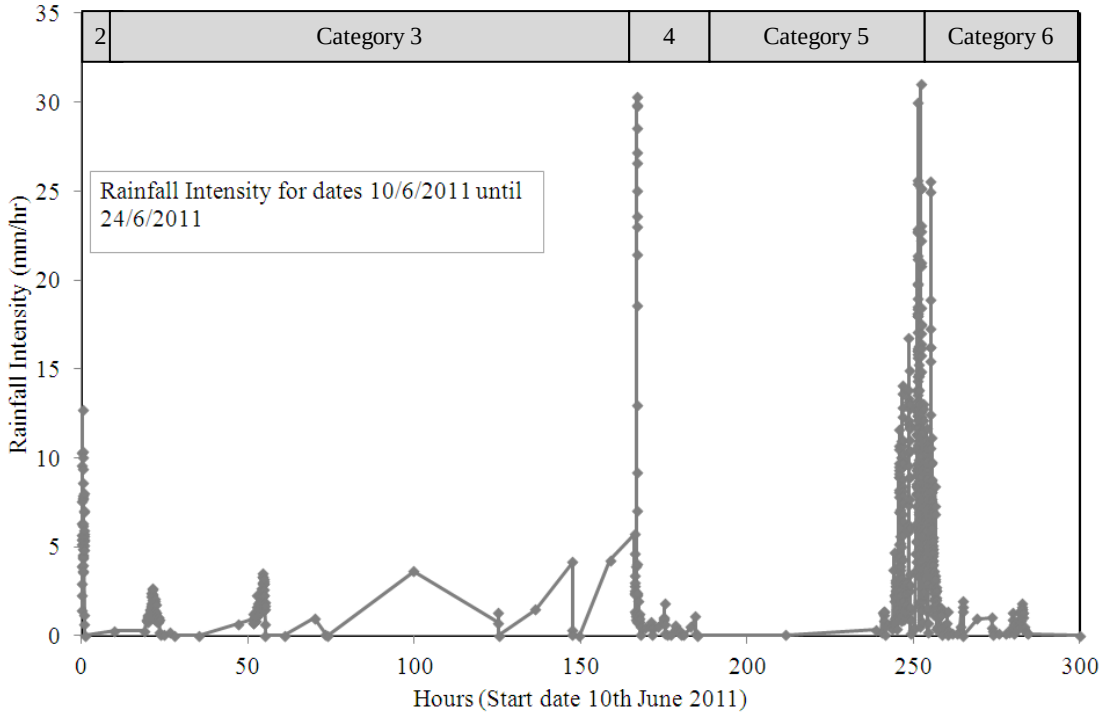

Figure 7.2(a) NRS, System 1-West: Start 10th June, detritus change.

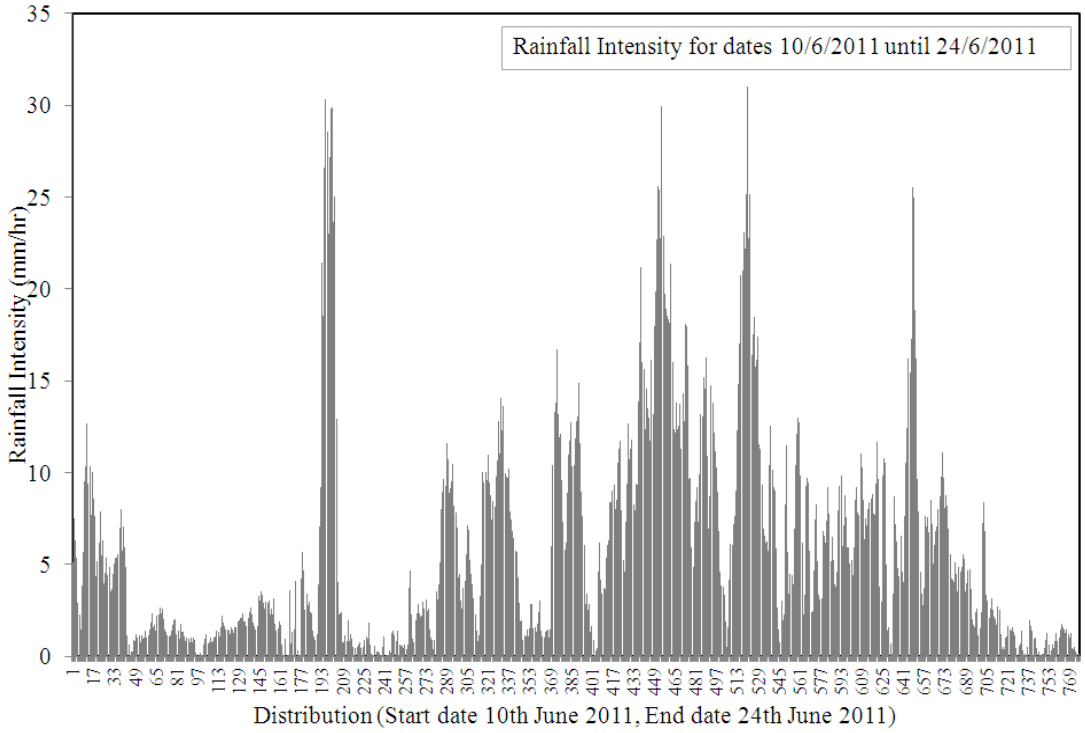

Figure 7.2(b) NRS, System 1-West: Start 10th June, rainfall distribution.

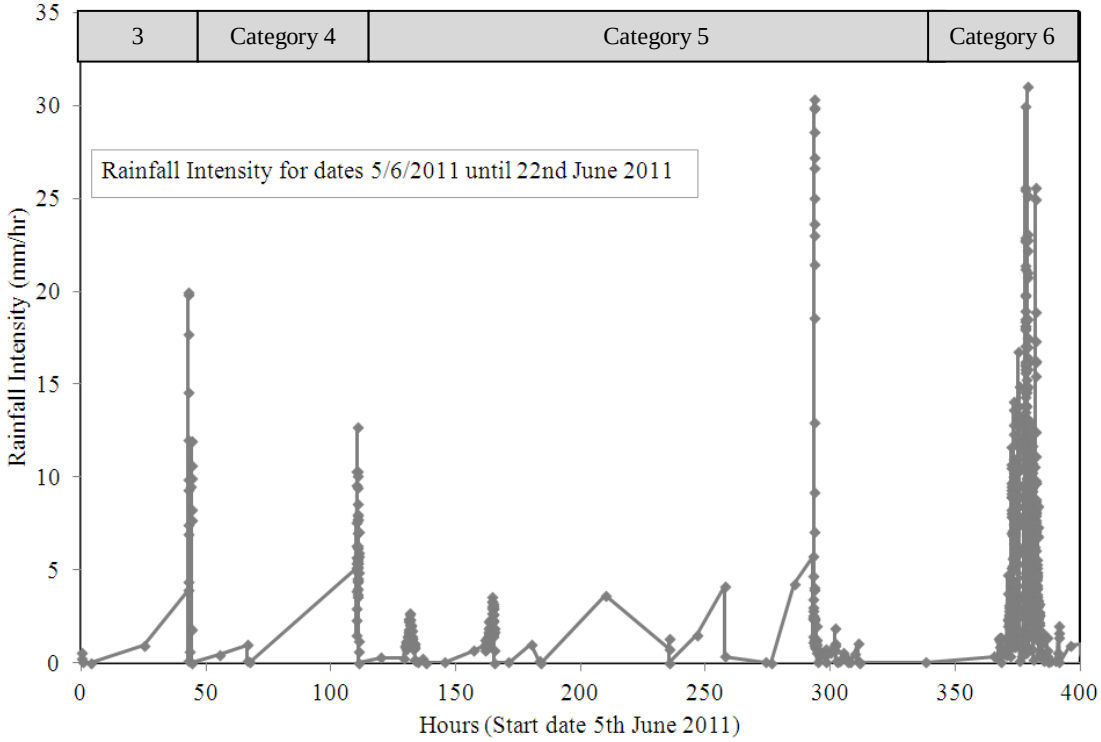

Figure 7.3(a) NRS, System 2-East: Start date 5th June, detritus change.

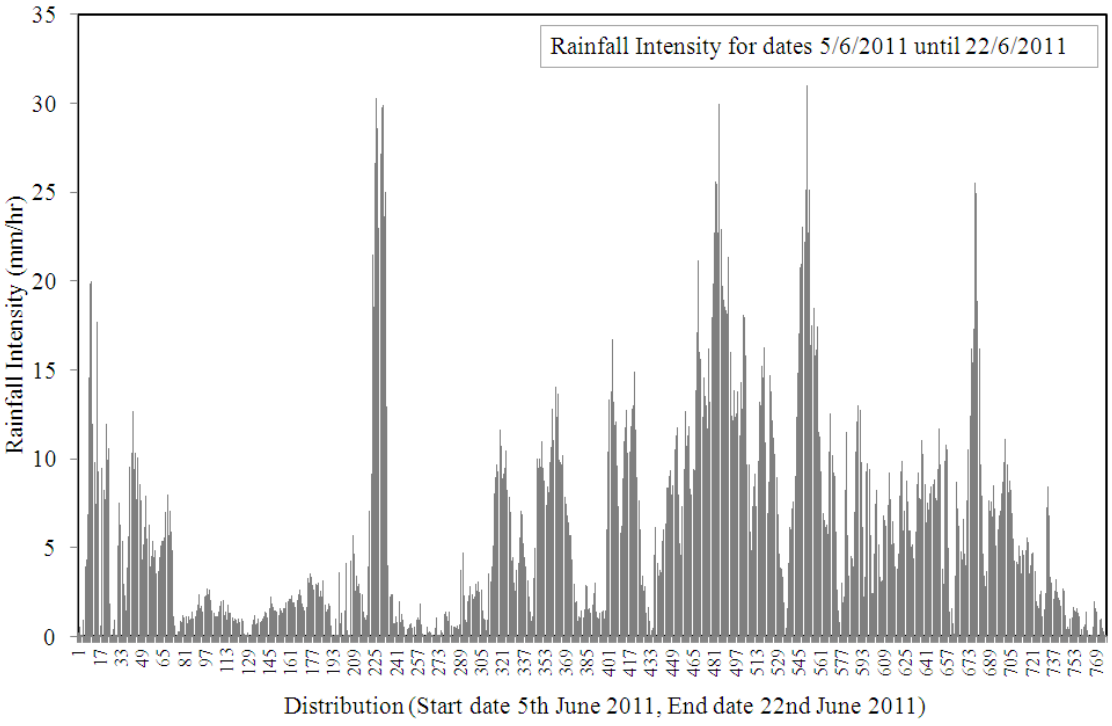

Figure 7.3(b) NRS, System 2-East: Start date 5th June, rainfall distribution.

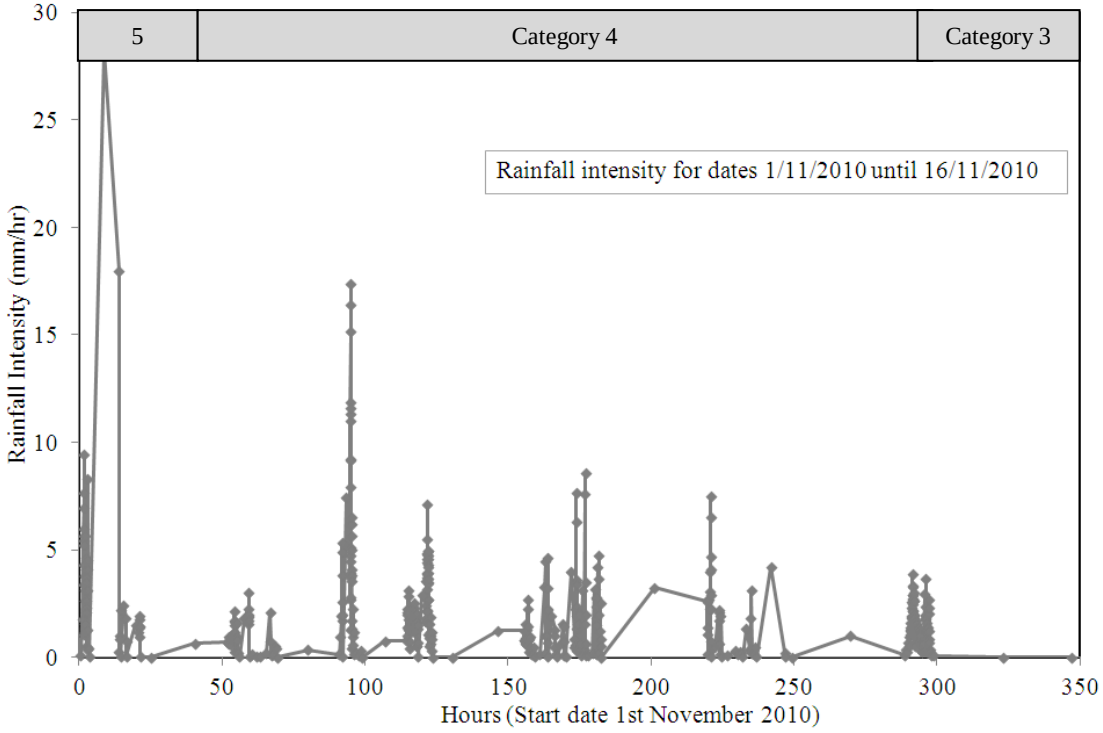

Figure 7.4(a) NRS, System 1-West: Start date 1st Nov, detritus change.

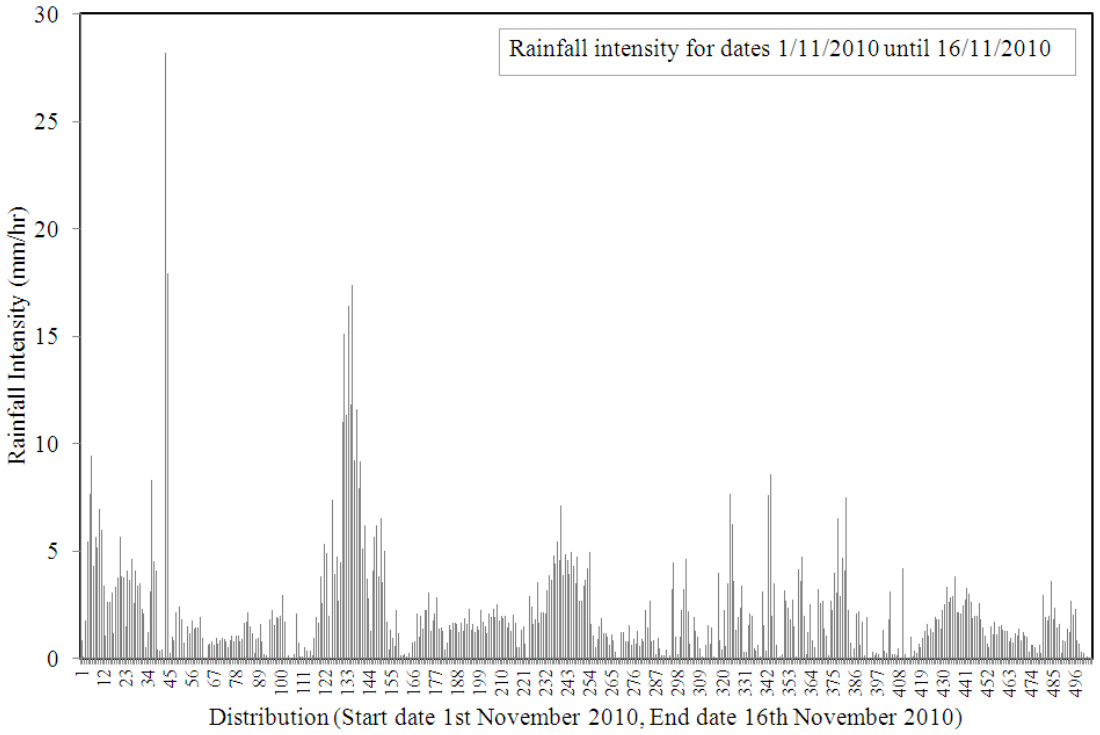

Figure 7.4(b) NRS, System 1-West: Start date 1st Nov, rainfall distribution.

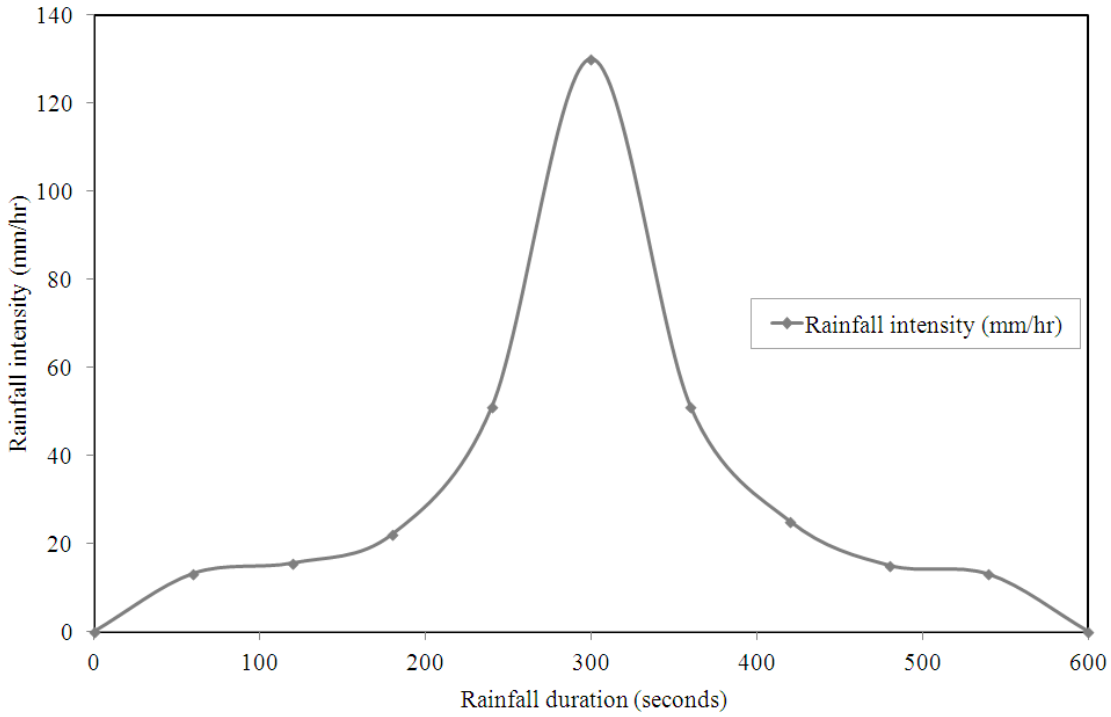

Figure 7.5 Simulation summer rainfall profile.

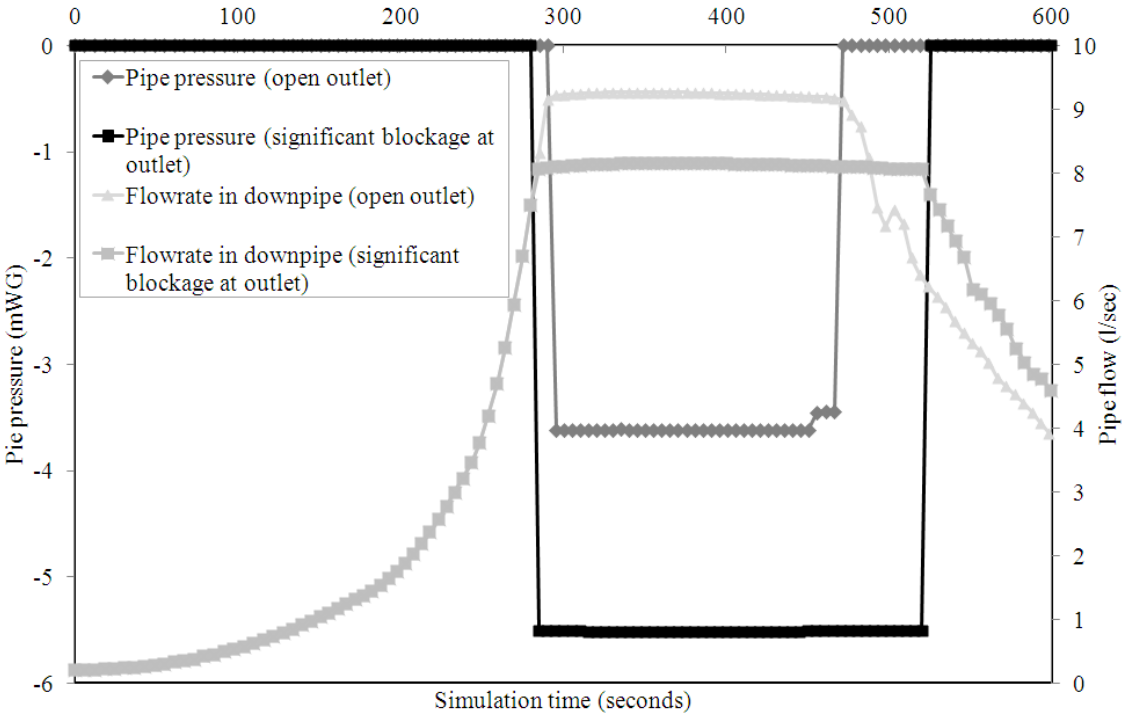

Figure 7.6 NRS System 1–West: Blockage impact on system pressure and flow. (refer to Fig 4.3 for system layout).

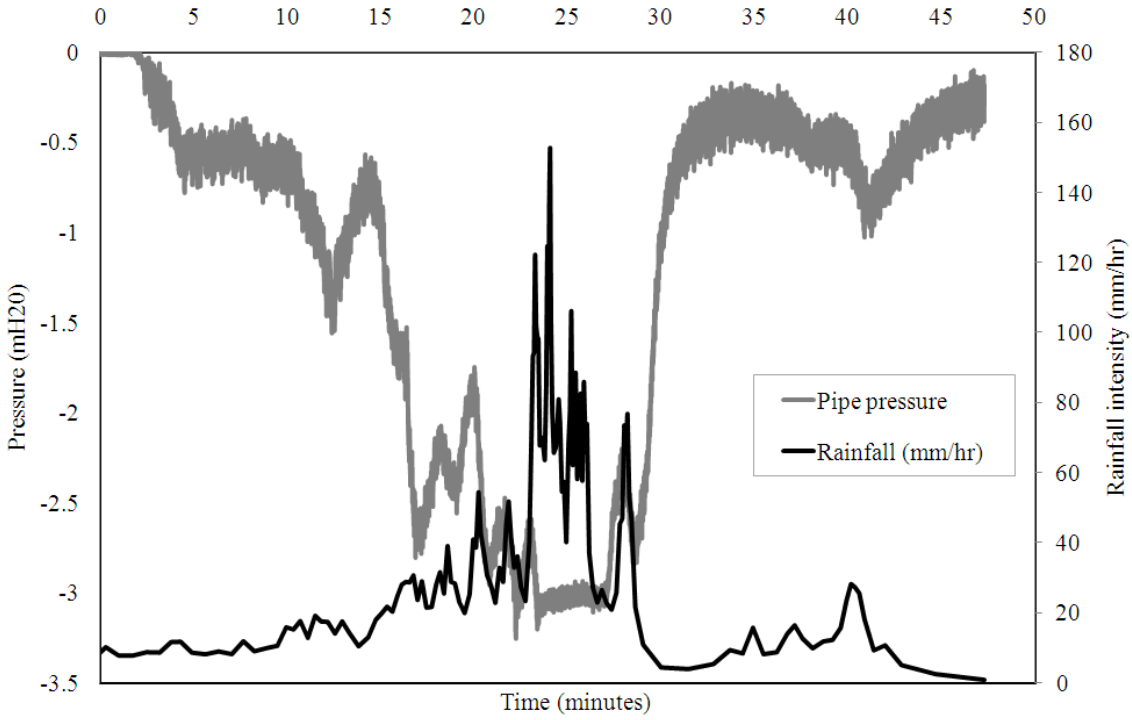

Figure 7.7 NRS System 1-West: Measured data on 8th July 14:18 2011 at top of discharge pipe (refer to Fig 4.3 for system layout).